THE HONG KONG POLYTECHNIC UNIVERSITY

DEPARTMENT OF CIVIL AND STRUCTURAL ENGINEERIG

CHARACTERIZATION OF ON-ROAD VEHICLE EMISSIONS AND AIR QUALITY IN DENSELY-BUILT ENVIRONMENT

LAU Cheuk Yin Jason

A thesis submitted in partial fulfilment of the requirements for the degree of

Doctor of Philosophy

April 2010

CERTIFICATE OF ORIGINALITY

I hereby declare that this thesis is my own work and that, to the best of my knowledge and belief, it reproduces no material previously published or written, nor material that has been accepted for the award of any other degree or diploma, except where due acknowledgement has been made in the text.

LAU Cheuk Yin Jason

ABSTRACT

Vehicle emission is one of the major contributors of gaseous pollutants such as carbon monoxide (CO), nitrogen oxides (NO_x), and hydrocarbons (HC) in the urban area. This work examines on-road gaseous emissions from vehicles of different vehicle and fuel types in order to gain a better understanding of emissions from vehicles operating under urban driving conditions and their effect on air quality in a city with a high density of high-rise buildings. The work described in this thesis has made four important contributions to the current understanding of vehicle gaseous emissions and their effects on the adjacent urban environment:

1. fostered a better understanding of the current methods of developing vehicle emission factors through a thorough review and critique exercise;

2. fostered a better understanding of the vehicle emission characteristics in relation to engine operating modes and developed instantaneous vehicle emission factors through intensive on-road emission measurements of four taxis and four light goods vehicles with a sophisticated portable emission measurement system (PEMS);

3. developed initial co-relations between two instantaneous vehicle emission data sets – one collected from on-road PEMS and the other from roadside remote sensing (RS) system so as to improve the confidence level of using the RS system in monitoring on-road vehicle emissions; and

4. discovered long memory effects of vehicle emissions in the microenvironment of the urban areas.

Measurement of on-road gaseous emissions from taxis and light goods vehicles were carried out using a portable emission measurement system (PEMS). This investigation was carried out to gain a better understanding of on-road emission characteristics of LPG taxis and diesel light goods vehicles (LGVs) under urban driving conditions. Emission indices and rates exhibit similar patterns in relation to speed while emission factors are inversely related to vehicle speed. Test vehicles emit lower amounts of gaseous pollutants when idling and higher levels of gaseous pollutants when undergoing hard acceleration. Emission level of one taxi is extraordinarily high when travelling at low speed. This is likely due to malfunction of control of fuel supply to the engine. Gaseous emissions from LGVs equipped with a catalytic converter are lower than those without one. Emissions from LGVs not equipped with a catalytic converter appear to depend mainly on engine size and power.

Over 250,000 vehicles emission measurements recorded by remote sensing techniques between 2007 and 2008 are examined to gain a better understanding of emission characteristics of the vehicle fleet in Hong Kong. Older model vehicles emit more gaseous pollutants compared to newer vehicles, possibly due to the cleaner engines of newer vehicles. Emissions from vehicles of the same vehicle type operating on different types of fuel are compared so as to examine fuel effects on gaseous emissions from vehicles. Light-duty diesel vehicles produce higher amounts of NO and lower amounts of CO and HC compared to both petrol and LPG vehicles, while LPG vehicles emit higher levels of gaseous pollutants than petrol vehicles. Older LPG commercial vehicles produce higher levels of gaseous emissions compared to non-commercial petrol and diesel vehicles of similar age, likely due to deterioration from the vehicles' extended use. Emissions from light-duty vehicles, fuelled by various fuel types, under a number of speed and acceleration modes are examined. The results show that emission factors and

vehicle speed are inversely related. High levels of gaseous pollutants are emitted when vehicles undergo heavy acceleration.

Emission factors derived from different measurement methods often vary greatly due to factors such as traffic conditions and emission variability of individual vehicles. To bridge the discrepancy between emission factors derived from different measurement methods, emission factors of LPG taxis and diesel light goods vehicles derived from on-road and remote sensing measurements are compared. The results show that emission factors are generally higher when measurements are collected on-board. This discrepancy is likely owing to the dilution and reaction of vehicle emission in the atmosphere. By establishing correlation with emission factors derived from on-road (PEMS) method that provides accurate measurements, capabilities of roadside remote sensing method which measures emissions from a large number of vehicles can be improved.

The effect vehicle emission has on air quality in different regions within a city is examined by comparing variations in traffic volume and air quality in built-up areas within Hong Kong. This comparison reveals that daily patterns in air quality at various parts of the city follow variations in traffic volume closely, indicating that vehicle emission has a strong effect on air quality in built-up areas. The effect vehicle emission has on urban air quality is illustrated by studying the correlation between air quality measurements at roadside and background monitoring stations, with the aid of two statistical techniques—principal component analysis and cluster analysis. The results show that vehicle emissions strongly influence variations in NO_2 concentration in the urban area and its effect on PM_{10} is smaller, due to the presence of other urban sources. The discrepancies in the station clusters identified by the two methods indicate that

variations in urban background air quality depend largely on local sources. Examination of variations in air quality in relation to variations in traffic indicates that dispersion of vehicle emission is hindered by tall buildings within the urban area. Vehicle emission's impact on urban air quality is also greatly affected by the level of development within the city, which can influence the effectiveness of the dispersion process. In addition, traffic conditions in the urban area can further contribute to deterioration of urban air quality, as frequent stops and acceleration results in higher levels of vehicle emissions.

LIST OF PUBLICATIONS

Journal Papers

1. Lau, J., Hung, W.T., Cheung, C.S., Yuen, D. (2008) Contributions of roadside vehicle emissions to general air quality in Hong Kong. *Transportation Research Part D: Transport and Environment,* Vol. 13, pp. 19-26

2. Lau, J., Hung, W.T., Cheung, C.S. (2009a) Interpretation of air quality in relation to monitoring station's surroundings. *Atmospheric Environment,* Vol. 43, pp. 769-777

3. Lau, J.C., Hung, W.T., Yuen, D.D., Cheung, C.S. (2009b) Long-memory characteristics of urban roadside air quality. *Transportation Research Part D: Transport and Environment,* Vol. 14, pp. 353-359

4. Lau, J., Hung, W.T., Cheung, C.S. On-road gaseous emission characteristics of LPG taxis under urban driving conditions. *Transportmetrica*, Under review

Conference and Workshop Papers

1. Lau, J., Hung, W.T., Cheung, C. S. (2007) Analysis of roadside air quality trends on Hong Kong Island. *Proceedings of the 12th International Conference of Hong Kong Society for Transportation Studies, Hong Kong, December 8-10, 2007*, pp. 743-750

2. Lau, J. (2008) A review of roadside vehicular emission measuring and calculation techniques. *Proceedings of the 13th International Conference of Hong Kong Society for Transportation Studies, Hong Kong, December 13-15, 2008,* pp. 321-330

3. Lau, J., Hung, W.T., Cheung, C. S. (2009c) An examination of air pollution behaviour in relation to monitoring station's surroundings. *Proceedings of the First International Postgraduate Conference on Infrastructure and Environment, Hong Kong, June 5-6, 2009,* pp. 75-82

4. Lau, J., Hung, W.T., Cheung, C. S. (2010) Scope of Application of Remote Sensing Technology in Motor Vehicle Emission Control. Paper presented at *Motor Vehicle Emission Control Workshop* (*MoVE*), *Hong Kong, March 4-6, 2010*

5. Lau, J., Hung, W.T. (2010) On-road gaseous emissions characteristics of diesel and LPG light buses. *Proceedings of the Third Transportation Arena Europe, Brussels, Belgium, June 7-10, 2010*

ACKNOWLEDGMENTS

I would like to express my gratitude to my supervisor, Dr. W. T. Hung, for his invaluable guidance, patience, and encouragement throughout the course of my study. I would also like to thank my co-supervisor, Dr. C.S. Cheung, for his support and helpful suggestions.

A note of thanks goes to Mr. C. Tsang, along with a number of my colleagues, for helping me conduct on-road emission measurements. I would also like to thank Mr. A. Wong for his invaluable guidance on operation of the portable emission measurement system.

The provision of a portable emission measurement system, air quality monitoring data, and remote sensing measurements from the Hong Kong Environmental Protection Department are appreciated.

Finally, I would like to thank my family members for their support and encouragement.

TABLE OF CONTENTS

NOMENCLATURE

a	Vehicle acceleration (in m/s^2)
C_P	Concentration of pollutant P (in μg/m^3 or number of particles/m^3)
D	Total trip length (in km)
D_{fuel}	Fuel density (in g/L)
EF_P	Emission factor of pollutant P (in g/km)
EI_P	Emission index of pollutant P (in g/L)
ER_P	Emission rate of pollutant P (in g/s)
FC	Fuel consumption rate (in L/km)
FR	Volumetric flow rate in exhaust pipe or sampling duct (in L/s)
h	Emission source height (in m)
L	Vehicle tunnel length (in km)
MW_P	Molecular weight of pollutant P (in g/mol C)
N	Traffic volume (in vehicles/h)
$[P]$	Concentration of pollutant P (in ppm)
Q_P	Emission source strength of pollutant P (in g/km)
T	Subset length of a time series
u	Wind speed perpendicular to road (in m/s)
V	Air flow volume within a tunnel (in m^3/h)
v	Vehicle velocity (in km/h)
ΔC_P	Change in concentration of pollutant P (in μg/m^3 or number of particles/m^3)
$\Delta[P]$	Contribution of vehicle emissions towards pollutant P (in ppm)
γ_G	Ground reflection coefficient
θ	Wind direction
ρ_P	Standard density of gas species P (in g/L)
σ_y	Horizontal dispersion coefficient (in m)
σ_z	Vertical dispersion coefficient (in m)
$\sigma(T)$	Variance of means of sub-series of length T
ω_C	Carbon fraction of fuel

Chapter 1

Introduction

1.1 Overview

Vehicle emission is a major source of gaseous and particulate pollutants in urban areas. Its effect on human health has been widely documented—previous studies have shown that incidence and hospitalization rates of respiratory and cardiovascular diseases are higher at the roadside or within street canyons, where higher levels of carbon monoxide (CO), nitrogen dioxide (NO_2), and particulate matter (PM) are observed (Scoggins et al., 2004; Namdeo and Bell; 2005; Curtis et al., 2006).

While there is an increasing trend in vehicle fleet size and vehicle-kilometre travelled in many cities (HKTD, 2009; Zamboni et al., 2009; Zavala et al., 2009), a decreasing trend in the amount of gaseous and particulate pollutants emitted by vehicles can be observed in some cities (HKEPD, 2008; Zamboni et al., 2009). The reduction in cumulative emission of gaseous and particulate pollutants from motor vehicles may be attributed to the replacement of older vehicles, which tend to emit a high amount of emissions, with newer vehicles complying with more stringent emission standards (Zavala et al., 2009). To further reduce vehicle emissions in cities, measures aimed to limit traffic volume in the urban area are implemented (Mediavilla-Sahagún and ApSimon, 2003; Westerdahl et al., 2009). However, in many cities, there is little improvement in roadside air quality in recent years (Carslaw et al., 2006; Lu and Wang, 2008). To verify the effectiveness of various control measures, there is a pressing need to monitor the changes of on-road vehicle emissions. Measurements of emissions from the vehicle fleet have been carried out in many cities with road-side sampling techniques (Shorter et al., 2005; Tang and

Wang, 2006). Only average emission factors/rates of certain vehicle categories can be deduced with such techniques. It is not possible to estimate vehicle emission factors under various operating modes for individual vehicles. Recent developments in emission measurement instruments and techniques, in particular the remote sensing systems and the on-board portable emission measurement systems, have facilitated instantaneous measurements of on-road emissions from individual vehicles. This has enhanced the understanding of emission characteristics of vehicles operating under different driving conditions.

In many cities, cumulative emission from vehicles is estimated from emission inventories (Yura et al., 2007). Such inventories are often derived from measurements of emissions from vehicles operating on conditions defined by drive cycles (Bush et al., 2008). The number of vehicles being tested is often limited and the results may not fully reflect emission characteristics of the vehicle fleet under urban driving conditions. The remote sensing systems enable measuring on-road emissions from a larger segment of the vehicle fleet at the roadside. Thus emission inventories derived from such measurements would likely be more representative of typical driving conditions within the city.

In many cities, a high percentage of gaseous and particulate emissions from vehicles are emitted from a small segment of the vehicle fleet (Mazzoleni et al., 2004a; Chan and Ning, 2005). Once high-emitting vehicles are identified, service of such vehicles can be carried out. The roadside remote sensing system can effectively identify such vehicles. However, accuracy of these measurements requires further validation before further action(s) against these dirty vehicles can be implemented. The on-board vehicle emission measuring system has high potential to serve this purpose.

With the emission inventory obtained by roadside remote sensing systems, it is possible to monitor the effectiveness of vehicle emission control schemes such as alternative fuelled vehicles including biodiesel, liquefied petroleum gas (LPG), and compressed natural gas (CNG) vehicles (Shorter et al., 2005; Jayaratne et al., 2008). While laboratory tests show that vehicles running on such fuels generally emit lower amounts of gaseous and particulate pollutants than vehicles running on convention fuels such as petrol and diesel (Ceviz and Yüksel, 2005; Yang et al., 2007), further understanding of the effectiveness of alternative fuels in reducing vehicle emissions under various driving conditions can be made with large volume of on-road emission data.

When abatement measures to reduce vehicle emissions are implemented, there are always arguments regarding contributing proportions. To quantify this proportion, gross estimation method based on fuel consumption of various activities in entire cities has been used. Source apportioning method based on emission data recorded at one or more carefully selected points has also been proposed. It is however very difficult to make any conclusive inference. And, in most cities, monitoring stations are set up at various points within the city to monitor roadside and background air quality in the urban area (Harrison et al., 2004; Pandey et al., 2008). Theoretically, the contribution of vehicle emissions towards concentrations of gaseous and particulate pollutants measured at monitoring stations can be quantified with statistical tools (Dongarrà et al., 2007); in particular, by analysing the difference between air quality measurements collected at roadside and background monitoring stations (Harrison et al., 2004). Nevertheless, few studies have ever performed to look into the cumulative effects of vehicle emissions on air quality.

1.2 Aim and Objectives

In the light of the above overview, the main aim of this research is to foster a better understanding of vehicle emission and its impacts on the densely-built urban environment. It therefore bears the following objectives:

1. To review thoroughly the prevailing methods of vehicle emission measurement and computation of vehicle emission rates and factors

2. To investigate on-road emission characteristics of light-duty vehicles by carrying out on-board measurements of vehicle emissions with a sophisticated portable emission measurement system

3. To conduct extensive analysis on road-side remote sensing records on vehicle emissions so as to explore the relationships of on-road emissions with vehicle types, fuel type, vehicle age, speed, acceleration, and road grade

4. To compare emission factors derived from (2) and (3) in order to validate emission factors derived from remote sensing data

5. To examine current methods in identifying contribution of vehicle emissions to urban air quality

6. To explore the cumulative effects of vehicle emission on urban and suburban air quality through critical examination of roadside and background air quality records over the years

1.3 Thesis Outline

This work looks into on-road vehicle emissions and its effect on air quality within a city with a high density of high rise buildings in the urban area. Chapter 1 contains an overview and outline of study aim and objectives. Chapter 2 reviews the methods of vehicle emission measurement as well methods in deriving emission factors and rates. The chapter also reviews methods for identifying contribution of gaseous and particulate pollutants from various emission sources.

Chapter 3 describes the design, implementation and analysis of on-road vehicle emission measurements using a sophisticated portable emissions measurement system. Instantaneous emissions from four taxis and four light goods vehicles operating varying speed and acceleration are recorded and examined.

Chapter 4 analyses the gaseous emissions from a wide range of vehicles recorded by the remote sensing systems over the years. Vehicle emissions by fuel type (petrol, diesel, LPG), model year, vehicle speed and acceleration, and road gradient are explored. The emission factors derived from remote sensing and on-board measurements are compared and the discrepancies between the two sets of emission factors are discussed.

Chapter 5 looks into the air quality at monitoring stations in the built-up area of Hong Kong. Variations in air quality at roadside and background stations are examined. The impact of vehicle emissions on background air quality in the urban and new town areas is examined with the aid of statistical tools. The characteristics of vehicular traffic and cumulative vehicle emission are also discussed.

1.4 Significance of This Research

This research, for the first time, looks systematically into different methods to measure and derive vehicle emissions factors. The results of the review will provide a guidance to researchers and practitioners in assessing appropriate methods to derive vehicle emission factors under their specific resource and skill constraints. This research will produce a comprehensive set of on-road instantaneous vehicle emission data for the test vehicles. This dataset will be very useful in constructing or modifying traffic emission models. Observations on the relationships between instantaneous emissions and vehicle characteristics will also be made. These observations will be very useful in formulating policy and measures to control vehicle emissions.

When the emission factors derived from the huge remote sensing dataset are validated with the on-board instantaneous emission data, the remote sensing data can then be used more effectively in identifying high pollution vehicles.

Last but not the least, identification of vehicle emission accumulation in the surrounding areas of main roads and its contribution to air quality will help policy makers to formulate effective measures to reduce human exposure to air pollution.

Chapter 2

Methods in Determination of Vehicle Emission and Contribution to Urban Air Pollution

2.1 Introduction

To gain a better understanding of emissions from motor vehicles, a number of methods and instruments have been developed to measure vehicle emissions and to derive emission factors from such measurements. In the past, emission factors were derived from measurement of vehicle fleet emissions at the roadside or within tunnels while measurement of emissions from individual vehicles was mainly carried out using a chassis dynamometer.

Development in rapid-response instruments has enabled measurements of particulate and gaseous emissions from individual vehicles under different traffic conditions to take place both at the roadside and on-board. Direct measurements of on-road vehicle emissions are made possible with the development of mobile emission laboratories and portable measurement instruments. Such developments enable comparison of emissions from vehicles operating under different conditions and fuels. The effect of vehicle weight, engine power, vehicle age, and road grade have on vehicle emissions can also be examined.

Statistical techniques are applied to identify contribution of gaseous and particulate pollutants, measured at various districts within a city, from various urban emission sources. The dispersion of vehicle emission within the urban area can be simulated with the aid of dispersion models. Vehicle emission's contribution towards deterioration of

air quality can be assessed by monitoring variations in air quality at roadside and background sites in the urban area.

In the following, prevalent methods in measuring emissions from both the vehicle fleet and individual vehicles are described and discussed. The methods used to derive emission factors from such measurements are outlined. A number of statistical techniques commonly used for identifying emission sources in the urban area and general descriptions of models simulating dispersion of vehicle emissions in the urban area are outlined. Monitoring of roadside and urban background air quality and how such measurements are applied in the study of vehicle emission and its dispersion in the urban area are discussed.

2.2 Measurement and Computation of Vehicle Fleet Emissions

2.2.1 Roadside measurements of fleet emissions

To study emissions from vehicles operating under real-world traffic conditions, mobile laboratories are developed to measure roadside air quality under different traffic conditions. These studies investigate gaseous and particle emissions from vehicles under both free-flowing and congested conditions and the measurements represent the total contribution from the full vehicle fleet travelling past the road segment where the mobile laboratory is stationed (Jones and Harrison, 2006). The roadside measurement campaigns are mainly carried out at roadways where the speed and acceleration of the vehicles travelling on it are similar (Jones and Harrison, 2006). Traffic counts are carried out to measure the traffic composition, classified by either fuel or vehicle type.

Background air quality is measured concurrently with the roadside measurements to

determine the contribution of vehicles towards the concentrations of particulate and gaseous pollutants at the roadside measurement site. Background air quality is generally monitored at a location far from the roadside measurement site or upwind of the roadside measurement site (Jones and Harrison, 2006). Meteorological measurements such as wind direction are collected at the roadside measurement site and valid measurement periods are considered to be those where the wind direction is close to perpendicular to the roadway (Gramotnev et al., 2003). Since air quality measurements can be strongly affected by changes in wind direction, monitoring equipment can be placed on opposite sides of a roadway to increase the length of measurement periods. Under such arrangements, the background and roadside measurement sites are determined from instantaneous wind direction (Corsmeier et al., 2005; Kohler et al., 2005). Such measurement campaigns are carried out on roadways where wind direction is generally perpendicular to the roadway (Imhof et al., 2005).

Differing traffic composition can often be observed on weekdays and weekends—weekend traffic generally consists of a smaller percentage of heavy-duty diesel vehicles than weekday traffic (Lonati et al., 2006; Mellios et al., 2006). Thus emission of vehicles of different fuel types and vehicle classes can be distinguished by examining roadside air quality measurements on different days.

2.2.2 Tunnel fleet emission studies

Roadside emission measurement results are often affected by variations in meteorological conditions at the roadside monitoring site. To monitor on-road vehicle emissions under more controlled conditions, emission measurements are often carried out within vehicle tunnels.

Monitoring of tunnel air quality within the tunnel may take place near the tunnel exit while background air quality is measured at the tunnel entrance or in the interior of the tunnel, near the tunnel entrance (Geller et al., 2005; Phuleria et al., 2006). This is done to maintain the consistency of background measurements. Such arrangements, however, can result in background measurements being affected by vehicle traffic. In general all traffic within a tunnel bore travel in one direction and it is assumed that air travels from the entrance to the exit (Kean et al., 2003; Kristensson et al., 2004). Thus the background measurement site is often considered upwind of the traffic measurement site. The air flow rate within the tunnel can be estimated by releasing an inert tracer gas at a constant rate at the background site and measuring the concentration of the tracer at the trafficked site (Kean et al., 2003). Alternatively, air flow rate can be estimated from wind speed measurements collected within the tunnel (Kristensson et al., 2004). The air fuel rate is then computed by multiplying the wind speed by the cross-section area of the tunnel.

Monitoring may take place within the interior of a tunnel bore, far from the tunnel entrance and exit, by placing sampling probes at ventilation ducts near the tunnel ceiling (Martins et al., 2006). Alternatively, measurement of gaseous and particulate emissions from vehicles can take place near the curb. Such measurements often take place near the midpoint of the tunnel so that interference from outside the tunnel has no effect on measurements (Imhof et al., 2006; Martins et al., 2006). Ventilation fans generally operate continuously to provide fresh air to the tunnel. Background concentrations of pollutants are measured at the inlet of the ventilation tunnel, at a site near the tunnel entrance or at a site far from the tunnels (Laschober et al., 2004; Imhof et al., 2006; Martins et al., 2006). Measurements may also be carried out at ventilation outlet to investigate size distribution of particulate matter at the roadside and the ventilation

outlet (Imhof et al., 2006).

Since the tunnel length is known, vehicle speed can be estimated by comparing the entrance and exit times of random vehicles (Phuleria et al., 2006). Traffic speed of the tunnel can also be estimated by driving a vehicle through the tunnel a number of times and recording the time needed to travel the length of tunnel (Kirchstetter et al., 1999). Speed measurements can also be obtained using road sensors. Total traffic volume and traffic composition can be acquired from video footage recorded from within the tunnel or vehicle license plate surveys, where license plates of random vehicles are recorded and matched with registration data (Kirchstetter et al., 1999; Phuleria et al., 2006).

At some tunnels, light-duty vehicles may travel in a dedicated bore, separate from heavy-duty vehicles. Thus measurement of air quality can be carried out in different bores to determine the emission factors of light- and heavy-duty vehicles. Since heavy-duty vehicles operate mostly on diesel, emission levels of diesel and petrol vehicles can also be derived from air quality and traffic measurements at different bores (Geller et al., 2005).

2.2.3 On-road measurement of fleet emissions

Instead of measuring fleet emissions at a stationary location, measurements of vehicle emissions can be carried out by driving a mobile laboratory on a fixed route. Compared to roadside and tunnel measurements, vehicle emission of gaseous pollutants and particulate matter under a wider range of traffic conditions can be measured using such methods.

Mobile laboratories used for on-road measurements are usually in the form of a

modified passenger car or van. Measurement instruments are installed within the laboratory and are connected to the sampling line. The sample intake is installed to the front end of the mobile laboratory to prevent contamination by the mobile laboratory's own exhaust and electric generators (Jiang et al., 2005). Separate inlets may be constructed for gaseous pollutants and particulate matter. The inlet for particulate matter is often set to a height where the sampled air would not be contaminated by road and tire wear while the gaseous inlet is often placed closer to the road surface (Bukowiecki et al., 2002; Tang and Wang, 2006). Gaseous and particulate inlets may also be placed next to one another so that gaseous and particulate emissions within the same plume can be sampled (Pirjola et al., 2004). The particle sample may pass through a filter, where it is diluted with ambient air at a fixed ratio, before measurement of particle number takes place. Separate monitors of one pollutant, commonly CO_2 detectors, may be connected to each inlet so that air quality measurements at separate inlets can be linked and compared (Bukowiecki et al., 2002). Monitoring instruments are calibrated periodically.

During road tests, concentrations of gaseous pollutants and particulate matter are constantly monitored by the mobile laboratory, which maintains a sufficiently large distance between itself and the preceding vehicle. This is done to avoid sampling exhaust from a single vehicle and to prevent impeding traffic flow (Kittelson et al., 2004; Jiang et al., 2005). Traffic volume, traffic conditions, and road type along the test route can be recorded manually or by video. Traffic volume can also be estimated by examining CO_2 concentrations while the number of petrol vehicles can be estimated from CO measurements collected during road tests. Traffic speed along the test route can be estimated by monitoring the speed of laboratory (Kittelson et al., 2004; Fruin et al., 2008; Westerdahl et al., 2009). Background air quality measurements are made at a fixed location along the route or a location far from the test route (Johnson et al., 2005;

Westerdahl et al., 2009). Measurements are considered to be reflective of on-road air quality, rather than contribution from a single vehicle, if the difference between on-road CO_2 measurements and the baseline value, defined to be a low percentile value over a moving time period, is sufficiently small (Jiang et al., 2005).

2.2.4 Derivation of fleet emission factors

The distance-based emission factors of the total vehicle fleet can be derived from traffic volume, mean vehicle speed of the roadway, and the net contribution of various pollutants from vehicle emissions, considered as the difference between roadside and background concentrations of each pollutant (Kohler et al., 2005; Jones and Harrison, 2006). The emission index, in g/L $_{fuel}$, can be derived from tunnel and on-road measurements as follows:

$$EI_P = \frac{\Delta[P]}{\Delta[CO_2] + \Delta[CO] + \Delta[HC]} \cdot \omega_C \cdot D_{fuel} \quad (2.1)$$

where $\Delta[P]$ is the net contribution of vehicle emissions towards pollutant P, computed as the difference between roadside and background measurements and expressed in terms of ppm. ω_C is the carbon mass fraction of the vehicle fuel and D_{Fuel} is the fuel density in g/L (Martins et al., 2006; Westerdahl et al., 2009). Fleet emission factor can then be derived by multiplying emission indices by fuel consumption rate of the fleet.

When air quality measurements take place at the tunnel entrance and exit, fleet emission factors can be computed using the following:

$$EF_P = \frac{C_{P,exit} \cdot V_{exit} - C_{P,entr} \cdot V_{entr}}{N \cdot L} \quad (2.2)$$

where $C_{P,\,exit}$ and $C_{P,\,entr}$ are concentrations of P at the tunnel exit and entrance, in μg/m^3, respectively. V_{exit} and V_{entr} are the air flow volumes, which are expressed in m^3/h and computed from wind speed and cross section area of the tunnel bore, at the tunnel exit and entrance respectively. N is the hourly traffic volume and L is the tunnel length in kilometres (Pierson et al., 1996; He et al., 2008). Air flow volume within the tunnel is sometimes considered constant throughout the tunnel (Moeckli et al., 1996, Cheng et al., 2006).

Emission factors of different vehicle types can then be computed from the vehicle fleet emission factors and traffic composition by means of regression analysis. The emission factors of different vehicle types can then be estimated from fleet emission factor traffic count as follows:

$$EF = EF_L \cdot N_L + EF_H \cdot N_H \quad (2.3)$$

where N_L and N_H are the number of light- and heavy-duty vehicles, respectively, and EF_L and EF_H are the emission factors of light- and heavy-duty vehicles respectively (Kristensson et al., 2004; Corsmeier et al., 2005). Emission factors of petrol and diesel vehicles can be estimated in a similar manner.

The emission factors can also be computed from roadside measurements of total emission by reverse modelling using a line source model such as CALINE4 or OSPM (Gramotnev et al., 2003; Ketzel et al., 2003). Traffic volume and meteorological conditions (wind speed and direction) are measured simultaneously as the air quality measurements. The cumulative emissions from vehicles over a period of time and the average wind conditions of this period are obtained from the measurements. Each set of measurements takes place over a long time segment (1 hour) to reduce the level of

uncertainly in the computation. The emission factor for the model can then estimated by comparing the model output and the roadside air quality measurements, using background air quality measurements, and meteorological and traffic conditions as input for the model (Gramotnev et al., 2003; Kühlwein and Friedrich, 2005). General descriptions of dispersion models are discussed in a later section.

2.3 Indirect Measurements of Emissions from Individual Vehicles

Emission measurements from roadside and tunnel measurements can provide information on emissions under specific traffic conditions. Such measurements are reflective of the emission from the total vehicle fleet at the time testing takes place. However, emission factors of different types of vehicles are derived based on traffic measurements and may not be reflective of actual emissions. To establish a better understanding of emissions from different types of vehicles, a number of methods have been developed to monitor emissions from individual on-road vehicles.

2.3.1 Roadside and tunnel measurements of emissions from individual vehicles

Development of rapid response instruments has enabled on-road measurement of gaseous and particulate emissions from individual vehicles to take place. A laboratory containing measuring instruments is stationed near a roadway to monitor roadside air quality. Instead of monitoring cumulative emission over a period of time, concentrations of particulate matter and gaseous pollutants are recorded continuously.

As a vehicle travels past the mobile laboratory, emissions from the vehicle would result in an increase in concentrations of various pollutants, which would be detected by the measurement instruments. The contribution of various pollutants from the vehicle can

then be obtained by comparing the concentrations of each pollutant prior to the vehicle's passage and the peak concentrations observed shortly after the passage of the vehicle. Placement of the sample inlets is determined by the type of vehicle being examined. Investigations of vehicle emissions using this method have been performed on roadways where local traffic consists mostly of one type of vehicle and within tunnels (Jayaratne et al., 2007; Ban-Weiss et al., 2009). During roadside tests, the mobile laboratory is placed at a spot where vehicles travelling past the laboratory operate at similar conditions (Kurniawan and Schmidt-Ott, 2006; Jayaratne et al., 2007). When measurements take place at a tunnel, the average speed of each vehicle can be estimated by recording its tunnel entry and exit times (Ban-Weiss et al., 2009).

Gaseous and particle emission of vehicles can be determined by studying the emission ratio between the increase in concentration of a specific pollutant and the increase in concentration of a tracer gas. In general, the tracer gas chosen is CO_2, as its emission is directly related to fuel consumption and its concentration under various operating modes are mostly similar (Jayaratne et al., 2007; Hak et al., 2009). It is generally assumed that perfect combustion takes place, which is often the case for diesel vehicles (Galindo et al., 2005). When CO_2 is the tracer gas, emission factors of particulate mass and NO_x (in grams per kilometre) can be derived from measurements values using Eq. 2.4. Particle number emission factor can be computed using Eq. 2.5.

$$EF_P = \frac{\Delta[P]}{\Delta[CO_2]} \cdot \frac{MW_P}{MW_{CO2}} \cdot EF_{CO2} \quad (2.4)$$

$$EF_P = \frac{\Delta C_P}{\Delta[CO_2]} \cdot \frac{N_A}{MW_{CO2}} \cdot EF_{CO2} \quad (2.5)$$

where $\Delta[P]$ is the difference between peak and background concentrations of a pollutant P in ppm, ΔC_P is the difference between peak and background particle number concentration (in number/μg^3), MW_P is the molecular weight of P in g/mol, N_A is the Avocado number (Hak et al., 2009). The emission factor of CO_2 can be estimated from vehicle fuel consumption rates and fuel carbon content. Emission factors can also be obtained from emission inventories such as ADCC (2009) and the background concentration is considered the concentration immediately prior to the passage of the vehicle.

In addition to pollutant concentrations, wind direction is also monitored to determine whether shifts in gaseous and particulate concentrations are induced by vehicles travelling past the laboratory. A video camera may also be deployed to identify the vehicles being monitored. This way emission from vehicles of various age, fuel, and emission standards can be compared (Jayaratne et al., 2008).

2.3.2 Remote sensing measurements

Roadside measurement of emissions from individual vehicles is carried out under the assumption that the vehicles travelling on the roadway have similar speed and acceleration at the time when they travel past the monitoring equipment. To obtain the operating condition of each vehicle as it passes through the monitoring site, a remote sensing system has been developed to measure both vehicle speed/acceleration and emission data.

Using remote sensing techniques, concentrations of major gaseous pollutants—carbon monoxide (CO), carbon dioxide (CO_2), hydrocarbons (HC), and nitric oxide (NO)—emitted by moving vehicles can be obtained. A laser beam, containing an infrared and

an ultraviolet beam, is emitted from a source detector module and reflected back to the module by a mirror on the opposite side of the lane. When a vehicle passes by the monitoring equipment, the vehicle's exhaust absorbs some of the light emitted. The strength of the beams is measured and the concentrations of gaseous emissions are determined by comparing the strength and waveform of the beams exiting and returning to the source detector module.

In addition to emission measurements, a remote sensing system can also record the speed and acceleration of each vehicle travelling past the system. A speed sensor, containing an emitter bar, which emits two laser beams, and a detector bar, is used to determine the speed and acceleration of each vehicle travelling past the measurement system. The speed and acceleration measurements can help determine the vehicle's driving modes and the derivation of distance-based emission factors. A video recorder records the license plate information of each vehicle travelling past the remote sensing system. Registration information of each vehicle (vehicle and fuel type, for example) can then be retrieved from a vehicle registration database (Kuhns et al., 2004; Chan and Ning, 2005). The vehicle's speed and acceleration provide information on the vehicle's operating conditions. By matching license plate numbers of the vehicles being measured to the vehicle registration database, the vehicle type, fuel type, and age of each vehicle being tested can be obtained.

CO, NO, and HC emission indices of each vehicle, expressed in terms of grams per litre of fuel, travelling past the remote sensing system can be determined from the following:

$$EI_P = \frac{[P]}{[CO]+[CO_2]+3\cdot[HC]/0.5} \cdot \frac{MW_P}{MW_{Fuel}} \cdot D_{Fuel} \quad (2.6)$$

where [P] is the measured concentration of pollutant P in ppm, MW_P is the molecular weight of P in g/(mol C), and D_{Fuel} is the fuel density in g/L (Ning and Chan, 2007). HC concentration is divided by a factor of 0.5 in Eq. 2.6 due to discrepancies in HC concentrations measured by NDUV and those measured with a flame ionization detector (FID), commonly used in dynamometer tests (Kuhns et al., 2004). A vehicle's gaseous emission factors can be derived from its emission indices using the following:

$$EF_{P,fuel} = EI_{P,fuel} \cdot FC_{fuel} \quad (2.7)$$

where FC_{fuel} is the fuel consumption rate in L/km.

Remote sensing techniques were originally developed to measure gaseous pollutants, but not particulate matter. Techniques have been developed to measure particulate matter emitted by individual vehicles travelling along a roadway. Particle mass can be measured with an ultraviolet Lidar (light detection and ranging) system. A laser pulse is transmitted from the light source towards the opposite side of a traffic lane. The pulse is then reflected back to an oscilloscope, where the waveform of the pulse is measured. A series of waveforms collected immediately before and after the passage of a vehicle is analysed and the increase in PM mass concentration as the result of the vehicle's passage can be computed based on assumptions on particle size distribution and bulk density (Mazzoleni et al., 2004b). Testing often takes place on busy roadways where vehicles are expected to be operated under higher engine load, such as highway on-ramps and inclined roadways, to increase the data capture rate (Mazzoleni et al., 2004a).

A method in identifying particle number and size distribution using remote sensing techniques has yet to be found, mainly due to the differing particle distribution of exhaust emissions from vehicles of different types and weight classes (Wåhlin et al.,

2001; Gross et al., 2005).

2.3.3 Chase car experiments

While remote sensing measurements can capture emissions from large number of vehicles operating under a wide range of operating conditions, such measurements only provide emission information of the vehicle the instant the vehicle passes through the monitoring equipment. To monitor an on-road vehicle's emission over a longer period of time, mobile laboratories can be deployed to monitor emissions from individual vehicles.

The mobile laboratory used for such studies is generally similar to the one used for on-road measurement of fleet emissions. The sample inlets are located at the front end of the mobile laboratory and directed forwards so that the air sample is not contaminated by the mobile laboratory's exhaust. The inlet for particulate matter is often placed on top of the vehicle while the gaseous inlet is often placed near to the road surface (Bukowiecki et al., 2002; Weijers et al., 2004). Power to instruments on-board is supplied by electric generators. The laboratory records instantaneous concentrations of gaseous pollutants and particulate matter to observe rapid changes in on-road air quality caused by a preceding vehicle.

During chase car experiments, the mobile laboratory travels along a route and air samples are captured continuously. This way, emissions from the vehicles preceding the mobile laboratory can be captured. Concentrations of gaseous and particulate pollutants are logged at short intervals to identify periods when emissions from a preceding vehicle are being captured. While the mobile laboratory chases a vehicle, the distance between the two vehicles should be kept small so that the driving pattern of the

laboratory mimics that of the preceding vehicle (Shorter et al., 2005).

Instruments with high temporal resolution are needed as it has been shown that, under normal urban traffic conditions, the time a vehicle spends trailing another vehicle is below 45 seconds and the period in which the laboratory captures a vehicle's emission lasts no longer than 15 seconds (Bukowiecki et al., 2002). The peak concentration observed during the period where emissions from the preceding vehicle are captured is often considered the combined contribution from the vehicle and ambient air (Bukowiecki et al., 2002). Meteorological conditions such as wind direction may also be monitored so that gaseous and particulate emission measurements are not contaminated by emissions from the generator, used to provide power to the instruments within the mobile laboratory, or emissions from the laboratory's own tailpipe (Jiang et al., 2005). To reduce contamination of air samples by emissions from the laboratory's tailpipe at times when the mobile laboratory is stationary, the mobile laboratory is generally in the form of an electric vehicle (Westerdahl et al., 2005; Fruin et al., 2008). The range of electric vehicles—2 hours and 120 km under highway driving conditions (Westerdahl et al., 2005)—indicates that such vehicles are capable of measuring vehicle emissions on highways in Hong Kong. Such vehicles may also be suitable for emission experiments on urban streets of Hong Kong over shorter distances (15-20km).

By monitoring the speed of the laboratory, the operating conditions of the vehicle preceding it can be estimated. This way measurements obtained throughout the period in which the laboratory follows a vehicle can be used to investigate emissions of the vehicle under different traffic conditions (Tang and Wang, 2006). During on-road tests, license plate number of the vehicles being followed may be recorded to facilitate comparison of emissions from different types of vehicles, classified by vehicle or fuel

type (Shorter et al., 2005).

Instantaneous emission indices and factors of vehicles being chased can be computed using Eq. 2.5 and 2.6 respectively. The cumulative emission factor can be computed from instantaneous emission factors by dividing the weighted sum of instantaneous emission factors, where weightings are defined to be vehicle speed, by the total distance the vehicle is being chased.

Since emissions from other vehicles can interfere with chase car measurements, emission measurement using chase car techniques are sometimes carried out on roadways closed to traffic such as racetracks. To maintain consistency of results, the distance between the test vehicle and the mobile laboratory is kept approximately constant during testing by attaching the two vehicles (Vogt et al., 2003; Bergmann et al., 2009). The distance between the two vehicles may vary between tests so that the dilution ratios at different distances can be investigated.

On-road emissions of a vehicle under steady driving conditions can also be measured by attaching a capture trailer, which contains a conductive sampling bag and a sampling probe tube, to the vehicle. The sampling probe tube opening is set a short distance away from the exhaust pipe. During on-road experiments, the vehicle's exhaust is captured by the sampling probe tube and stored in the sample collection bag. A remotely-controlled valve is constructed within the trailer to divert the emission sample to a bypass vent while the emission is not being collected (Morawska et al., 2007). The valve also prevents contamination of the filled sampling bag by ambient air after sample collection is completed. The sampling bag can be transported to a laboratory upon completion of a road test. At the laboratory, the sampling bag is replaced and its contents is analysed. The test vehicle is driven repeatedly in a circuit prior to the first test run to warm up the

engine. Between test runs the vehicle is kept at idling mode. Collection of emission takes place while the test vehicle travels at steady speed. Gaseous and particle mass emission factors can be estimated as stated in Eq. 2.8, assuming that exhaust flow rate can be approximated by the air flow rate to the engine.

$$EF_P = \frac{[Tracer]_{exhaust}}{[Tracer]_{bag}} \cdot \frac{FR \cdot [P]}{v} \cdot D_{fuel} \quad (2.8)$$

where $[Tracer]_{exhaust}$ and $[Tracer]_{bag}$ are the tracer gas, chosen to be NO_x, concentrations (in ppm) within the exhaust and sampling bag respectively, $[P]$ is the concentration of a pollutant P within the sampling bag in ppm, FR is the air flow rate in L/s, calculated from air velocity measurements and sampling duct dimensions, v is the vehicle speed and D_{fuel} is the fuel density in g/L (Morawska et al., 2007).

2.4 Direct Vehicle Emission Measurement Techniques

Indirect on-road emission measurement techniques such as roadside monitoring, remote sensing measurements, and chase car experiments provide useful information on emissions from on-road vehicles under different operating conditions. Emission measurements collected using these methods can be affected by factors such as wind conditions, turbulence from other vehicles, and emissions from other vehicles or road maintenance. To eliminate the effect of external factors, techniques have been developed to directly measure vehicle emissions in the tailpipe before emission is being discharged into the atmosphere.

2.4.1 Dynamometer testing

To measure vehicle emission under a controlled setting, emissions from a vehicle can be

measured using a chassis dynamometer. During a test, a vehicle is parked on a test bed and the vehicle's exhaust pipe is attached to a sampling line. A number of sampling probes, each connected to an analyser, are placed inside the sampling line. Instead of directly connecting the sampling line to the exhaust, a vehicle's emission may pass through a dilution tunnel before its contents are sampled (Holmén and Ayala, 2002; Yao et al., 2009). Within the dilution tunnel a vehicle's exhaust is diluted by ambient air, which is pre-cleaned with the filter so that particles are removed (Robert et al., 2007). The flow rate of the dilution tunnel can be adjusted to accommodate different types of vehicles. During a test, flow rate within the dilution tunnel is generally kept constant. Thus the higher the exhaust flow rate, the lower the dilution ratio (Holmén and Ayala, 2002). Concentrations of regulated gaseous pollutants (CO, CO_2, NO_x, HC) can be measured directly from the sampling line or at the end of the dilution tunnel (Dearth et al., 2005; Alvarez et al., 2008). Further dilution may be necessary when measuring concentrations particulate matter. This is done so that measurements would not exceed an instrument's detection range. The dilution factor can be determined by the ratio between the concentration of a tracer gas, typically CO_2, in the raw exhaust and within the dilution tunnel (Bergmann et al., 2009).

CO and CO_2 emissions of a vehicle are measured by non-dispersive infrared (NDIR) absorption. Concentration of HC is measured by a flame ionization detector (FID). Exhaust sample is transported to the sensor through a heated line, whose temperature is maintained at 190℃. NO_x concentration is measured by a chemiluminescence detector (Durbin et al., 2003; Yang et al., 2005). Particulate matter emitted by a vehicle is collected with filters, which are heated to approximately 47℃, and particle mass concentration is measured by weighing the filters. Particle number within the exhaust is measured using a particle counter. The sample may be heated during transport to

remove volatile particles (Giechaskiel et al., 2008).

Tests measuring emissions from a vehicle operating under steady state conditions or conditions defined by established driving cycles generally take place using a chassis roll dynamometer (Yang et al., 2005; Yao et al., 2009). Drive cycles are a fixed set of acceleration, deceleration, and cruise segments that a driver attempts to follow. Cold-start emission of a vehicle is generally higher than emission from a warmed up vehicle, due to that engine temperature is not sufficiently high for the catalytic converter to function effectively (Yang et al., 2005; Gao and Checkel, 2007). Thus cold start operation is incorporated into a number of drive cycle emission tests (Yang et al., 2005). Prior to a cold-start emission test, a vehicle's engine is kept off and the vehicle is stored in a temperature-controlled room for a minimum of 12 hours. The vehicle is then moved to the dynamometer immediately before testing begins (Sodeman et al., 2005; Bergmann et al., 2009). Meanwhile, emission under steady state conditions are generally carried out after the vehicle is sufficiently warmed up so that measurements are more stable. This is generally done by leaving the vehicle at idle mode or driving the vehicle at constant speed for a period of time shortly before testing begins (Dearth et al., 2005; Sodeman et al., 2005). Between tests a vehicle is left at idle mode or kept running at constant speed. Total emission of a vehicle for the duration of a drive cycle can be determined by collecting the vehicle's exhaust in sampling bags and analysing the contents immediately after the completion of a cycle (Durbin et al., 2003; Yang et al., 2005).

Studies comparing emission from vehicles fuelled by conventional fuels such as gasoline and diesel and alternative fuels such as compressed natural gas (CNG), liquefied petroleum gas (LPG), alcohols, and biodiesel are often carried out using a

dynamometer (Wang et al., 2000; Ristovski et al., 2004; Yang et al., 2007; Yao et al., 2009). In such investigations, vehicles are operated under conditions defined by drive cycles or steady state conditions (constant vehicle speed) and the vehicle's emissions using different test fuels are examined and compared. Prior to testing of a vehicle running on a specific type of fuel, the vehicle's fuel tank is drained to reduce contamination. The vehicle's emission levels under specific modes of a driving cycle and over the entire cycle can be found and the vehicle's emission while running on different types of fuel can then be compared.

2.4.2 Mobile emission laboratory

A vehicle's emission under a wide range of conditions can be obtained from a chassis dynamometer measurement system. However, such tests cannot simulate parameters such as variations in road geometry and topography (Li et al., 2007). The dynamometer may also be less effective in simulating large variations in speed and rapid speed changes, situations that frequently arise under urban driving conditions. As a result, techniques and instruments have been developed to continuously monitor a vehicle's exhaust emissions while on-road.

On-road measurements of emissions from individual heavy-duty vehicles can be carried out by attaching the vehicle and its exhaust to a mobile laboratory, in the form of a cargo trailer. The test vehicles may be operated under conditions defined by standard driving cycles. Ideally, such measurement should be carried out on a closed circuit or roadways with free-flowing traffic so that measurements would not be disrupted by other vehicles. Measurements can also take place on pre-defined routes to mimic actual traffic conditions (Shah et al., 2004). By comparing emissions of a vehicle operating of different types of fuel, fuel effect on emissions can also be investigated using a mobile

emission laboratory (Kittelson et al., 2008).

Measurement instruments similar to those used for dynamometer tests are installed within the trailer. The test vehicle's exhaust is transported to the trailer through a sampling line. Inside the trailer, sampling probes connect the sampling line to various instruments and the concentrations of gaseous pollutants and particulate matter are monitored in real time. The exhaust flow rate and temperature are measured by a flow meter, placed near the point where the vehicle's exhaust pipe connects with the sampling line, so that the vehicle's emission rate can be measured (Shah et al., 2004; Johnson et al., 2009a). The vehicle's speed may be recorded to investigate the vehicle's emission under different operating conditions.

The gaseous emission indices of the vehicle can be derived using Eq. 2.6. Instantaneous emission rates, expressed in terms of g/s, and factors can be determined from emission and flow rate measurements as follows:

$$ER_P = [P] \cdot FR \cdot \rho_P \quad (2.9)$$

$$EF_P = \frac{ER_P}{v} \quad (2.10)$$

where $[P]$ is the concentration of the gas P in ppm, FR is the exhaust mass flow rate in L/s, ρ_P is the standard density of P in g/L, and v is the vehicle speed in km/h. Trip emission factor can be computed from the following

$$EF_P = \frac{\Sigma ER_P}{D} \quad (2.11)$$

where ΣER_P is the sum of instantaneous emission rate of P over the entire trip and D is

the trip length in km.

2.4.3 On-board measurement devices

Mobile laboratory may not be suitable for measuring emission from light-duty vehicles because of the size and weight of the monitoring equipment. As a result, more compact emission measurement instruments have been developed to facilitate on-board measurement of emissions from light-duty vehicles.

To measure emissions directly from light-duty vehicles, measurement device monitoring gaseous emissions are installed to the test vehicle. A sampling probe is inserted into the test vehicle's tailpipe and a small portion of the tailpipe exhaust is transported to the portable measurement device for analysis. Gaseous emissions are monitored continuously using an on-board measurement device such as a five-gas analyser, which monitors emissions of CO, CO_2 and HC using a non-dispersive infrared monitor and concentrations of O_2 and NO_x using electrochemical transducers (Holmén and Niemeier, 1998; Silva et al., 2006b). Emissions can also be monitored using a Fourier-transform infrared (FTIR) spectrometer. The spectrometer is capable of measuring concentrations of major species of volatile organic compounds and gaseous pollutants such as ammonia, CO, NO_x, and THC in a vehicle's exhaust in real-time (Collins et al., 2007). The spectrometer releases beams over a wide range of wavelengths and a specific range of wavelengths corresponds to a single pollutant. Concentration of each pollutant is determined using the classical least-squares method (Collins et al., 2007).

The speed of the test vehicle is recorded to examine the vehicle's emissions under different operating conditions. To compute the vehicle's emission rate, the vehicle's instantaneous exhaust flow rate is measured by connecting a flow meter to the exhaust

pipe. Alternatively, instantaneous fuel flow rate of the test vehicle can be measured by connecting a fuel meter to the vehicle's fuel supply line so that instantaneous emission rate can be determined from the air and fuel flow rates.

It has been shown that HC emissions obtained from FTIR measurements can be lower by a factor of 2 or larger compared to the actual HC concentration (Unal et al., 2004). Likewise, NDIR measurements of HC concentrations are approximately half the actual concentration (Tang and Wang, 2006). To improve the accuracy of HC measurements from on-board emission measuring instruments, portable emission measurement systems (PEMS) incorporating the flame ionization detector (FID), commonly used for measurement of HC emissions from vehicles in dynamometer tests, have been developed (Oestergaard et al., 2004; Dearth et al., 2005).

Simultaneous measurements shows that instantaneous concentration measurements of gaseous pollutants obtained from a PEMS and a chassis dynamometer are highly correlated and, on average, within 5% of each other (Dearth et al., 2005). Meanwhile, on-road tests have shown that PEMS measurements of gaseous pollutants generally have a slight positive bias compared to measurements from a mobile emission laboratory while second-by-second PEMS measurements correlate well with measurements obtained from a mobile emission laboratory (Johnson et al., 2009a).

In addition to major gaseous pollutants (Chen et al., 2007), measurements of toxic pollutants such as mercury can also be carried out using portable measurement devices. During a test, a vehicle travels on a designated route, generally chosen to be a route with low traffic volume. Emissions of vehicles can be determined by collecting a sample from the exhaust. The sampled exhaust passes through filters and impingers, where the toxic pollutant is collected and measured (Won et al., 2007). By computing

the emission rate of vehicles running on different types of fuel, fuel effects on toxic emission can be examined.

On-board instruments measuring particle mass emission from vehicles have also been developed (O'Sullivan and Timoney, 2005; Booker et al., 2007). A small portion of a vehicle's exhaust is drawn through a filter unit. The exhaust flow rate is measured by a built-in flow meter. The ratio between exhaust and sample flow is kept constant by mixing the vehicle's exhaust with ambient air. The flow rate within the sample inlet is controlled by a series of solenoid valves. Particulate matter is collected using filters or vibrating quartz crystals. The particle mass concentration is determined by measuring changes in filter mass or the crystal's vibration frequency. To date measurement of particle mass emission from vehicles using on-board instruments is carried out mostly on diesel vehicles (Booker et al., 2007).

A vehicle's instantaneous emission indices can be computed using Eq. 2.6 while instantaneous emission rates and factors are derived from Eqs. 2.9 and 2.10 respectively.

2.5 Evaluation of emission measurement and computation methods

2.5.1 Advantages and shortcomings of emission measurement methods

When emission from the total fleet is measured at the roadside or within tunnels, the derived emission factors can be segregated into emission factors of different vehicle types based on the composition of traffic at the roadway where emission measurement takes place. By carrying out measurements at periods where traffic composition differs, emission factors of various vehicle types can be determined. On-road measurement of fleet emissions generally enables measurement of emission under a wider range of

traffic conditions than roadside and tunnel measurements. Measurement of fleet emissions assumes that operating conditions are similar for all vehicles.

The amount of air quality measurements collected at the roadside are highly dependent on variations in wind direction. To remedy this, measurement campaigns in which air quality monitors are placed on the two sides of a roadway had been carried out—the monitoring station located on the windward side of the roadway is considered the background station and the station on the leeward side is considered the roadside station (Corsmeier et al., 2005; Kohler et al., 2005). In some tunnel studies, background air quality measurements may take place at the interior of the tunnel or at the tunnel entrance. This can result in background measurements that are directly influenced by vehicle emissions (Geller et al., 2005).

Since the measurement data used in the derivation of emission factors through reverse modelling are obtained from the roadside, issues such as accumulation of emissions due to traffic congestion may arise. Factors such as meteorological conditions, traffic composition and conditions, fuel characteristics, choice of background measurement site, and particle size range (for PN emission factors) can also have an effect on on-road emission measurement results and therefore emission factors derived using modelling methods (Jamriska and Morawska, 2001).

Roadside measurement of emissions from individual vehicles enables rapid collection of emission data from a large number of vehicles. This way, emissions from different types of vehicles can be compared and high emitters can be identified. Similar to roadside measurement of total fleet emissions, the operating condition is often assumed to be the same for all vehicles (Hak et al., 2009). Thus roadside measurement of emissions is best suited for roadways where vehicles operate under similar conditions,

such as free-flowing highways. Tunnel measurement of emissions are sometimes preferred over roadside measurements due to that wind has a smaller effect on emission measurements within a tunnel than at the roadside. Traffic at the measurement site should be sufficiently sparse. Otherwise peaks associated with each vehicle's passing may be difficult to distinguish (Jayaratne et al., 2007).

Emission data from vehicles of various types operating at a vast variety of conditions can be measured at a single location using remote sensing techniques. Since remote sensing techniques measure a vehicle's emission over an instant (~0.5s), remote sensing is capable of measuring emissions from a higher number of vehicles in comparison with roadside measurements of individual vehicles (Kuhns et al., 2004). It is assumed that particle size distribution are the same for vehicles of different type, although it has been shown that particle size distribution may be different for petrol and diesel vehicles (Wåhlin et al., 2001). As particle number measurements cannot be made by remote sensing techniques, remote sensing is less effective in measuring particulate emissions compared to other emission measurement methods.

A common limitation of roadside, tunnel, and remote sensing measurements of emissions from individual vehicles is that they only provide instantaneous emission characteristics. However, the measurements can be conducted at roadways with different traffic composition so that emission factors of the total vehicle fleet can be estimated (Kuhns et al., 2004).

Emission measurements of individual vehicles under different real world traffic conditions can be obtained through chase-car experiments. In particular, a vehicle’s emission level under a large range of traffic conditions (idle, cruising, stop-and-go) can be observed rapidly through such experiments (Tang and Wang, 2006). The number of

vehicles being tested would be smaller than roadside or remote sensing measurements and the representativeness of the vehicles being tested would depend on traffic at the time of measurements. The laboratory should be set up so that the air sample is not contaminated with the laboratory's own exhaust emissions (Jiang et al., 2005). Chase-car techniques can be considered for measurement of on-road emission from a specific vehicle type such as buses, where the mobile laboratory travels on a route frequently travelled by the specified vehicle type (Shorter et al., 2005).

Direct measurement of vehicle emissions collects a vehicle’s exhaust from its tailpipe. Thus interference by external factors such as wind and traffic turbulence is mostly eliminated. Dynamometer testing of vehicle emissions enables measurement of emissions under a controlled setting. Thus emissions of vehicles operated under steady state conditions or conditions prescribed by drive cycles are best measured using a chassis dynamometer. However, a dynamometer may be less effective in simulating certain conditions, such as uphill and downhill driving (Li et al., 2008).

On-board emission measurements, such as those collected using mobile emission laboratory or portable measurement devices, tend to be more reflective of the actual operating condition of the test vehicle than measurements obtained from chase-car experiments, as the exhaust sample is obtained directly from the test vehicle's exhaust pipe. Such techniques also enable measurement of emissions from a wider range of operating conditions compared to chase-car methods. However, the number of vehicles that can be tested tends to be small due to time and cost constraints.

Additional properties of each measurement method are outlined in Table 2.1.

	Vehicle Sample size	Test duration for each vehicle	Additional measurements needed	Operating conditions	Pollutants measured	Selectivity of vehicles measured	Accuracy of fleet average Emission Factors	Reference (Examples)
Roadside or Tunnel Testing (Total Fleet)	Fleet average	Short	Traffic count, meteorological conditions	Average driving mode on roadway	All	Major vehicle classes	Reflects average driving mode and fleet composition of roadway	Jones and Harrison (2006)
Roadside or Tunnel Testing (Individual Vehicles)	Large	Short	Traffic count, meteorological conditions	Average driving mode on roadway	All	Variable; depends on traffic	Reflects average driving mode of roadway; may be extrapolated to reproduce average emission for total fleet	Kurniawan and Schmidt-Ott (2006)
Remote Sensing	Large	Instantaneous (0.5s)	Vehicle license plate information	Variable; depends on vehicle	CO, CO_2, HC, NO, PM	Excellent	May be extrapolated to reproduce average emission for total fleet	Kuhns et al. (2004)
Chase-car Experiment	Medium	Depends on length of time a vehicle is followed	Instantaneous speed and acceleration of mobile laboratory	Variable; depends on traffic	All	Variable; depends on traffic	Reflects driving mode of vehicles being followed	Shorter et al. (2005)
Dynamometer Tests	Small	Defined by user	Exhaust flow rate	Defined by user	All	Excellent	Limited; small number of vehicle samples due to cost	Durbin et al. (2003)
On-board Measurement	Small	Defined by user	Exhaust flow rate, vehicle speed	Defined by user	All	Excellent	Limited; small number of vehicle samples due to cost	Chen et al. (2007)

Table 2.1 Properties of emission measurement methods

2.5.2 Examination of emission computation and comparison of emission factors

When measurement of vehicle fleet emissions is carried out at the roadside, background air quality measurements should reflect ambient air quality in the neighbourhood of the roadway. Thus monitoring of background air quality preferably should take place at a location upwind and near the roadside measurement site (Imhof et al., 2005; Jones and Harrison, 2006).

The computation of vehicle fleet emissions from tunnel measurements (Eq. 2.2) assumes that pollutants emitted by vehicles travelling within the tunnel are accumulated towards the exit. This is generally the case as vehicles travel in the same direction within a tunnel bore (Geller et al., 2005). However, vehicle traffic travels in both directions in some tunnels. Under such circumstances, it may be preferable to replace P_{entr} in Eq. 2.2 by measurements outside the tunnel and assume that air flow rate is constant throughout the tunnel. Alternatively, fleet emission factors within the tunnel can be derived using Eqs. 2.1 and 2.7.

When emissions of individual vehicles are measured at the roadside or tunnels (Eqs. 2.4 and 2.5), the background concentration is often defined as the concentration shortly before the vehicle's passage. Background air quality measurements can be influenced by residual emissions from a previous vehicle or instrument signal noise (Jiang et al., 2005). To reduce the influence from these factors, background concentration can be considered as a low percentile value over a short period prior to the vehicle's passage (Bukowiecki et al., 2002; Tang and Wang; 2006).

CO_2 is considered as the tracer gas in the roadside and tunnel measurement of emissions from individual vehicles (Hak et al., 2009). The emission index of CO_2 is incorporated

in the computation of gaseous and particulate emissions (Eqs. 2.4 and 2.5). This is based on the assumption that vehicle engine combustion is stoichiometric, which may not necessarily be the case (Li et al., 2008). If CO concentration is also monitored by the mobile laboratory, gaseous and particle emissions from individual vehicles can be computed using Eq. 2.1 instead. Emission factors can then be derived from Eq. 2.7.

If a vehicle's fuel consumption rate is known, a vehicle's emission factors can be computed from emission indices using Eq. 2.7. A vehicle's fuel consumption rate can be retrieved from the vehicle manufacturer, direct measurements, or estimations. Fuel consumption rates provided from manufacturer are generally a single value and may not reflect fuel consumption under different conditions (Won et al., 2007). Direct measurements generally yield more accurate fuel consumption rates (Gao and Checkel, 2007). A vehicle's fuel consumption can be estimated from CO_2 emission rate or the ratio between emission factor and index of vehicles of the same type (Zhai et al., 2008). Estimation of fuel consumption rates under different speeds should be made so that fuel consumption estimations better reflect a vehicle's operating conditions (Kudoh et al., 2004).

Variations in the dilution ratio between tracer gas concentration in the exhaust and that in sampling bag can have a large effect on emission factors derived from Eq. 2.8. Thus exhaust and sampling measurements of tracer gas concentrations is best carried out under calm wind conditions, under which exhaust flow rate and air flow rate within the sample tube are not affected by perpendicular winds and therefore better correlated (Vogt et al., 2003).

Instantaneous emission of a vehicle can be computed using Eqs. 2.9 and 2.10. Lags in exhaust emission and flow rate measurements, caused by instrument response delays,

can result in inaccurate emission factors. Thus exhaust flow rate and emission and speed measurements can be aligned so that the instantaneous emission factors derived from on-board measurements correspond with actual driving conditions better. This would also improve the accuracy of trip emission factor, derived from Eq. 2.11.

To compare the emission factors derived from data obtained using different measurement methods, Table 2.2 shows the emission factors of CO, NO_x, particle mass (PM) and particle number (PN), derived from measurements obtained using the data measurement methods discussed in previous sections.

a)	EF g/(km veh.)	Traffic Condition	Veh. Type	Method	Reference
	11±2	Variable	Mostly LD	Model[1]	Ketzel et al. (2003)
	6.55±0.40	Variable	LD	Roadside (Fleet)	Jones and Harrison (2006)
	2.62±0.13	Free Flowing	All	Roadside (Fleet)	Kohler et al. (2005)
	1.85±0.43	Free Flowing	All	Tunnel (Fleet)	Cheng et al. (2006)
	5.27±0.10	Free Flowing	Mostly LD	Tunnel (Fleet)	Kristensson et al. (2004)
	5.32 [2]	Variable	LD	On-road (Fleet)	Westerdahl et al. (2009)
	3.65 [2]	Variable	HD	On-road (Fleet)	Westerdahl et al. (2009)
	11.21	Variable	Passenger Car	Chase-car	Tang and Wang (2006)
	3.31	Variable	Diesel Truck	Chase-car	Tang and Wang (2006)
	2.17	Variable	Diesel Bus	Chase-car	Tang and Wang (2006)
	2.73 [2]	Variable	Passenger Car	Remote Sensing	Mazzoleni et al. (2004a)
	0.73 [2]	Variable	Diesel Truck	Remote Sensing	Mazzoleni et al. (2004a)
	0.52	Variable	Passenger Car	On-board	Silva et al. (2006b)
	4.96	Variable	Diesel Truck	On-board	Chen et al. (2007)

b)	EF g/(km veh.)	Traffic Condition	Vehicle Type	Method	Reference
	1.30±0.20	Variable	Mostly LD	Model[1]	Ketzel et al. (2003)
	0.59±0.09	Variable	LD	Roadside (Fleet)	Jones and Harrison (2006)
	5.19±0.52	Variable	HD	Roadside (Fleet)	Jones and Harrison (2006)
	0.68±0.12	Free Flowing	LD	Roadside (Fleet)	Kohler et al. (2005)
	6.86±1.57	Free Flowing	HD	Roadside (Fleet)	Kohler et al. (2005)
	0.08±0.28	Free Flowing	Non-Diesel	Tunnel (Fleet)	Cheng et al. (2006)
	1.93±0.31	Free Flowing	Diesel	Tunnel (Fleet)	Cheng et al. (2006)
	1.36±0.03	Free Flowing	Mostly LD	Tunnel (Fleet)	Kristensson et al. (2004)
	1.02±0.40	Variable	HD	On-road (Fleet)	Johnson et al. (2009b)
	0.28	Variable	Passenger Car	Chase-car	Tang and Wang (2006)
	1.27	Variable	Diesel Truck	Chase-car	Tang and Wang (2006)
	2.19	Variable	Diesel Bus	Chase-car	Tang and Wang (2006)
	0.59 [2]	Variable	All	Remote Sensing	Mazzoleni et al. (2004b)
	0.49	Variable	Passenger Car	On-board	Silva et al. (2006b)
	6.54	Variable	Diesel Truck	On-board	Chen et al. (2007)

c)	EF mg/(km veh.)	Traffic Condition	Vehicle Type	Method	Reference
	172	Variable	All	Model[1]	Kühlwein and Friedrich (2005)
	33±6	Variable	LD	Roadside (Fleet)	Jones and Harrison (2006)
	370±32	Variable	HD	Roadside (Fleet)	Jones and Harrison (2006)
	26±11	Free Flowing	LD	Roadside (Fleet)	Imhof et al. (2005)
	275±67	Free Flowing	HD	Roadside (Fleet)	Imhof et al. (2005)
	45.3±17.5	Free Flowing	Mostly LD	Tunnel (Fleet)	Laschober et al. (2004)
	4.2	Free Flowing	LD	Tunnel (Fleet)	Geller et al. (2005)
	79.6	Free Flowing	HD	Tunnel (Fleet)	Geller et al. (2005)
	3.7±0.7	Variable	Petrol	Remote Sensing	Mazzoleni et al. (2004b)
	170±40	Variable	Diesel	Remote Sensing	Mazzoleni et al. (2004b)
	166±122	Variable	Diesel Trucks	Emission Lab	Shah et al. (2004)

d)	EF 10^{14}/(km veh.)	Traffic Condition	Size Range (nm)	Vehicle Type	Measurement Method	Reference
	2.80±0.50	Variable	10-700	All	Model[1]	Ketzel et al. (2003)
	2.82±0.25	Free Flowing	15-700	All	Model[1]	Gramotnev et al. (2003)
	0.12	Variable	11-450	LD	Roadside (Fleet)	Jones and Harrison (2006)
	6.36	Variable	11-450	HD	Roadside (Fleet)	Jones and Harrison (2006)
	1.22	Free Flowing	30-10000	LD	Roadside (Fleet)	Corsmeier et al. (2005)
	7.79	Free Flowing	30-10000	HD	Roadside (Fleet)	Corsmeier et al. (2005)
	4.6±1.9	Free Flowing	3-900	All	Tunnel (Fleet)	Kristensson et al. (2004)
	1.01 [2]	Variable	6-560	LD	On-road (Fleet)	Westerdahl et al. (2009)
	8.03 [2]	Variable	6-560	HD	On-road (Fleet)	Westerdahl et al. (2009)
	0.23	Free Flowing	>10	Petrol	Roadside (Individual)	Hak et al. (2009)
	1.5	Free Flowing	>10	Diesel	Roadside (Individual)	Hak et al. (2009)
	3.43±4.82 [2]	Free Flowing	>3	HD	Tunnel (Individual)	Ban-Weiss et al. (2009)

Table 2.2 Comparison of a) CO, b) NO_x, c) PM_{10}, and d) particle number (PN) vehicle emission factors derived from different measurement methods (LD—light duty, HD—heavy duty)

Notes:

[1] Emission factors are derived from models using data obtained from roadside measurements

[2] Emission factors are converted from g/kg_{fuel} assuming a fuel consumption rate of 0.056 kg/km for light duty vehicles and 0.073 kg/km for heavy duty vehicles (Tang and Wang, 2006)

Table 2.2 shows a wide discrepancy in fleet emission factors derived from different measurement methods, even among vehicles of the same class. This may be the result of differences in meteorological conditions, traffic composition and conditions, fuel content, and background air quality in various cities (Morawska et al., 2005). Large variation in emission factors of individual vehicles, resulting from each vehicle's conditioning and operating mode, can also contribute to large variations in emission factors derived from different methods (Bishop and Stedman, 1996).

In many cities, a large percentage of gaseous and particulate emissions from vehicles are emitted by a small number of vehicles (Mazzoleni et al., 2004b; Ko and Cho, 2006). Due to a smaller number of vehicles being tested, emission factors derived from

measurements of individual vehicles can be more easily skewed by high-emitting vehicles than fleet emission factors.

2.6 Identification of Emission Contribution from Urban Sources

A number of methods have been developed to identify contribution of gaseous pollutants and particulate matter from various emission sources at different monitoring sites. Mass concentrations of various particulate species such as trace metals, elemental and organic carbons, and water-soluble ions can be determined from samples gathered at monitoring sites. The contribution from each major source is then estimated using statistical techniques. Statistical methods are also considered in identifying emission sources and the contribution from each source towards gaseous and particle mass concentrations at different monitoring sites (Castanho and Artaxo, 2001; Pires et al., 2008).

2.6.1 Speciation of particulate matter

To identify the contribution of various emission sources towards particulate matter in the urban area, concentrations of major species of particulate matter are monitored. Major sources of particulate matter include soil dust, road dust, on-road vehicle emissions, marine emissions, biomass burning, oil combustion, and secondary aerosols. Concentrations of coarse and fine particulate matter are often measured simultaneously to determine the composition of the two types of particles (Park and Kim, 2005). Some of the major species of particulate matter mostly originate from one single source. For example, elemental and organic carbon are generally associated with vehicle emissions; water soluble ions is generally associated with road dust while trace metals mostly originate from oil burning and soil dust (Castanho and Artaxo, 2001; Karanasiou et al.,

2009).

Generally, each air sample is collected over a 6- or 24-hour period. Concentrations of various species are measured using a number of methods. For instance, concentrations of elemental and organic carbon can be measured by evolving carbonaceous species into gas phase, using vaporisation and oxidation, followed by applying a thermal/optical transmittance method (Yuan et al., 2006). Concentrations of trace metals may be measured using particle induce X-ray emission (Castanho and Artaxo, 2001). Concentrations of water-soluble ions are measured by extracting a part of the sample with water. Ion chromatography is then used to analyse the extracted sample (Yuan et al., 2006).

Each emission source's contribution toward different particulate species is then determined using techniques such as those outlined below. Such methods generally identify similarities in concentrations of various pollutants and categorises pollutants into groups. The major source of each pollutant can be identified by comparing results with pollutants associated mostly with one emission source.

2.6.2 Principal component analysis

Principal component analysis (PCA) is a statistical technique that transforms a set of inter-related variables into a set of uncorrelated variables. The newly formed variables are ordered such that most of the variation present in the original variables is retained by the first few variables (Jolliffe, 2002). This is done by ordering the variables so that the first variable, or principal component (PC), explains the largest proportion of variability within the original data, the second variable explains the largest proportion of the variability not explained by the first PC, and so forth (Jolliffe, 2002; Pires et al., 2008).

The PCs representing a large percentage of variability (70-90%) are then retained for further analysis. PCA requires that observations be available at all target stations.

The general method used to determine the number of PCs that should be retained is by examining the log plot of the variation attributed to each PC. The number of PCs retained can then be chosen to be the component beyond which the plot is close to linear (Jolliffe, 2002). To better illustrate the relationship between the PCs and the original variables, the retained PCs can be transformed by applying a rotation algorithm such as Varimax rotation. The variables that are highly correlated would have similar PC loadings (Jolliffe, 2002; Pires et al., 2008). By comparing the PC loadings of each station, similarities between temporal variations in air quality at different stations can be found. Station redundancy within the air quality network of a city can then be identified—highly similar PC loadings at multiple stations is an indication that air quality observed at such stations may be duplicates of each other (Pires et al., 2008). The effect one specific emission source, such as vehicle emissions, has on background air quality can be identified from PCA results by examining the level of similarity between PC loadings at two monitoring sites, one of which is located in close proximity to an emission source, such as a heavily-trafficked roadway (Väkevä et al., 1999; Karar and Gupta, 2007). PCA can also be applied to gaseous and particulate measurements at one monitoring site to identify the major emission sources at the site (Pandey et al., 2008).

Contribution of various emission sources towards concentrations of a specific particulate species can be identified by comparing the PC loadings of this species with that of another species, with the latter originating mostly from a single source. For instance, particle species having similar PC loadings with elemental carbon generally

originate from vehicle emissions (Almeida et al., 2005; Park and Kim, 2005).

2.6.3 Cluster analysis

Cluster analysis (CA) is a method to partition objects into a number of clusters so that objects within a cluster are similar to each other while objects located in different clusters are different from each other (Pires et al., 2008). To classify objects into clusters, individual objects are first considered as separate clusters. The pair-wise distances between clusters are then computed and the pair with the lowest distance is connected to form a new cluster (Pires et al., 2008). This process is repeated until all objects, monitoring stations in this case, belong to a single cluster.

The classification of the objects can be illustrated with a dendrogram, which shows the similarity level or the Euclidean distance between any two objects. This method can be used to identify monitoring stations within a monitoring network whose pollutant observations can be reproduced by data from other stations within the network (Gramsch et al., 2006) and to identify sources of pollutants at different sections within a city (Pires et al., 2008). If one station is located in close proximity to an emission source such as vehicle emissions, the Euclidean distance between this station and another station may be considered an indicator of the level of influence this emission source has on air quality at the latter station—the lower the distance between two stations, the more likely the emission source contribute greatly towards concentration of a pollutant observed at the latter station.

Sources of individual particulate species can be identified by examining the Euclidean distance or degree of similarity between this particle species and another species that originates mostly from one source (Viana et al., 2006; Dongarrà et al., 2007). For

instance, vehicle emissions often contribute greatly towards concentrations of particulate species belonging to the same cluster as elemental carbon.

2.6.4 Positive matrix factorization

PCA results may yield negative loadings for certain factors, which can be difficult to interpret. Thus methods in deriving positive contribution from each emission source have been developed. One of which is the positive matrix factorization (PMF) method.

The objective of PMF is to quantify the contribution of various emission sources towards concentration levels of a number of pollutants and to minimize cumulative residuals. PMF computes the contribution of each source using the least-squares method. Non-negative constraints are applied so that contribution from each source is non-negative. Similar to PCA, emission sources can be identified by examining the dominant factor of one pollutant that is closely associated with a specific emission source.

PMF is primarily applied to identify sources of particulate matter at different monitoring stations within a city (Yuan et al., 2006; Song et al., 2007). It has also been applied to identify sources of gaseous pollutants such as CO and ozone (Paterson et al., 1999).

2.6.5 Interpretation of results

The methods outlined above are applied to identify clusters of pollutants or measurement sites. Such clusters by themselves do not have any meaning. However, association between a cluster and an emission source can be established through examination of the elements within a cluster. If a cluster contains a pollutant that originates mainly from one source, the cluster can be associated with this particular

source. In many cities, CO and elemental carbon originate mostly from vehicle emission (Väkevä et al., 1999; Almeida et al., 2005). Thus vehicle emission can be considered the main source of pollutants belonging to the same cluster as these two.

The contributions from various urban emission sources, computed from the methods outlined above, are considered estimations. Thus results obtained from such methods may not reflect the actual contribution from each source. To address this, multiple identification methods are applied to one set of measurements and results from different methods are compared to determine whether the results converge (Yuan et al., 2006; Pires et al., 2008). Convergent result from different source apportionment methods would indicate that the apportionment techniques provide a fairly accurate estimation of contributions from various emission sources.

The source apportionment methods described above are sometimes applied to identify clusters of monitoring stations in a city with similar air quality patterns (Pires et al., 2008). Station clusters identified from measurements of multiple pollutants can be examined to determine whether measurements of different pollutants yield similar clusters. Such a result would indicate that variation in air quality at stations contained in each cluster are similar, indicating air quality of these stations is influenced by a common emission source. If the stations contained in a cluster are scattered throughout the city and no clear emission source is present in the neighbourhood of the stations, this may be interpreted as air quality being influenced mainly by regional sources rather than local sources. If the stations within a cluster are located within a small region, the result would be an indication that air quality is influenced by local sources. Likewise, if apportionment analysis of different pollutants yield divergent station clusters, the result would indicate that air quality in the city is largely affected by local emission sources.

2.7 Modelling of Air Quality near Urban Roadways

In many cities, vehicle emission is a major source of air pollutants. Vehicle emissions tend to have a larger effect on air quality in the urban area, particularly at the ground level, since emission from other sources such as power generation and industrial activity are generally dispersed more widely compared to vehicle emissions (Peace et al., 2004).

A number of studies investigating vehicle emissions' impact on urban air quality have been carried out. Contribution of vehicle emissions towards deterioration of air quality can be illustrated by model simulations. Such models are often applied to estimate concentrations of gaseous pollutants and particulate matter at various locations within a street canyon (Ketzel et al., 2003). Models are also used to estimate vehicle's effect on air quality in the neighbourhood of major roadways and intersections (Yura et al., 2007). Box model, Gaussian plume model, and computational fluid dynamics simulations are frequently applied to simulate air quality in the neighbourhood of a roadway or intersection.

The box model considers the area in the immediate surrounding a roadway as a box, inside which emissions are released and removed at the same rate. Vehicle emissions are considered the major source of gaseous and particulate pollutants within the box. The box may be oriented in such a way that wind or a roadway is perpendicular to one face of the box (Collett and Oduyemi, 1997; Jamriska and Morawska, 2001). It is assumed that air quality within the box is uniform. Thus gaseous and particulate pollutants emitted by vehicles are immediately mixed with surrounding air.

The input required for such models include air quality measurements within and outside the model area, wind direction and speed measurements, and traffic volume, total and

by vehicle type. The height of the box is determined by the plume height (Gokhale and Pandian, 2007). Concentrations of pollutant *P* within the box can be computed from the following:

$$C_{P,box} = \frac{EF_P \cdot N}{\Delta z \cdot (u \cdot \sin\theta + u_0)} \quad (2.12)$$

where EF_P is the emission factor (in g/(km vehicle)), u is the wind speed (in m/s) and θ is the wind direction, u_0 is the vehicle wake factor (in m/s), Δz is the box height (in metres), and N is the traffic volume within the box (in vehicle/s) (Gokhale and Pandian, 2007). The emission factor is considered a weighted sum of emission factors of different vehicle types under free flow, interrupted, and congested traffic conditions (Gokhale and Pandian, 2007). Such models are generally considered in the study of concentrations of inert pollutants such as CO near urban roadways.

A box model can also be incorporated to a model simulating air quality within a street canyon (Berkowicz, 2000). Circulation within a street canyon and street level turbulence, created by incoming wind and on-road traffic, are considered in the model (Berkowicz, 2000). The incoming wind component, which depends on the wind speed and direction, has a strong effect when wind speed is high. Conversely, turbulence due to on-road traffic becomes dominant when wind speed is low. Contribution of gaseous pollutants and particulate matter from vehicles are computed from emission factors and traffic count (Ketzel et al., 2003). Air quality on both sides of the canyon at a specified height is then computed. The building configuration used for simulation are generally assumed to be uniform or highly homogeneous (Berkowicz, 2000).

In Gaussian plume models, vehicle emission is assumed to be dispersed evenly in

different directions under calm wind conditions and unobstructed surroundings. In addition, the topology surrounding the roadway should be flat and meteorological condition within the simulated area is considered homogeneous. It is also assumed that no chemical reaction and deposition take place within the area being simulated. A proportion of the vehicle exhaust plume is reflected by the ground (Collett and Oduyemi, 1997; Nagendra and Khare, 2002). Inputs for such models include hourly traffic volume, vehicle emission factor, and meteorological data. Meteorological data are generally collected from weather stations within or close to the study area.

It is generally assumed that meteorological conditions are homogeneous throughout the simulated area while traffic emission, which is defined by the user, is considered to be fixed on each road segment. The model considers the area immediately above road surface as a mixing zone, separate from the area above. In the mixing zone, vehicle-induced turbulence dominates air movement (Nagendra and Khare, 2002; Greco et al., 2007). The model computes concentrations of various pollutants at a number of specified points, or receptors, by summing the contribution of vehicle emissions from all points upwind of each receptor. Assuming an emission source has a coordinate of (0,0,0), the contribution of pollutant *P* from the emission source towards at the receptor located at (*x*,*y*,*z*) is defined as follows:

$$C_P = \frac{Q_P}{2\pi \cdot u \cdot \sigma_y \cdot \sigma_z} \cdot \exp\left(\frac{-y^2}{2{\sigma_y}^2}\right) \cdot \left(\exp\left(\frac{-(h-z)^2}{2{\sigma_z}^2}\right) + \gamma_G \cdot \exp\left(\frac{-(h+z)^2}{2{\sigma_z}^2}\right)\right) \quad (2.13)$$

where Q_P is the emission source strength, which is determined from vehicle emission factor and traffic volume. u is the average wind speed perpendicular to the road and h is the source height. γ_G is the ground reflection coefficient, whose value is between 0 and 1. The σ_y and σ_z values are dependent on the distance between a receptor and the

emission source and the atmospheric stability class (Collett and Oduyemi, 1997). The latter parameter is determined by wind speed and, depending on the time of day, amount of cloud cover or solar radiation levels (Benson, 1992; Nagendra and Khare, 2002). The contribution from motor vehicles towards pollutant levels at a receptor is computed as the sum of contributions from road segments upwind of the receptor.

Pollutants such as CO and PM_{10} are generally considered to be inert in the model. Meanwhile, concentrations of nitrogen oxides (NO_x) at receptors are computed from vehicle emission factor of NO_x and background levels of ozone (O_3). In some studies, NO_x is considered as a single, inert pollutant (Gidhagen et al., 2004; Kenty et al., 2007). Model input may allow separate vehicle emission factors for different fuel and vehicle classes—passenger car, goods vehicles, buses, etc.

Models employing computational fluid dynamics (CFD) methods are often applied to simulate air quality within street canyons and the neighbourhood of traffic intersections (Gidhagen et al., 2004; Di Sabatino et al., 2008). Such models are based upon the numerical solution of mass-conservation equations, momentum-conservation equations, and transport equations (Vardoulakis et al., 2003). Turbulence within the model area is generally governed by Reynolds Averaged Napier-Stokes (RANS) equations (Vardoulakis et al., 2003; Baik et al., 2007). While CFD is generally applied to simulate dispersion of inert pollutants, reactions between pollutants, such as that between NO, NO_2, and O_3, can be incorporated into the model by introducing equations governing such reactions to the model (Vardoulakis et al., 2003; Baik et al., 2007).

A grid that replicates the model domain is set up. The grip is comprised of cells of varying size, with cells of smaller dimensions located in regions closer to the road surface and boundary regions (Vardoulakis et al., 2003). Models employing CFD

methods are capable of modelling dispersion of vehicle emission within a complex domain. The model domain should be sufficiently large that incoming and outgoing air flows are stable. Initial wind speed and temperature, and boundary (reflectiveness of walls and road surface, dissipation rate) conditions are defined (Baik et al., 2007). Contribution of gaseous pollutants and particulate matter from vehicles is computed from emission factors and traffic volume. Background concentrations of inert pollutants are generally assumed to be zero. Incoming wind conditions are assumed to be constant throughout the domain being modelled (Baik et al., 2007; Di Sabatino et al., 2008). Traffic movement can be simulated by considering cells near the road surface as a moving plane or by fixing cells representing the road surface and moving cells representing walls and buildings (Gidhagen et al., 2004).

Beginning with an initial approximation of flow within the domain, the model estimates the numerical solution to the governing equations iteratively until a solution, whose residual for each equation is within a predetermined threshold, to the equations is reached. The effect changes in wind direction and emission factor has air quality at various points within the model domain can be illustrated by incorporating different input to the model (Gidhagen et al., 2004). Concentrations of gaseous pollutants and particulate matter at various spots within the study area can be observed. Background concentrations are added to simulated results to facilitate comparison between model and measured concentration values (Gidhagen et al., 2004).

The results derived from the models are compared with measurements from selected sites within the test area and the effectiveness of the models are evaluated by performance benchmarks such as correlation, mean square error, and the “factor-of-two” envelope, which measures the percentage of model-predicted concentration values that

are between 50% and 200% of the measured values (Yura et al., 2007).

As discussed in a previous section, models can be used to estimate gaseous and particle emission factors of a vehicle fleet. Instead of computing air quality in the vicinity of a roadway, the roadside and background air quality measurements, along with meteorological and traffic measurements, are entered to the model to compute vehicle emission factors.

2.8 Urban Air Quality Monitoring

The ambient air quality measurements used for model simulations are often collected at permanent air quality monitoring sites in the urban area. Measurements at the stations are assumed to be reflective of the general urban air quality. A number of studies have been carried out to identify the pollution sources in the neighbourhood of the station and to determine whether measurements obtained from the monitoring stations reflect air quality of the surrounding area.

In many cities, permanent monitoring stations are often placed within areas where gaseous and particulate pollutants originate from one major emission source, or emission hotspots (Kukkonen et al., 2001). To monitor air quality at the roadside, a monitoring station is constructed a short distance away from a major roadway. Continuous monitoring generally takes place at a height close to street level (1.5-5 metres) to monitor air quality the population is exposed to at street level. Air quality measurements at background monitoring stations in the urban area should reflect urban air quality in general and be influenced by the integrated contribution from all sources upwind of each station. Thus such stations should be located at sites where there is sufficient distance between the site and major emission sources so that air quality at the

stations is not strongly affected by a single emission source.

Permanent background air quality monitoring stations are generally selected based on the following criteria: the highest pollutant concentration within the urban area, air quality the general population within the urban area is exposed to, the amount of obstructive objects (hills, tall buildings) in the surrounding area, the site's proximity to a busy roadway and other major emission sources, and prevailing wind direction at the site (USEPA, 1998; EU, 2005). The most common settings selected for monitoring of urban background air quality are rooftop and parks (Harrison et al., 2004; Gramsch et al., 2006; Johansson et al., 2007). Rooftop level is considered as a suitable location for monitoring urban background air quality as there tends to be few obstructive objects and major emission sources in the immediate surroundings of the site. Since vehicle emission generally has little effect on air quality within parks, background monitoring stations may also be placed within parks (Kuttler and Strassburger, 1999).

Many cities and countries set short- and long-term air quality objectives on acceptable concentration levels of pollutants (Gramsch et al., 2006; Wang and Lu, 2006). Based on observations made at monitoring stations, advisories and warnings are issued when concentration of one or more pollutants exceeds these objectives. Measurements collected over the long term may be used to investigate the relationship between population exposure to air pollutants and the incidence rate of diseases (Chang et al., 2005; Namdeo and Bell, 2005).

In many cities, measures aimed to improve roadside air quality—restriction of vehicle operation on certain days, congestion charging programs, removal of vehicles not abiding to emission standards from the vehicle fleet—are introduced based on trends observed from measurements at urban air quality monitoring stations (Mediavilla-

Sahagún and ApSimon, 2003; Nurrohim and Sakugawa, 2005). Once implemented, the effectiveness of specific measures can be evaluated by comparing air quality at monitoring stations before and after the enactment of such measures (Lee et al., 2005; Carslaw et al., 2006).

In many cities, studies examining whether measurements at monitoring stations accurately reflect general air quality within the urban area are carried out periodically. Review of the air quality monitoring network often involves examination of variations in air quality at individual stations. Monitoring stations whose observations can be reproduced by measurements at other stations are identified (Gramsch et al., 2006). Such stations may be closed and stations are set up in areas where pollution level is high and air quality is yet to be monitored instead. The location of individual stations may be investigated to determine whether measurements at the station are representative of air quality of the surrounding area (Vardoulakis et al., 2005).

2.9 Vehicle Emission and its effect on Urban Air Quality

The variation in air quality within an urban street canyon can be examined by monitoring air quality measurements at various heights between street and rooftop levels (Monn et al., 1997; Wu et al., 2002; Xie et al., 2003). Generally monitoring takes place at opposite sides of a street canyon where building height on both sides are similar. Wind speed and direction measurements are collected at the rooftop level on one side of the street canyon. Traffic volume is measured by manual counting or collected from local transportation authorities. This way the effect of traffic volume and wind direction have on air quality at various points within the street canyon can be examined. Temporal variations in air quality at various heights on the windward side of the canyon often are similar to those found at street level while the correlation between temporal variations

in air quality at street level and sites at the leeward side of the canyon is weaker. Concentrations of gaseous and particulate pollutants tend to be higher on the leeward side of a roadway compared to the windward side, due to wind carrying vehicle emissions from street level towards the leeward side of the canyon (Xie et al., 2003). When wind speed is low, concentrations of gaseous pollutants and particulate matter tend to be higher due to accumulation of vehicle emissions.

Air quality can also be monitored at various spots within a small region, generally a street canyon, to study the spatial variability of air quality within the area. Monitoring takes place at multiple locations along a busy roadway. Background air quality is monitored at a site located a short distance away from the study area. From such studies it is often found that, within a street canyon where there are large variations in building height, concentrations of gaseous pollutants within the canyon can vary greatly (Vardoulakis et al., 2005). This indicates that large variations in meteorological conditions may be observed at different parts of the canyon.

The general aim of such measurement campaigns is to investigate the dispersion of vehicle emissions within a street canyon. The methods adopted for these campaigns have been applied to examine air quality at monitoring sites where building configuration is less condensed (Harrison et al., 2004). This indicates that such measurement set-up can be considered for investigation of vehicle emission's effect on air quality at monitoring stations with different surroundings, particularly in terms of building height and configuration.

Urban air quality can be investigated through examination of air quality measurements at permanent roadside, urban background, and rural monitoring stations. The difference between roadside and urban background air quality measurements is often considered to

be the contribution of vehicle emissions towards gaseous and particulate pollutants in the urban area (Peace et al., 2004). The level of contribution vehicle emissions have on major pollutants within the urban atmosphere can be obtained by comparing air quality at roadside and background monitoring stations located in close proximity. The contribution of major air pollutants from motor vehicles can be determined by studying the ratio between air quality measurements at roadside and background monitoring stations (Pandey et al., 2008). A large ratio between average roadside and background air quality measurement values indicates that there is a great amount of vehicle emissions in the area near the roadside station while a low ratio can be considered as an indicator of a lack of vehicular activity.

The difference and ratio between pollutant levels at roadside and background sites can be considered indicators of ventilation effectiveness within the area—an area is considered to be well ventilated if the ratio between roadside and background pollutant concentrations within the area remain relatively constant at various concentration levels; a generally constant difference in pollutant concentrations between roadside and background measurements may be an indication that the ventilation within the area is poor, which can hinder dispersion of emissions such as those from motor vehicles (Harrison et al., 2004).

In the study of the vehicle emission's impact on urban air quality, a site in close proximity to the roadside measurement site is frequently selected as a background measurement site as mountains and valleys can strongly affect air quality measurements at different parts of a city (Pires et al., 2008). Having roadside and urban background stations located in close proximity may also be motivated by observations showing that large variations in meteorological conditions such as wind speed and direction can often

be observed in different districts within a city (Gramsch et al., 2006).

Urban background air quality is often influenced by more than one emission source. Thus the difference between roadside and background air quality may not fully reflect vehicle emission's contribution of gaseous and particulate pollutants. Comparison of daily variations in roadside and background air quality and statistical methods such as PCA and CA have been applied to identify the level of impact various emission sources have on background air quality within a city.

2.10 Analysis of Air Quality Time Series

Since air quality measurements at monitoring stations are generally collected at uniform intervals, such measurements can be considered as a time series. A number of methods are developed to investigate the relationship between air quality time series and those of traffic and meteorological conditions. Analysis of the correlation between air quality measurements collected at different times can also be carried out.

Regression analysis is frequently applied to model urban air quality time series. Time series of gaseous and particulate concentrations, traffic volume, wind speed, and temperature are collected at monitoring sites. An equation expressing the relationship between concentrations of one pollutant and traffic volume, meteorological conditions is derived by the least-squares method (Prybutok et al., 2000; Sousa et al., 2006). Regression analysis can also be applied to examine the relationship between concentrations of different pollutants at a monitoring site (Sousa et al., 2006).

Modelling of air quality time series can also be carried out using the autoregressive integrated moving average (ARIMA) model (Prybutok et al., 2000; Slini et al., 2002;

Dueñas et al., 2005). The model considers air quality measurements at one moment a weighted sum of measured values and residuals at earlier times. The model computes an initial solution. A new solution is derived until there is little difference between the residual sums of squares of the current solution and the previous one (Chatfield et al., 1996).

Since many air quality time series follow periodic patterns (Pandey et al., 2008; Pires et al., 2008), periodic effects can be incorporated into an ARIMA model, or a seasonal ARIMA (SARIMA) model. A SARIMA $(p,d,q)(P,D,Q)_s$ model can be expressed as follows:

$$w_t = \sum_{i=1}^{p} \phi_i w_{t-i} + \sum_{j=1}^{P} \Phi_j w_{t-sj} - \sum_{i=1}^{p}\sum_{j=1}^{P} \phi_i \Phi_j w_{t-i-sj} + \sum_{k=0}^{q}\sum_{l=0}^{Q} \theta_k \Theta_l z_{t-k-sl} \quad (2.14)$$

where w_t is the differenced series at time t; d and D are the order of ordinary and seasonal differencing respectively; φ_i, Φ_j, θ_k, Θ_l are the regular and seasonal autogressive and regular and seasonal moving average terms respectively; z_t is the residual term; and s is the length of the seasonal periodic component. θ_0 and Θ_0 are defined to be 1 (Chatfield, 1996).

The parameters of the SARIMA model are determined by examination of autocorrelation functions. If autocorrelation of the series converges to zero rapidly no differencing is needed. Differencing is performed by subtracting each value from another in some time-dependent order. For example, if d=1, a new series is derived by subtracting each measurement by the measurement immediately preceding it. While repeated differencing can be applied, d and D generally have values of 0 or 1 when the SARIMA model is applied to simulate air quality (Slini et al., 2002; Dueñas et al., 2005). The parameters p and q are determined from the autocorrelation and partial

autocorrelation functions respectively. This is done by identifying the time lag beyond which a function converges to zero rapidly. *P* and *Q* are determined in a similar manner by examining values at lags that are multiple of *s* (Chatfield, 1996).

Air quality time series can also be modelled with neural networks (Prybutok et al., 2000; Sousa et al., 2006). A network consists of an input layer, a single or multiple hidden layers, and an output layer. Each layer consists of a number of nodes. A single hidden layer is generally sufficient to model air quality (Nagendra and Khare, 2004; Sousa et al., 2006). Data are entered to the input layer, where each node corresponds to one input variable, and the network transfers the data to subsequent layers using a series of equations. Input data (air quality, traffic, and meteorological measurements) is partitioned into a training set and a validation set. For each node, a weighted sum of values of nodes within the previous layer is computed. An output is generated by applying a transfer function to the weighted sum (Prybutok et al., 2000). The output values are compared with the corresponding measurement values. The training set data is entered to the network to establish the weights for each node. The aim is to arrive at a network that minimizes the mean square error of the output (Nagendra and Khare, 2004; Sousa et al., 2006). The validation set is then applied to the network to examine the performance of the network and to prevent over-fitting. The best network is generally one that yields the lowest mean square error from the validation dataset (Lu and Chang, 2005; Sousa et al., 2006).

It has been shown that air quality measurements taken a long time apart can remain highly correlated (Varotsos et al., 2005; Weng et al., 2008). A time series with such a property is said to possess the long-memory property (Windsor and Toumi, 2001). In other words, the series is persistent or trend-reinforcing. A number of methods are developed to determine whether a time series possesses the long-memory property.

One way to identify whether a time series is a long-memory process is the ST method (Windsor and Toumi, 2001). The series is divided into non-overlapping sub-series of equal length. For each length T ($T \geq 2$), the means of a sufficient number of sub-series are computed. The standard deviation of the sub-series means, denoted S or $\sigma(T)$, is then computed as follows:

$$\sigma(T) = \sqrt{\sum_{i=1}^{N} (C_i(T) - C)^2 / N} \quad (2.15)$$

where $C_i(T)$ is the mean of sub-series i, C is the series mean, and N is the number of sub- series, with N being 5 or greater (Windsor and Toumi, 2001). The logarithm of sub-series lengths, T, is then plotted against the logarithm of $\sigma(T)$ (Beran, 1994). For a short-memory time series, where autocorrelation converges to zero rapidly, the fitted line has a slope of approximately -0.5; for a long-memory process, the slope of the fitted line is between -0.5 and 0. A slope closer to 0 indicates a stronger persistence (Beran, 1994; Windsor and Toumi, 2001).

A long-memory process can also be identified using the rescaled range method (Weng et al., 2008). Similar to the ST method, the series is dividing into non-overlapping sub-series of length T ($T \geq 2$). The mean for each sub-series is computed. A rescaled series is derived by subtracting each measurement by the mean of the sub-series containing the measurement. The range of the rescaled series, R, is defined to the difference between the series' maximum and minimum values. The standard deviation, S, of new series is computed. This same process is repeated for different values of T (Windsor and Toumi, 2001; Weng et al., 2008). The relationship between R/S and T can be expressed in the following:

$$\frac{R}{S} = (cT)^H \quad (2.16)$$

for some constant *c*. A time series is considered a short-memory if *H*=0.5; mean-reverting if 0<*H*<0.5 and a long-memory process if *H*>0.5 (Windsor and Toumi, 2001; Weng et al., 2008).

In some time series, long-memory and seasonal fluctuations are both present (Varotsos et al., 2005). Seasonal pattern of a time series is removed before examination of long-memory property is carried out. In the case of a season being 24 hours long (daily cycle), this can be achieved by subtracting each hourly value by the mean of the observations for that hour of the day (Windsor and Toumi, 2001).

2.11 Application of Measurement and Analytical Methods

As shown in Table 2.2, a wide discrepancy in gaseous and particle emission factors can be observed, even when measurements are collected using similar techniques. The discrepancy can be attributed to differences in traffic composition, fuel content, traffic condition, and background air quality at various measurement sites. In this work, emission factors are derived from two sets of measurements collected in the urban area of Hong Kong. Emission from diesel and LPG light-duty vehicles under a wide range of operating conditions are measured using on-board instruments, which measure emission directly in the tailpipe, to investigate vehicle emissions under urban driving conditions. Emission measurements collected using remote sensing instruments are examined to investigate on-road emissions from different vehicle types and to complement on-board measurements. The emission factors derived from remote sensing measurements reflects fleet emission well because of the large sample size. The emission factors of light-duty

diesel and LPG vehicles derived from the two measurement methods are then compared and the differences between the two sets of emission factors are discussed.

Variations in air quality at roadside and background monitoring stations in Hong Kong are compared to evaluate vehicle emission's effect on background air quality in various parts of the city. Two methods often used for identifying contribution of urban emission sources—principal component analysis (PCA) and cluster analysis (CA)—are applied to determine similarities in variations of air quality at roadside and background stations in Hong Kong. PCA has previous be applied to measurements at two monitoring sites within a street canyon so that vehicle emission's impact on background air quality can be examined (Väkevä et al., 1999). In this work PCA and CA is applied to measurements collected at roadside and background monitoring stations scattered throughout Hong Kong to examine the level of impact vehicle emission has on air quality at background stations in various parts of the city. In particular, vehicle emission's impact on background air quality in the urban and sub-urban areas of Hong Kong, a highly developed city, is investigated by comparing variations in air quality at background stations with those at roadside stations. This is achieved by comparing PC loadings at roadside and background stations and examining CA distance between roadside and background stations. Time series of air quality measurements at urban and rural monitoring stations are examined using the ST method to determine whether such series possess the long-memory property. These results are examined to discuss the effect vehicle emissions, traffic conditions, and a station's surroundings have on air quality at monitoring stations in urban and sub-urban areas.

Chapter 3

On-road Emissions Characteristics of Light-duty Vehicles

3.1 Introduction

As discussed in Chapter 2, emissions of vehicles operating under a variety of driving modes can be measured using the chassis dynamometer measurement system. However, such methods may be less effective in simulating urban driving conditions, such as stop-and-go conditions and abrupt changes in speed. To obtain measurements that are more representative of real-world traffic conditions, study of vehicle emissions using on-board equipment has become more commonplace (El-Shawarby et al., 2005; Gao and Checkel, 2007).

In this chapter, on-road gaseous emissions from light-duty diesel and LPG vehicles adhering to Euro 2, 3 and 4 emission standards are measured using a portable emission measurement system (PEMS). Vehicle speed measurements are collected to facilitate comparison of emissions under different driving conditions. The CO, NO, and HC emission indices, rates, and factors of different taxis and light goods vehicles are examined and compared. The emission characteristics of a range of vehicle operating conditions are investigated.

3.2 Road Test Methodology

3.2.1 Vehicle specifications

Four taxis and four light goods vehicles (LGVs) were selected for measurement of gaseous emissions. These eight vehicles, albeit small in sample size, do have a good

representation of the taxi and LGV fleet available on the roads of Hong Kong. The differences in vehicle age enable the comparison of emissions with different generations of vehicle technology. The general properties of the vehicles are outlined in Table 3.1. The taxis have mostly identical specifications and operate on liquefied petroleum gas (LPG) while the LGVs are fuelled by diesel. Each taxi is equipped with a three-way catalyst while an oxidation catalytic converter is installed to LGV 4.

	Taxi 1	Taxi 2	Taxi 3	Taxi 4
Manufacturer	Toyota			
Model Year	2001	2003	2005	2007
Engine Capacity (cc)	1998			
Vehicle Weight (kg)	1400			
Odometer Reading (km)	1040000	560000	454000	170000
Emission Standard	Euro 2	Euro 2	Euro 3	Euro 4
Engine Power	58 kW @ 4400rpm			
Maximum Torque	160 Nm @ 2400rpm			
Catalytic Converter	Yes	Yes	Yes	Yes

	LGV 1	LGV 2	LGV 3	LGV 4
Manufacturer	Mitsubishi	Isuzu	Mitsubishi	Isuzu
Model Year	2001	2003	2005	2007
Engine Capacity (cc)	3907	4751	3907	5193
Vehicle Weight (kg)	4700	4800	5300	4600
Odometer Reading (km)	147000	276000	113000	30000
Emission Standard	Euro 2	Euro 3	Euro 3	Euro 4
Engine Power	108 kW @ 2900rpm	124 kW @ 2300rpm	105 kW @ 2700rpm	126 kW @ 2400rpm
Maximum Torque	373 Nm @ 1600rpm	530 Nm @ 1600rpm	412 Nm @ 1600rpm	460 Nm @ 1600rpm
Catalytic Converter	No	No	No	Yes

Table 3.1 Properties of test vehicles

The number of vehicles being tested is limited by time and cost constraints. However,

measurements collected from road tests enables investigation of a vehicle's emissions under different conditions.

3.2.2 Measurement instruments and methods

Measurement of exhaust emissions was carried out using a Semtech-DS portable emission measurement system (PEMS). The system contains a non-dispersive infrared sensor, which monitors levels of CO, CO_2, a non-dispersive ultraviolet sensor, which measures concentrations of NO and NO_2, and a flame ionization detector, fuelled by a hydrogen/helium mixture, that measures concentration of THC. A heated sample tube, which connects the test vehicle's exhaust pipe and the PEMS unit, collects a portion of the exhaust for analysis. A vehicle's exhaust passes through a catalytic converter, if one is equipped to a vehicle, before being collected by the sampling tube. The exhaust sample first passes through a filter, heated to 190℃, to prevent condensation of heavy hydrocarbon species present in the exhaust sample. Zero calibration of various analysers takes place shortly before and immediately after each test run by measuring concentrations of various gaseous pollutants in the ambient air for a period of time. Zero calibration is performed to establish the baseline concentration of various gaseous pollutants and to reduce drift in measurements. To maintain the accuracy of road test measurements, zero calibration was performed hourly during road tests. On each day, span calibrations are carried out prior to the first test run and after the completion of the final test run. Audit calibrations are carried out between consecutive test runs. A linearity check of the instruments is carried out approximately once every five weeks to maintain instrument precision. This is done by monitoring concentrations of a number of gas mixtures, a percentage of which consists of pure nitrogen while the rest consists of span gases, and comparing the concentrations as measured by the PEMS with those

computed from values stated on the span gas bottle.

Ambient temperature and relative humidity are monitored using a temperature and humidity sensor connected to the PEMS unit. The exhaust flow volume and temperature is measured using a flow and temperature probe attached to the exhaust pipe. The probe is connected to a SEMTECH exhaust flow meter, which computes flow volume and temperature and transmit the information to the PEMS in real-time. Measurements are recorded to memory card. After the completion of each test run, measurement data collected from the test run are downloaded to a computer. A post-processor converts measurements to second-by-second records and computes the instantaneous air-fuel ratio using the oxygen balance method (Heywood, 1988).

Vehicle speed measurements are collected using a Corrsys-Datron Microstar speed sensor. The sensor measures vehicle speed by releasing radar beams towards the road surface, which would reflect the beams back to the sensor and the vehicle's speed is derived by computing the difference in beam frequency. The error in each speed measurement is less than 1% of the measured value. The data is transmitted to a laptop computer in real time. The interval between consecutive speed measurements is set to 1 second and acceleration is defined as the difference between consecutive speed measurements. The arrangement of the on-board measurement system is outlined in Fig. 3.1.

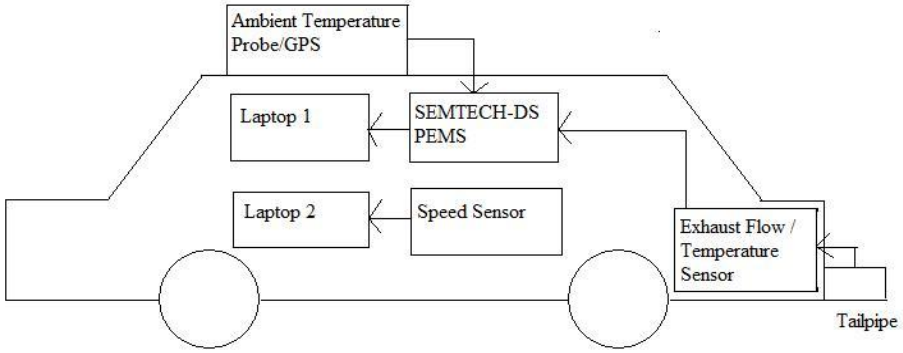

Fig. 3.1 Sketch of on-board measurement system

3.2.3 Road test descriptions

Testing took place between January and May 2009. The test vehicles were operated by professional drivers. Road tests took place within the urban area of Hong Kong. The test vehicles did not follow a fixed route. Instead a test vehicle trailed another vehicle of the same type (taxi or LGV) whenever possible to simulate typical driving patterns of a vehicle of the same type within the urban area of Hong Kong. Testing mainly took place on city streets, where stoppages and changes in vehicle speed due to traffic lights and congestion were frequent. Each test run lasted approximately two hours. 12 test runs were made for each taxi and six test runs were made for each LGV. The temperature on test days ranged between 14 and 30℃.

3.2.4 Data analysis

The collected data has to be collated to rectify the time lags among various data signals. Vehicle emission, exhaust flow rate, and speed measurements of each test are aligned by matching increases in gaseous concentrations and exhaust flow rate with changes in vehicle speed.

The instantaneous emission index of a pollutant, expressed in terms of grams per litre of fuel, is computed as follows:

$$EI_{CO} = \frac{[CO]}{[CO]+[CO_2]+[HC_1]} \cdot \frac{28}{MW_{fuel}} \cdot D_{fuel} \quad (3.1)$$

$$EI_{NO} = \frac{[NO]}{[CO]+[CO_2]+[HC_1]} \cdot \frac{30}{MW_{fuel}} \cdot D_{fuel} \quad (3.2)$$

$$EI_{HC} = \frac{[HC_1]/3}{[CO]+[CO_2]+[HC_1]} \cdot \frac{44}{MW_{fuel}} \cdot D_{fuel} \quad (3.3)$$

where [*P*] is the real-instantaneous concentration of the pollutant *P* in ppm; MW_{fuel} is the molecular weight of the fuel and D_{fuel} is the fuel density. The density and molecular weight per mole of carbon of LPG are 558.6g/L and 14.54g/(mol C) respectively while the density and molecular weight per mole of carbon of diesel are 850g/L and 13.86g/(mol C) respectively (Holmén and Niemeier, 1998; Kean et al., 2001; Ning and Chan, 2007). The molecular weight per mole of carbon is normally used for diesel fuel since the molecular structure of diesel fuel varies. Emission index is adopted in this discussion because the emission index facilitates examination of emission under different fuel consumption levels. High emission indices indicate periods of low fuel consumption, during which lower levels of CO_2 is emitted.

The instantaneous emission rate, expressed in terms of grams per second, is computed from the emission, exhaust flow, and speed measurements as follows:

$$ER_P = [P] \cdot FR \cdot \rho_P \quad (3.4)$$

where *FR* is the exhaust volumetric flow rate in L/s, obtained from the exhaust flow

meter, and ρ_P is the standard density of the gas *P* in g/L. Instantaneous emission factor in terms of g/km can then be computed from the instantaneous emission rate and vehicle speed, *v* in km/h, acquired by the speed sensor, as follows:

$$EF_P = \frac{ER_P}{v} \quad (3.5)$$

The definitions of idle, deceleration, cruising, and acceleration modes are listed in Table 3.2 to compare levels of gaseous emissions under different operating modes. In many on-road emission studies, a low bound ($0.2 m/s^2$) for acceleration mode is considered (André et al., 2006). A bound of $0.1 m/s^2$ is chosen for this work as this definition is frequently adapted for on-road emission studies (Gao and Checkel, 2007; Huo et al,, 2009; Saleh et al., 2009).

Operating Mode	Definition
Idle	$v < 2.5$ km/h and $\|a\| <= 0.1$ m/s^2
Deceleration	$a < -0.1$ m/s^2
Cruising	$v >= 2.5$ km/h and $\|a\| <= 0.1$ m/s^2
Acceleration	$a > 0.1$ m/s^2

Table 3.2 Definition of operating modes (*v* denotes instantaneous speed and *a* denotes instantaneous acceleration)

3.3 Traffic Conditions in the Urban Area

Table 3.3 shows the operating conditions of the eight test vehicles. It shows that the distribution of major operating conditions is generally similar among vehicles of the same type. The table also shows that, under urban driving conditions, taxis undergo frequent acceleration and deceleration. LGVs travel under cruising conditions more frequently, but also spend a majority of the test period undergoing acceleration or deceleration. Vehicles spend approximately 25% of the time in idle mode, indicating that congestions and stoppages due to traffic lights are commonplace in the urban area

of Hong Kong.

The speed distribution of the taxis and LGVs are shown in Fig 3.2. It shows that vehicles travel below 30km/h a majority of the time in urban driving conditions. In general taxis spend a slightly larger percentage of time travelling at speeds of 70km/h or higher compared to LGVs. Test vehicles generally reach such speeds when travelling on urban highways, where traffic is more free-flowing. The amount of time test vehicles spent travelling at various speed reaches up to 60km/h are evenly distributed in general.

	Average speed (km/h)	Idle (%)	Deceleration (%)	Cruise (%)	Acceleration (%)
Taxi 1	29.31	24.76	31.66	9.86	33.72
Taxi 2	27.36	27.17	30.68	9.16	32.98
Taxi 3	26.20	28.12	29.84	9.18	32.85
Taxi 4	26.94	25.53	31.64	9.50	33.33
LGV 1	23.24	27.25	27.48	15.34	29.94
LGV 2	29.61	21.21	33.08	13.41	32.20
LGV 3	25.43	27.85	29.12	11.38	31.65
LGV 4	29.04	25.74	31.99	10.23	32.04

Table 3.3 Vehicle speed and operating conditions of taxis and LGVs

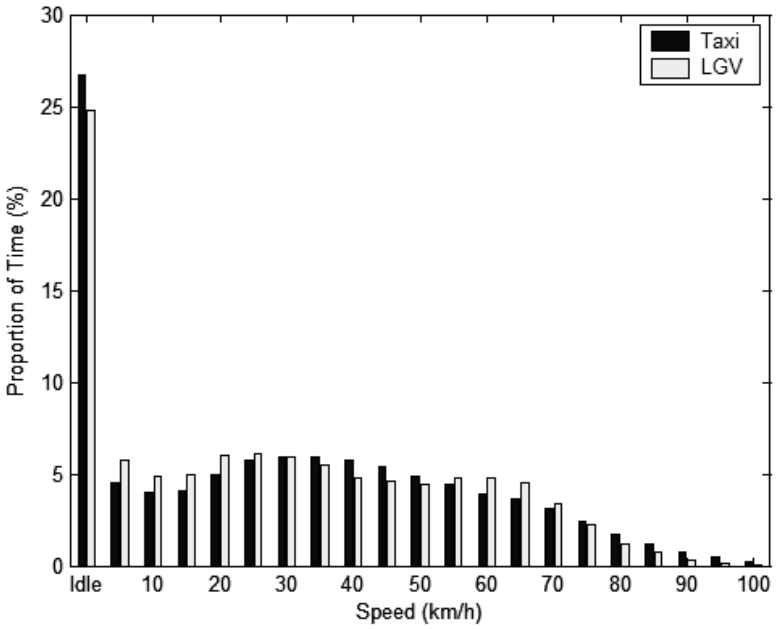

Fig. 3.2 Speed distribution of test taxis and LGVs

3.4 Emission Characteristics of LPG taxis

The average trip emission factors of the four taxis are shown in Table 3.4a. The emission factors of a trip are obtained by dividing a vehicle's cumulative emissions over a test run by the total distance travelled. The table shows that taxi 1 has the highest NO emission factor while taxi 4 has the lowest. CO and HC emission factors of taxi 3, a vehicle that adheres to Euro 3 emission standards, are lower than those of taxis 1 and 2, which are Euro 2 vehicles. The lower emissions from taxi 3 is expected since it adheres to more stringent emission standards, which requires improvements in engine design and additional emission control measures. Meanwhile, CO and HC emission factors of taxi 4, which adheres to Euro 4 emission standards, are extra-ordinarily high. The high CO and HC emissions of taxi 4 will be further explored later.

The emission factors of taxis 1, 2, and 4 are significantly higher compared to the specified emission standards (Table 3.4b). For taxis 1 and 2, the discrepancy is likely

due to the high vehicle mileage travelled, and thus engine and vehicle deterioration. In addition, taxis in Hong Kong often run on road for 24 hours daily and consequently maintenance is poor. These factors can lead to engine deterioration and increased emission. On-road emission of taxi 3 is closer to the emission standards compared to other taxis, indicating the deterioration of taxi 3 has not been to the same extent of taxi 1 and 2.

a)	CO (g/km)	NO (g/km)	HC (g/km)
Taxi 1	9.10±0.56	2.13±0.06	1.19±0.06
Taxi 2	5.65±0.14	1.25±0.04	0.77±0.05
Taxi 3	1.98±0.24	0.30±0.02	0.24±0.04
Taxi 4	9.33±0.75	0.26±0.01	0.81±0.14

b)	CO (g/km)	NO (g/km)	HC (g/km)
Euro 2	2.20	0.29	0.21
Euro 3	2.30	0.20	0.15
Euro 4	1.00	0.10	0.08

Table 3.4 a) Trip emission factors of taxis and b) Euro 2-4 emission standards for LPG vehicles

3.4.1 Influence of vehicle speed on emissions

To examine the relationship between vehicle speed and instantaneous emission, on-road emission measurements are grouped according to instantaneous vehicle speed and acceleration. In the following, emission measurements are classified by instantaneous speed in 5 km/h increments.

The relationship between instantaneous speed and emission indices of taxis, derived from Eqs. 3.1 to 3.3 are shown in Fig. 3.3. CO emission indices of taxis 1-3 are lower at idle mode. CO emission indices of these vehicles decrease gradually as vehicle speed increases. Meanwhile, CO emission index of taxi 4 follows a different trend—at idle

and low speeds, CO emission index of this taxi is much higher than those of other taxis. CO emission index of taxi 4 declines rapidly as vehicle speed increases—CO emission index of taxi 4 at 80km/h is 96% lower than the emission index at 10km/h, compared to a reduction of 13-70% for taxis 1-3. At speeds of 70km/h or higher, taxis 3 and 4 have similar CO emission indices.

Fig. 3.3 shows that NO emission index increases as vehicle speed increases, particularly at low vehicle speed. This increase is more prominent for taxis 1 and 2. At various speeds, the NO emission indices of taxis 1 and 2 vehicles are higher than those of taxis 3 and 4. HC emission indices are the highest when the vehicle speed is between 10 and 20 km/h and decreases at high vehicle speeds. Meanwhile, HC emission index of taxi 4 are high at low speed and declines rapidly as speed increases. As speed increases, HC emission indices of the other taxis also decrease, but the reduction is smaller compared to taxi 4—HC emission indices of taxis 1-3 at 80km/h are 37-69% lower than the emission index at 10km/h, compared to a reduction of 94% for taxi 4.

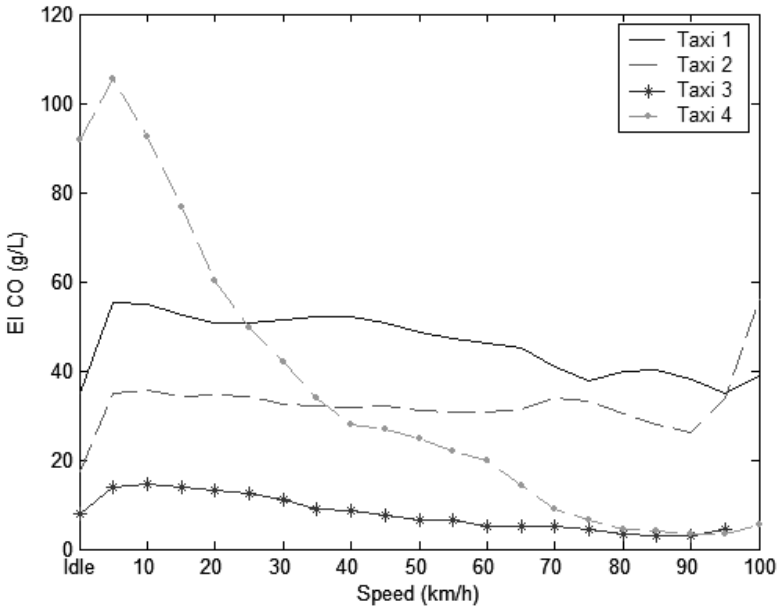
Taxi 1
Taxi 2
Taxi 3
Taxi 4
EI CO (g/L)
Idle
Speed (km/h)

a)

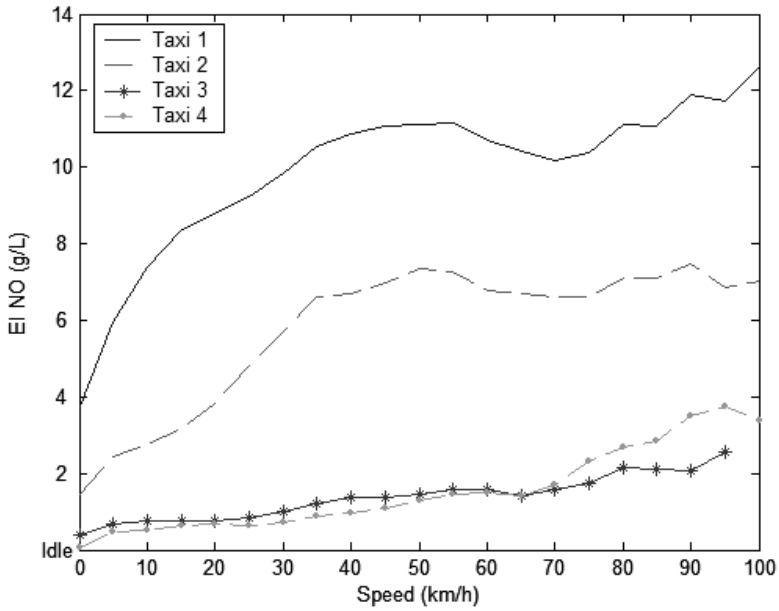
Taxi 1
Taxi 2
Taxi 3
Taxi 4
EI NO (g/L)
Idle
Speed (km/h)

b)

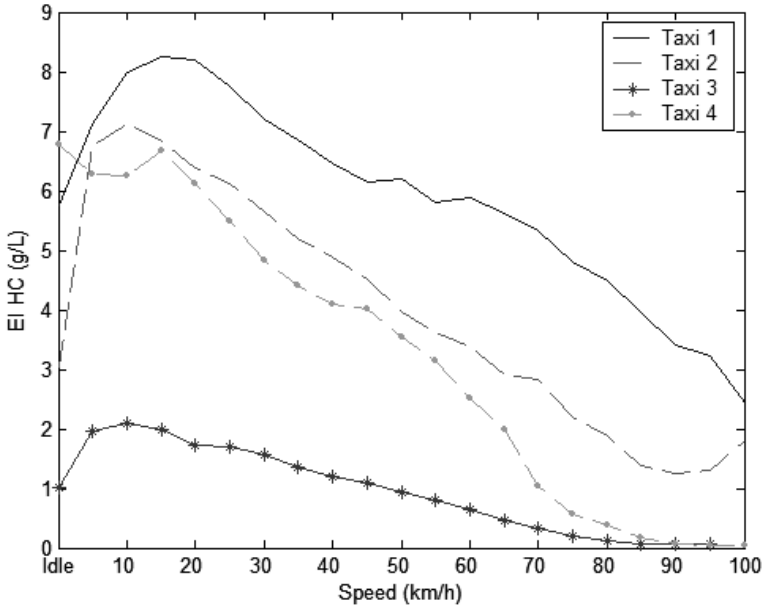

c)

Fig. 3.3 a) CO, b) NO, and c) HC emission indices of taxis

The CO, NO, and HC emission rates, computed using Eq. 3.4, for the four taxis are shown in Fig 3.4. The figure shows that, at various speeds, taxi 1 has the highest NO emission rate while taxis 3 and 4 have the lowest NO emission rate. The lowest NO emission of the four taxis can be observed when a vehicle is idling and emission rates increase as vehicle speed increases. CO emission rates of taxis 1 and 2 are also the lowest during idling and increase as vehicle speed increases. Variation between CO emission rates of taxi 3 at different speeds is smaller. In contrast, CO emission rate of taxi 4 is higher when idling and at low speed and decreases as vehicle speed increases.

Among taxis 1-3, taxi 1 has the highest HC emission rates, followed by taxis 2 and 3. Meanwhile, HC emission rate of taxi 4 are similar to those of taxi 2 while travelling at speeds below 60km/h. At higher speeds, CO and HC emission rates of taxi 4 are similar to those of taxi 3, a Euro 3 vehicle.

Comparing Figs. 3.3 and 3.4 shows that gaseous emission indices and rates follow

similar trends in relation to vehicle speed. This suggests that the two emission indicators reflect a vehicle's emission under different fuel consumption levels.

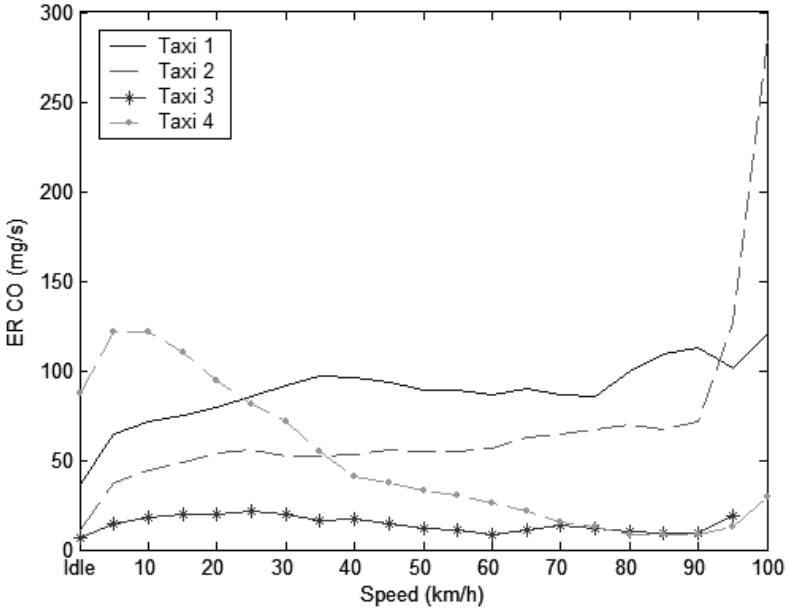

a)

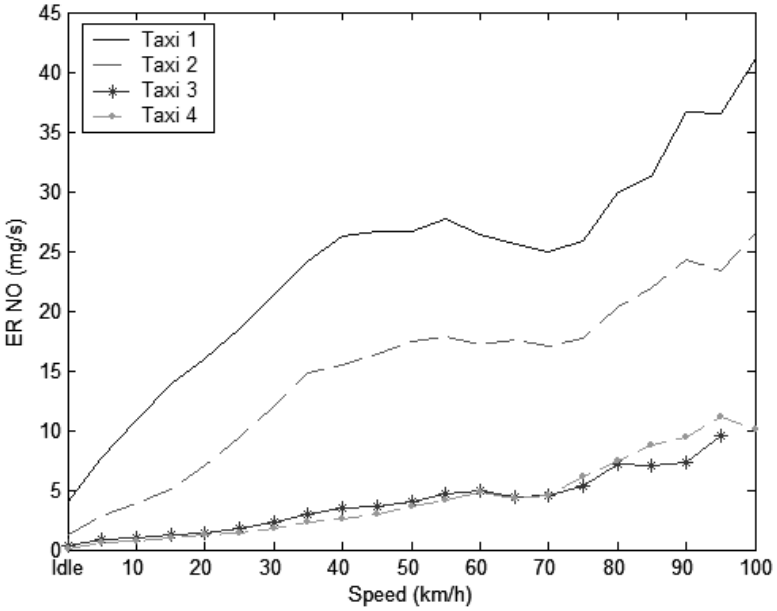

b)

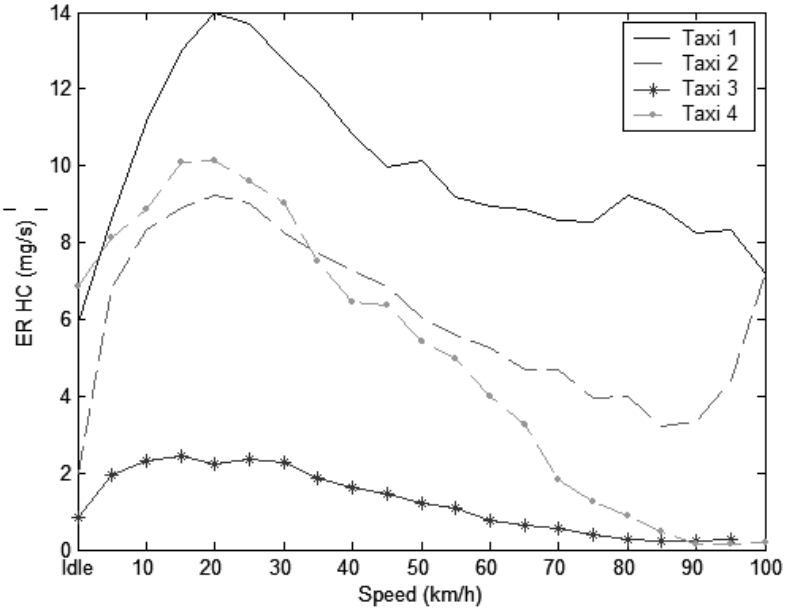

c)

Fig. 3.4 a) CO, b) NO, and c) HC emission rates of taxis

The CO, NO, and HC emission factors, computed using Eq. 3.5, for the four taxis are shown in Fig. 3.5. The figure shows that NO emission factors of taxis generally decreases as vehicle speed increases—NO emission factors of taxis 1 and 2 at 80km/h are 35% and 66% lower compared to the emission factors at 10km/h respectively. The decrease is less noticeable for taxis 3 and 4. CO and HC emission factors of taxis 1-3 also decrease as vehicle speed increases—CO and HC emission factors of each vehicle at 80km/h are 81-93% and 90-98% lower than the respective emission factors at 10km/h. HC emission factors of taxi 4 are similar to those of taxis 1 and 2 when travelling at speeds of under 60km/h. Taxi 4 has the highest CO emission factors when vehicle speed is below 20km/h. At speed exceeding 80km/h, CO and HC emission factors of taxi 4 are similar to those of taxi 3.

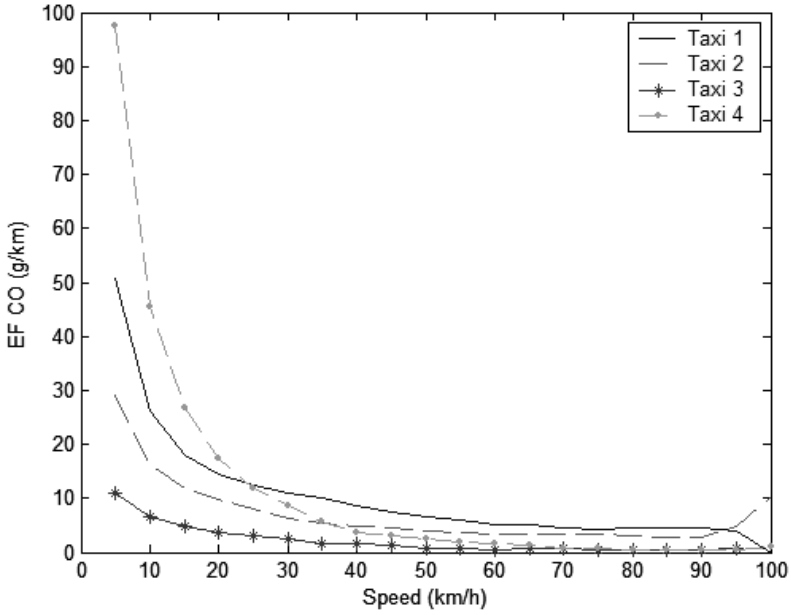
Taxi 1
Taxi 2
Taxi 3
Taxi 4
EF CO (g/km)
Speed (km/h)
0
10
20
30
40
50
60
70
80
90
100

a)

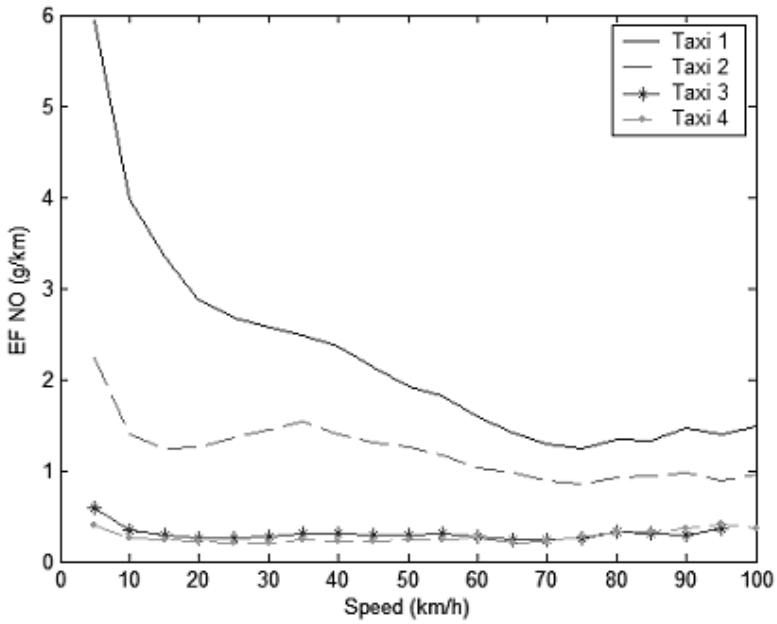
Taxi 1
Taxi 2
Taxi 3
Taxi 4
EF NO (g/km)
Speed (km/h)
0
1
2
3
4
5
6
10
20
30
40
50
60
70
80
90
100

b)

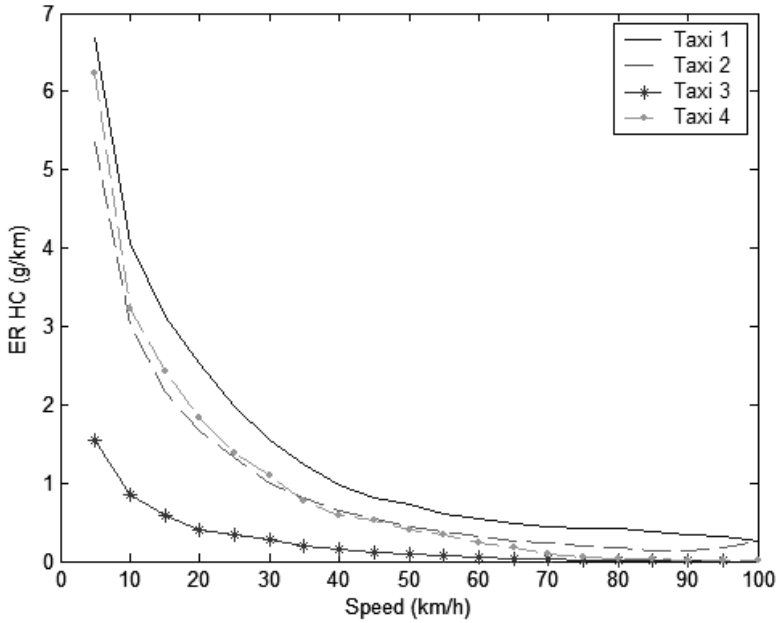

c)

Fig. 3.5 a) CO, b) NO, and c) HC emission factors of taxis

3.4.2 Effect of acceleration on emissions

To examine the effect of vehicle acceleration on vehicle emissions, emission rates of the four taxis under idling, acceleration, cruising, and deceleration modes, defined in Table 3.2, are listed in Table 3.5. For each vehicle, the emission rate of each mode is computed by taking the average of the instantaneous emission rates while the vehicle operates under that particular mode. The table shows that gaseous emission from taxis 1-3 are the lowest when the vehicle is in idle mode. Taxis 1-3 generally emit less CO and NO when decelerating compared to when operating under cruising or accelerating modes. Taxi 4 emits the lowest amount of NO and the highest amounts of CO and HC while idling. All four taxis emit less HC while travelling under cruising mode than acceleration or deceleration modes.

Flow Rate (L/s)	Idle	Deceleration	Cruising	Acceleration
Taxi 1	8.57±0.01	9.72±0.02	14.25±0.06	20.69±0.04
Taxi 2	7.17±0.01	9.77±0.02	14.71±0.07	19.63±0.04
Taxi 3	7.13±0.01	9.04±0.02	13.75±0.06	19.24±0.03
Taxi 4	8.02±0.01	9.38±0.02	13.83±0.06	19.22±0.04
CO (mg/s)				
Taxi 1	35.90±0.22	67.95±0.25	73.96±0.60	107.29±0.47
Taxi 2	10.75±0.09	43.39±0.23	57.31±0.96	63.06±0.38
Taxi 3	6.36±0.08	12.20±0.11	11.36±0.31	20.31±0.23
Taxi 4	87.42±0.40	58.40±0.30	42.53±0.49	67.81±0.41
NO (mg/s)				
Taxi 1	4.02±0.014	9.86±0.04	19.73±0.14	32.91±0.10
Taxi 2	1.19±0.006	5.69±0.04	12.08±0.12	18.86±0.08
Taxi 3	0.38±0.005	1.07±0.02	2.83±0.06	4.67±0.04
Taxi 4	0.09±0.004	0.99±0.02	3.07±0.05	4.48±0.08
HC (mg/s)				
Taxi 1	5.93±0.06	8.56±0.04	8.46±0.09	13.34±0.08
Taxi 2	1.99±0.03	7.23±0.04	5.91±0.06	6.96±0.04
Taxi 3	0.85±0.02	1.84±0.02	1.12±0.02	1.61±0.02
Taxi 4	6.87±0.10	5.64±0.08	4.71±0.16	8.10±0.15

Table 3.5 Exhaust flow and gaseous emission rates of taxis under various operating modes

From Table 3.5 it can be observed that taxis 1-3 generally have the lowest gaseous emissions at idle and emit the highest amount of gaseous pollutants while accelerating. This may be due to that, as shown in Table 3.5, the exhaust flow rate of vehicles are the lowest at idle while higher exhaust flow rate are observed during acceleration (Ko and Cho, 2006). A vehicle's exhaust flow rate depends on the speed and load of the vehicle's engine—the higher the acceleration rate, the higher the engine speed and load (Won et al., 2007). However, engine speed under different modes is not known as such measurements were not collected during on-road tests. Taxi 4, meanwhile, emits higher amounts of CO and HC during idling compared to cruising and deceleration modes. NO emission rates of taxi 4 under different operating modes follow similar patterns as the

other taxis.

In addition to exhaust flow rate, a vehicle's emission is affected by the condition of engine combustion. This is generally reflected by the air-fuel ratio (Li et al., 2008). Fig. 3.6 shows that the highest air-fuel ratio of a taxi is observed when the vehicle is idling, similar to previous results (Silva et al., 2006a). The stoichiometric air-fuel ratio for LPG vehicles is 15.4. At idle the air-fuel ratio as shown in Fig. 3.6 is 17.3. This results in lower CO and HC emissions from vehicles while idling. At idle, NO emission is inherently low due to lower combustion temperature (Ceviz and Yüksel, 2005).

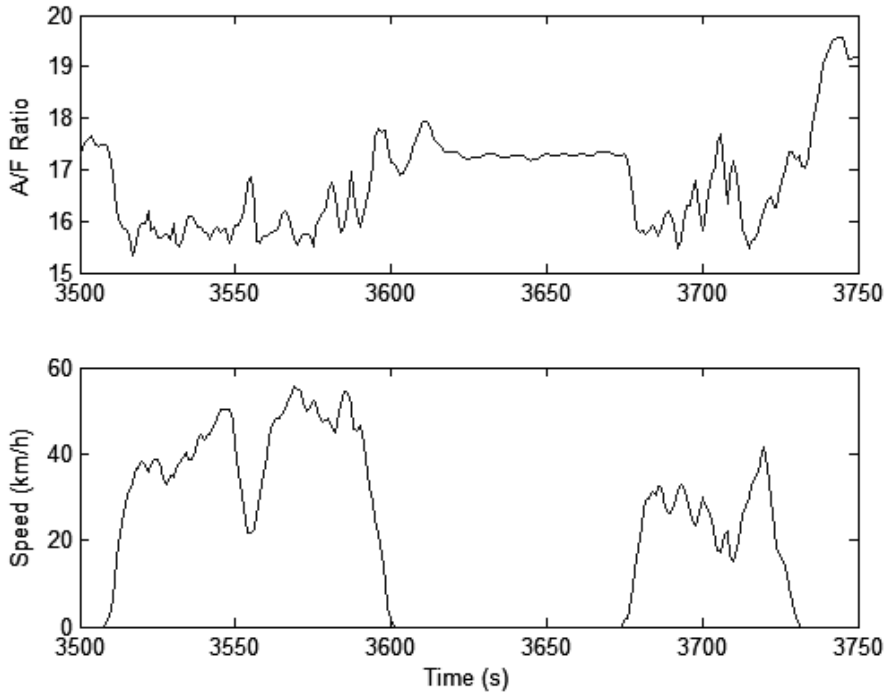

Fig. 3.6 Air-fuel ratio of taxi 3 under various driving modes

Previous studies have shown that that vehicles undergoing hard acceleration emit the highest amounts of CO and HC (El-Shawarby et al., 2005). However, the relationship between acceleration and NO emissions of light-duty vehicles have yielded contradictory results—El-Shawarby et al. (2005) showed that a vehicle undergoing aggressive acceleration has lower NO emissions compared to a vehicle accelerating at a

more moderate rate while Heeb et al. (2006) found that vehicles undergoing hard acceleration have higher NO emissions compared to cruising and decelerating vehicles. To further explore the relationship between acceleration and gaseous emissions of taxis, emissions rates of vehicles travelling at various speed and acceleration rates are plotted. Gaseous emissions rates of taxis 3 and 4 under different speed and acceleration are shown in Fig. 3.7 and 3.8 respectively. The relationship between speed and acceleration and gaseous emission rates of taxis 1 and 2 are similar to those of taxi 3.

Fig. 3.7 shows that, in general, gaseous emissions from taxi 3 are low when the vehicle is decelerating. As acceleration rate increases, gaseous emissions from the vehicle also increase. A large difference in CO and NO emissions of taxi 3 between acceleration and deceleration modes can be found. When the taxi accelerates rapidly (2 m/s^2), its CO and NO emission rates are 11-142 mg/s and 1.6-17.5 mg/s respectively. When the taxi decelerates rapidly (-2 m/s^2), CO and NO emission rates of the vehicle are 2-20 mg/s and 0.5-1.6 mg/s, respectively. Meanwhile, HC emission rate of the taxi is at the highest level when the vehicle undergoes rapid deceleration and the lowest when a vehicle is cruising—the vehicle has a HC emission rate of 0.2-2.1 mg/s while cruising and a HC emission rate of 0.6-3.5 mg/s when undergoing deceleration. This is likely due to vehicles having lower engine loads and higher air-fuel ratios (Fig. 3.6) during deceleration (Kean et al., 2003), which results in higher levels of unburnt fuel and thus higher amounts of HC within the exhaust.

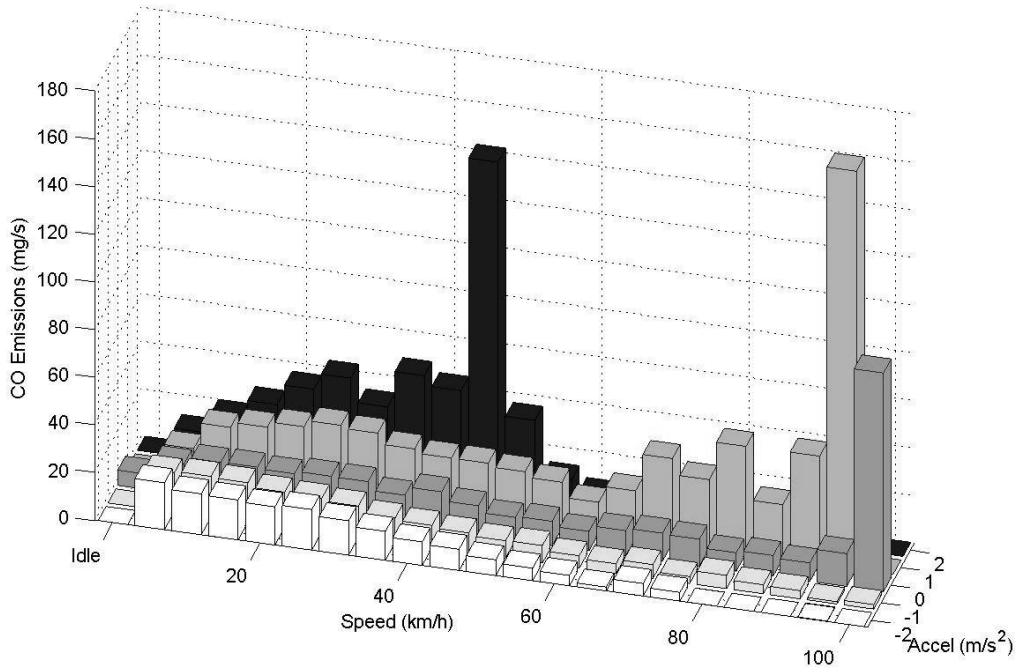
CO Emissions (mg/s)
180
160
140
120
100
80
60
40
20
0
Idle
20
40
60
80
100
Speed (km/h)
2
1
0
-1
-2
Accel (m/s2)

a)

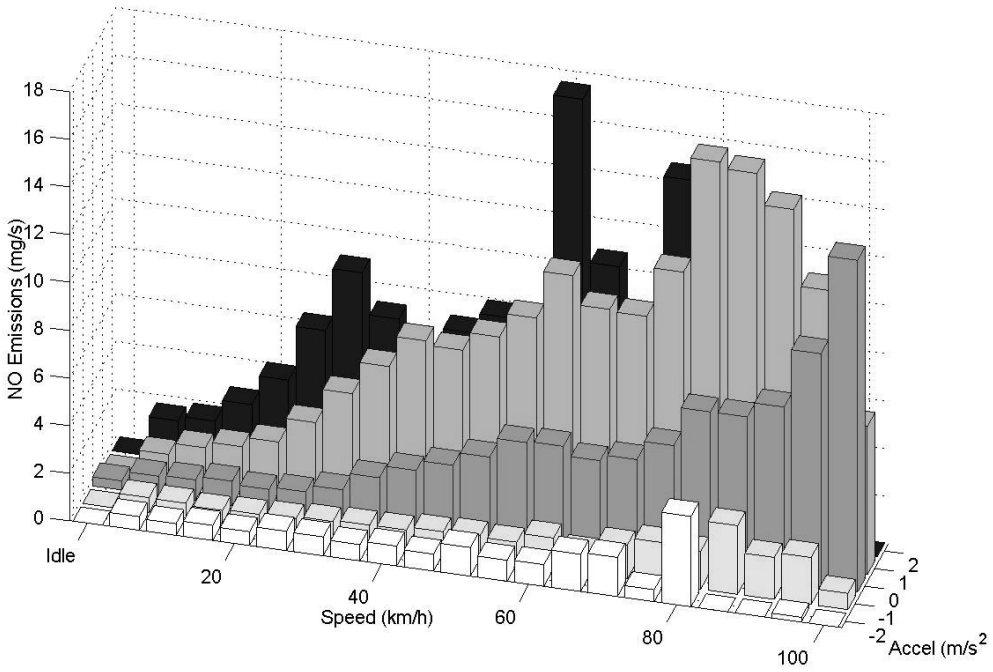
NO Emissions (mg/s)
18
16
14
12
10
8
6
4
2
0
Idle
20
40
60
80
100
Speed (km/h)
2
1
0
-1
-2
Accel (m/s2)

b)

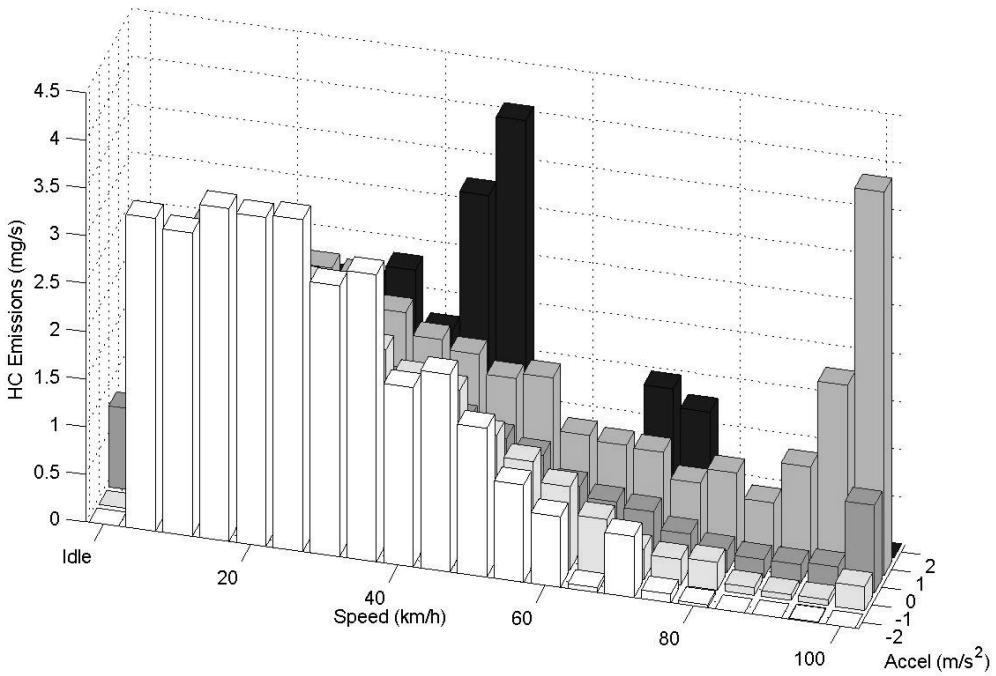

c)

Fig. 3.7 a) CO, b) NO, and c) HC emission rates of taxi 3 under acceleration, cruising, and deceleration modes

As shown in Fig. 3.8, gaseous emissions from taxi 4 while accelerating are higher compared to emissions of the vehicle when it is decelerating. When the vehicle accelerates aggressively (2 m/s^2), it emits 22-167, 0.9-9.6, and 5-33 mg of CO, NO, and HC per second, respectively; when the vehicle undergoes rapid deceleration (-2 m/s^2), the emission rates of CO, NO, and HC are 7-95, 0.2-4.0, and 2-9 mg/s, respectively. Similar to other taxis, HC emission from taxi 4 is the lowest in cruising mode. At various acceleration rates, CO and NO emissions generally are higher when the vehicle travels at a higher speed while HC emissions tend to be the highest when the vehicle is travelling between 30 and 50km/h.

At speeds below 60km/h, CO and HC emissions of taxi 4 under various acceleration rates are vastly higher compared to those of taxi 3. At a given speed and acceleration, NO emissions of taxis 3 and 4 are generally similar.

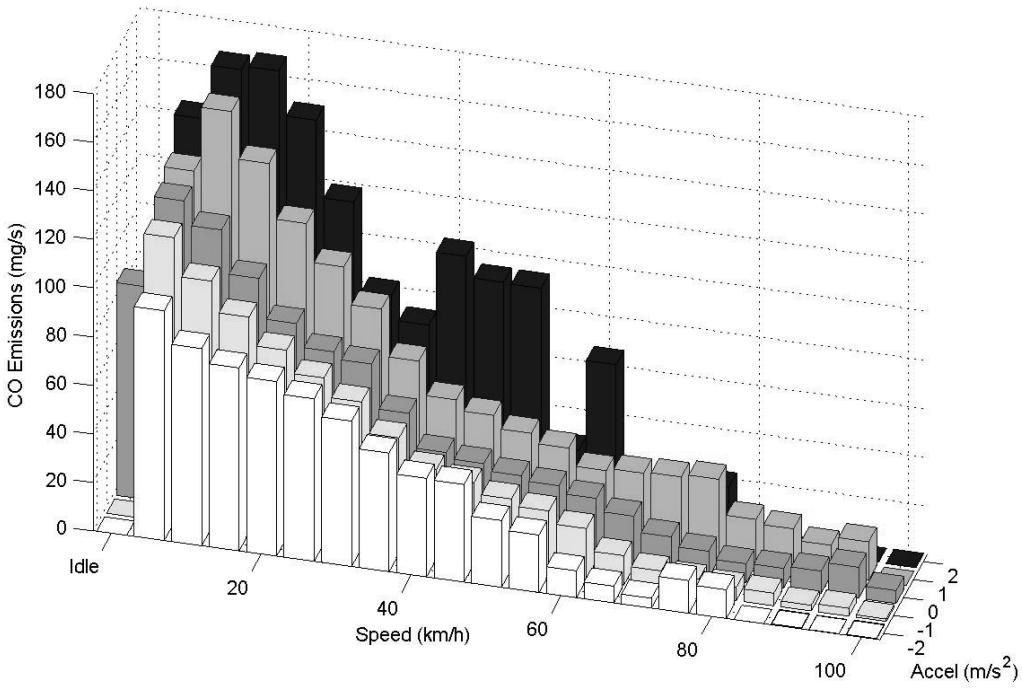
CO Emissions (mg/s)
180
160
140
120
100
80
60
40
20
0
Idle
20
40
60
80
100
Speed (km/h)
2
1
0
-1
-2
Accel (m/s^2)

a)

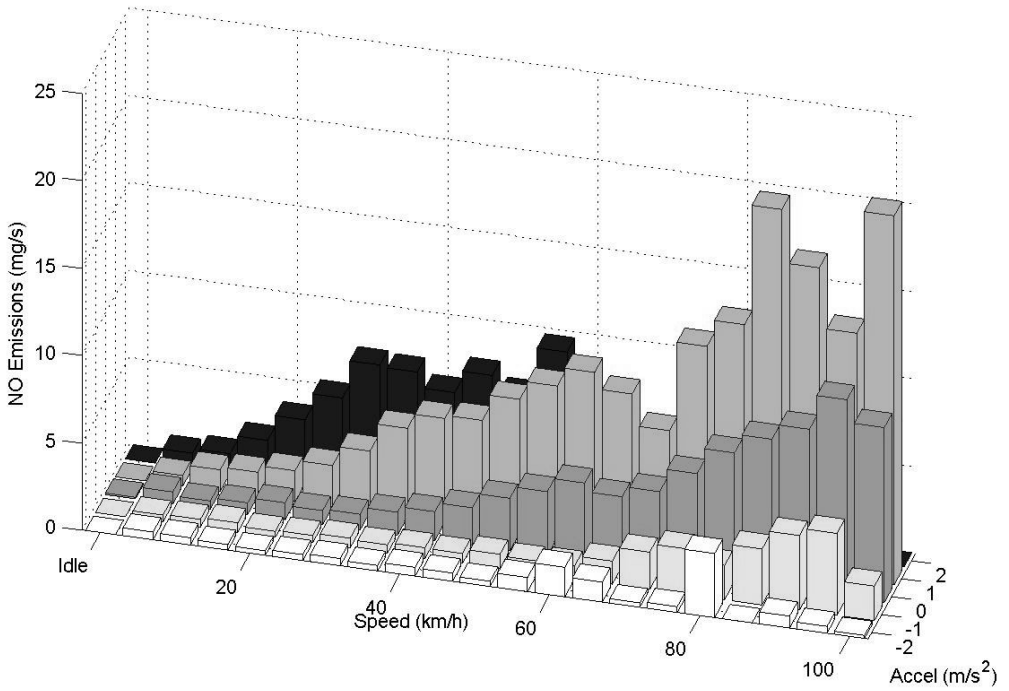
NO Emissions (mg/s)
25
20
15
10
5
0
Idle
20
40
60
80
100
Speed (km/h)
2
1
0
-1
-2
Accel (m/s^2)

b)

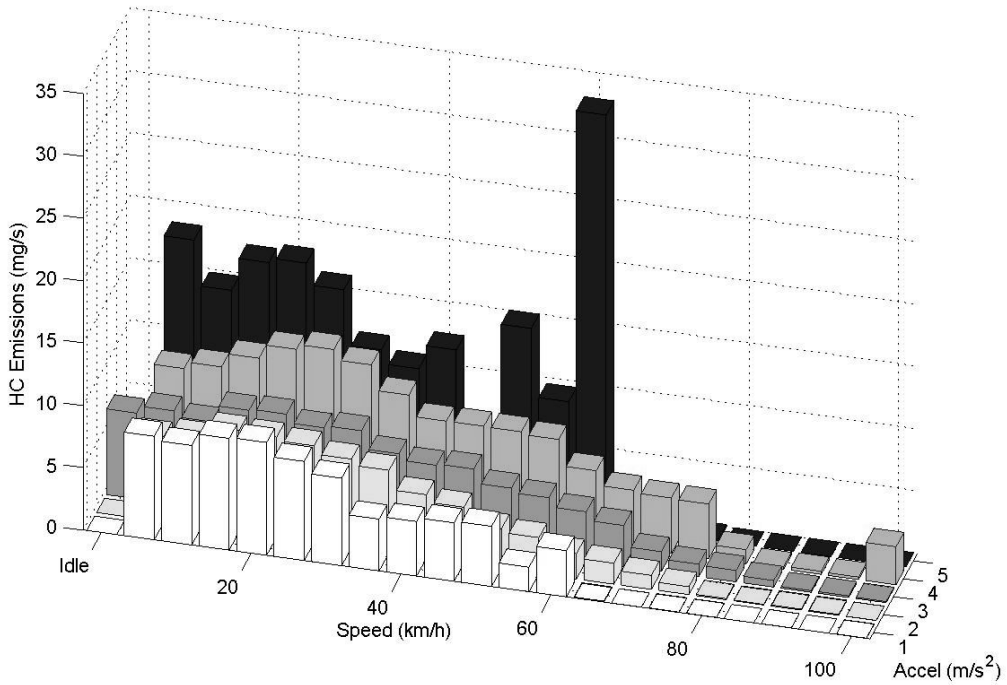

c)

Fig. 3.8 a) CO, b) NO, and c) HC emission rates of taxi 4 under acceleration, cruising, and deceleration modes

Fig. 3.8 shows that CO and HC emissions of taxi 4 at idle and low speeds are extraordinarily high. Meanwhile, CO and HC emissions of the vehicle at higher speeds are similar to those of taxi 3 (Fig. 3.7). Instantaneous gaseous emission rates, air-fuel ratio, and speed of taxis 3 and 4 are shown in Fig. 3.9 to illustrate typical emission characteristics of each taxi while idling. The instantaneous emission and air-fuel ratio profiles for taxis 1 and 2 during idling are mostly similar to those of taxi 3. The figure shows that gaseous emissions of taxi 3 remained stable when the vehicle is in idle mode. Meanwhile, large fluctuations in CO and HC emissions can be observed from taxi 4 when the vehicle operates in idle mode. The figure shows that, during idling, there are little variations in air-fuel ratio of taxi 3 and large variations in air-fuel ratio of taxi 4.

Likewise, consistent instantaneous air-fuel ratios can be observed from taxi 3 during acceleration while large variations in air-fuel ratios can be observed from taxi 4 as the

vehicle accelerates. The fluctuations in air-fuel ratio of taxi 4 during idling and acceleration indicate that control of fuel supply to the engine is not working properly, suggesting that the vehicle management system is not working properly. Thus the engine is not operating at stoichiometric conditions and hence affects the performance of the catalytic converter and emissions.

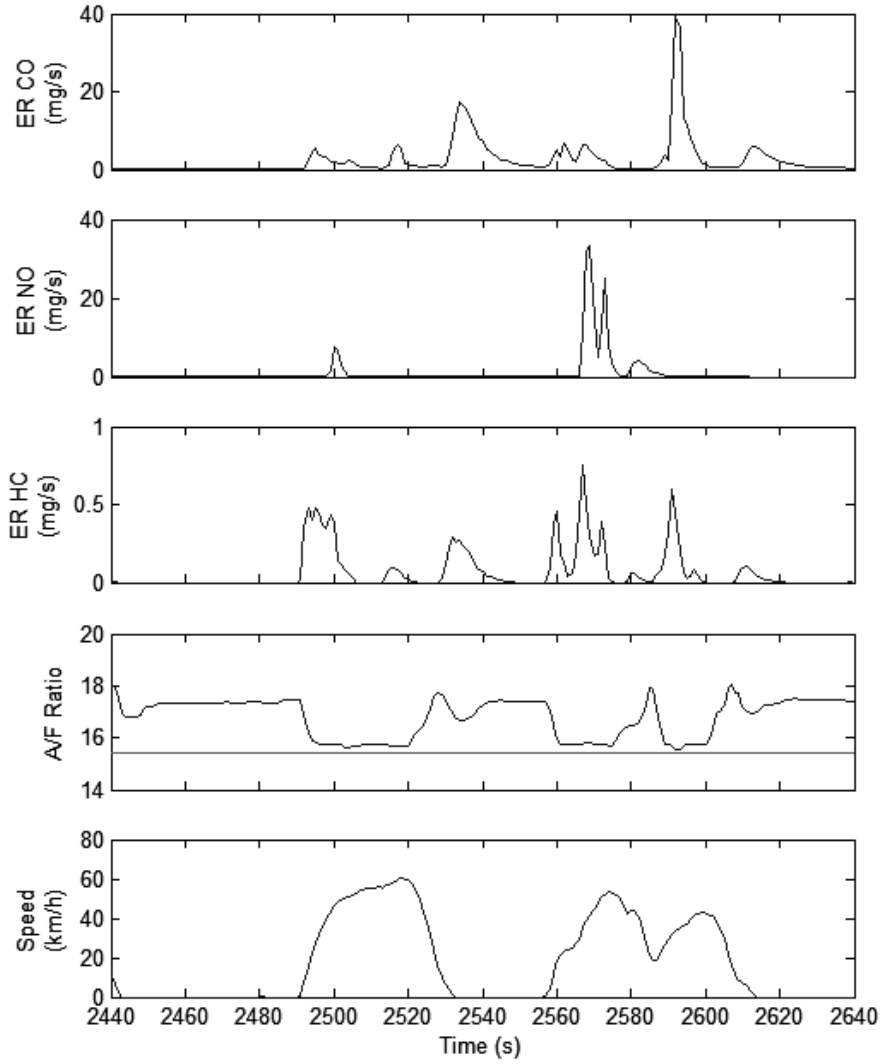

a)

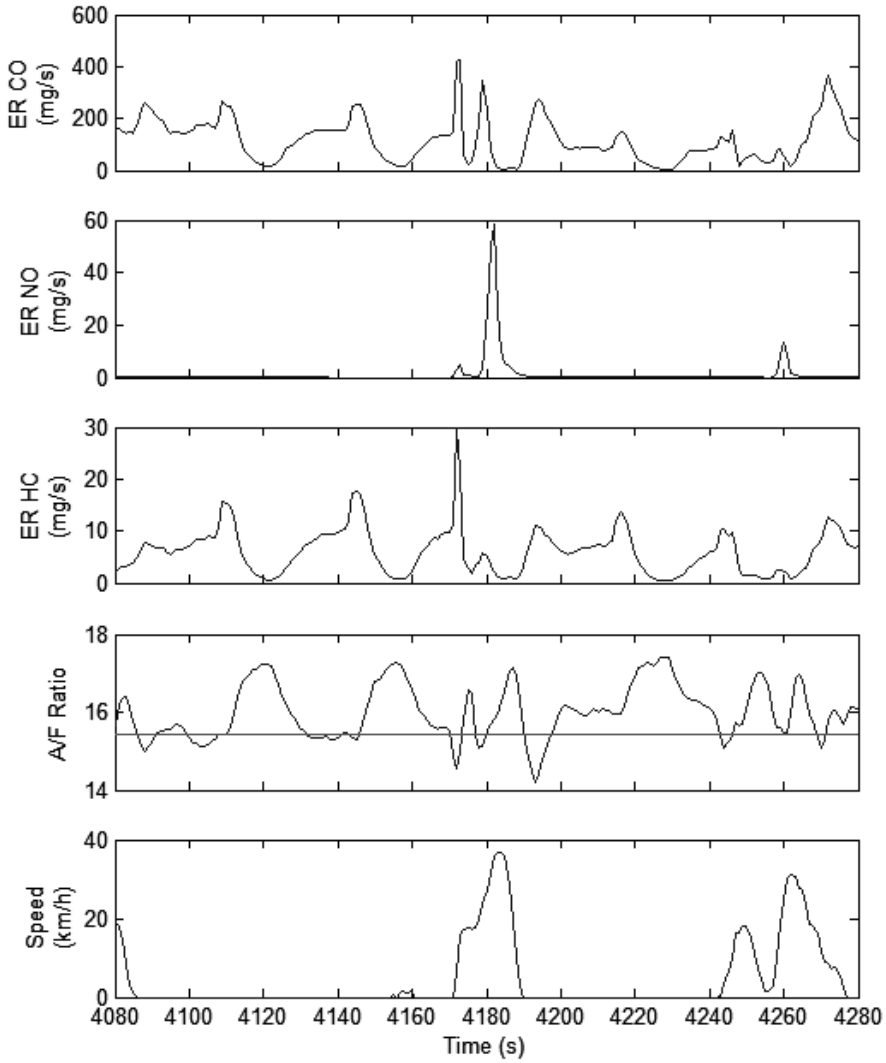

b)

Fig. 3.9 Instantaneous emission profiles of a) taxi 3 and b) taxi 4 during idling

3.5 On-road Emission Characteristics of Diesel LGVs

The average trip emission factors of LGVs are shown in Table 3.6. The emission factor of a trip is derived by dividing each vehicle's cumulative emissions over a single test run by the total distance travelled. It shows that HC emission factors of LGV 1 is the highest and LGV 4 has the lowest HC emission factor. The CO emission factor of LGV 3 is lower than that of LGVs 1 and 2 but its NO emission factor is the highest among the

LGVs. LGV 2 has higher CO and NO emission factors than LGV 1. LGV 2 has higher engine capacity and power than LGV 1 (Table 3.1), which can contribute to high emission factors. LGV 4 has lower gaseous emission factors compared to the other LGVs because it follows Euro 4 emission standards and has lower mileage.

Table 3.6 suggests that NO emissions of LGVs are positively correlated with vehicle weight, as indicated in Gajendran and Clark (2003). Meanwhile, there appears to be little correlation between vehicle weight and emissions of CO and HC. CO emission factors appear to be related to vehicle mileage, but not NO and HC.

	CO (g/km)	NO (g/km)	HC (g/km)
LGV 1	3.36±0.09	7.04±0.14	2.12±0.06
LGV 2	3.84±0.27	7.67±0.25	1.62±0.13
LGV 3	2.89±0.09	8.04±0.12	0.98±0.05
LGV 4	1.21±0.07	5.73±0.21	0.19±0.03

Table 3.6 Trip emission factors of LGVs

As LGV 4 has the largest engine size and power output among the LGVs tested, the low gaseous emission from LGV 4 may be attributed to the installation of an oxidation catalytic converter to this vehicle, as the other LGVs are not equipped with one. Kim and Choi (2008) found that a large percentage of a diesel vehicle's CO and HC emissions could be removed by a catalytic converter. Fig. 3.10 shows emission levels of LGVs 3 and 4 at the beginning of a test run to illustrate the effect of an oxidation catalytic converter. A large reduction in HC emission rate from LGV 4 can be observed after exhaust temperature reaches 150℃. No such reduction in HC emission rate is observed from LGV 3 after exhaust temperature reaches 150℃. A smaller reduction in CO emission can also be observed from LGV 4. While pre-catalyst temperature is not measured, the reduction in HC emission rate indicates that exhaust temperature is

sufficiently high for the catalyst to function.

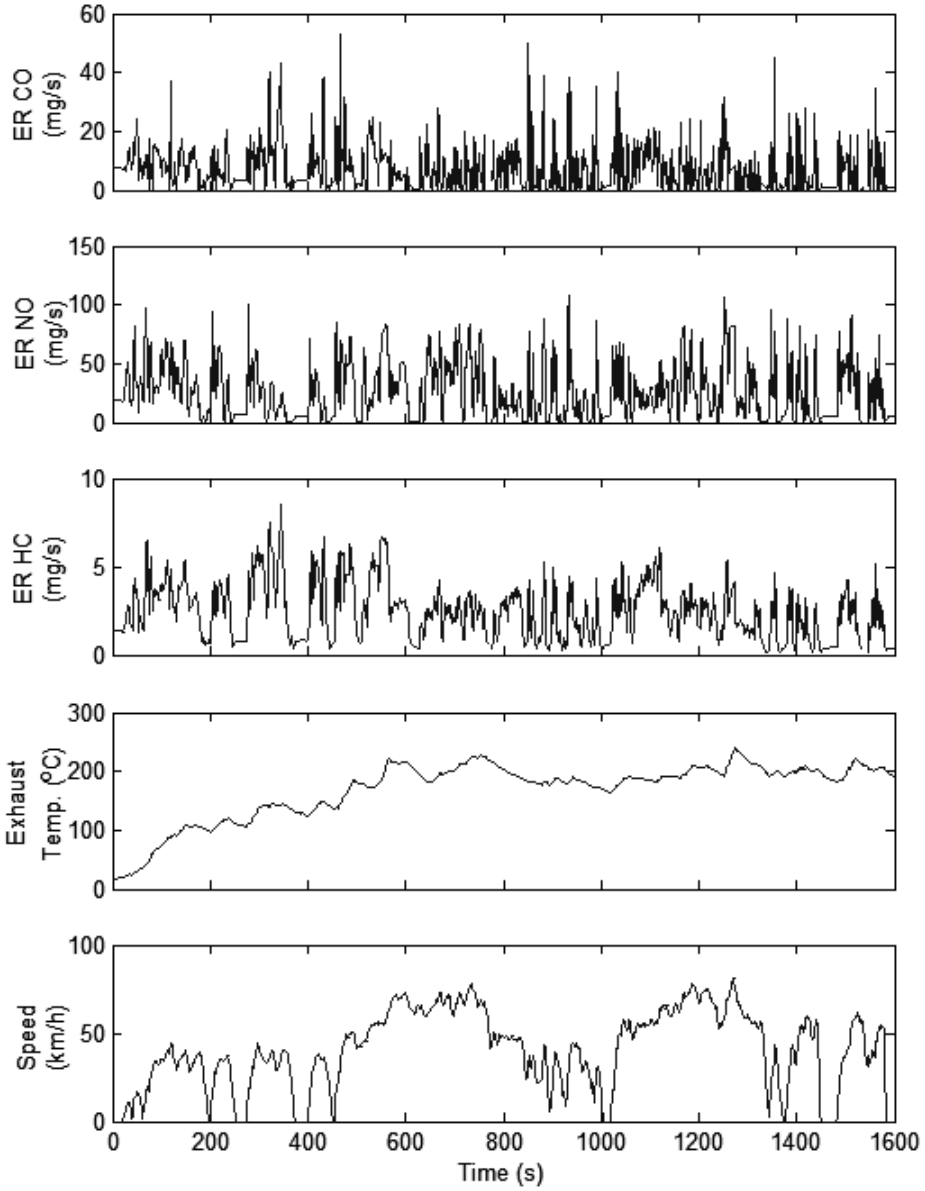

a)

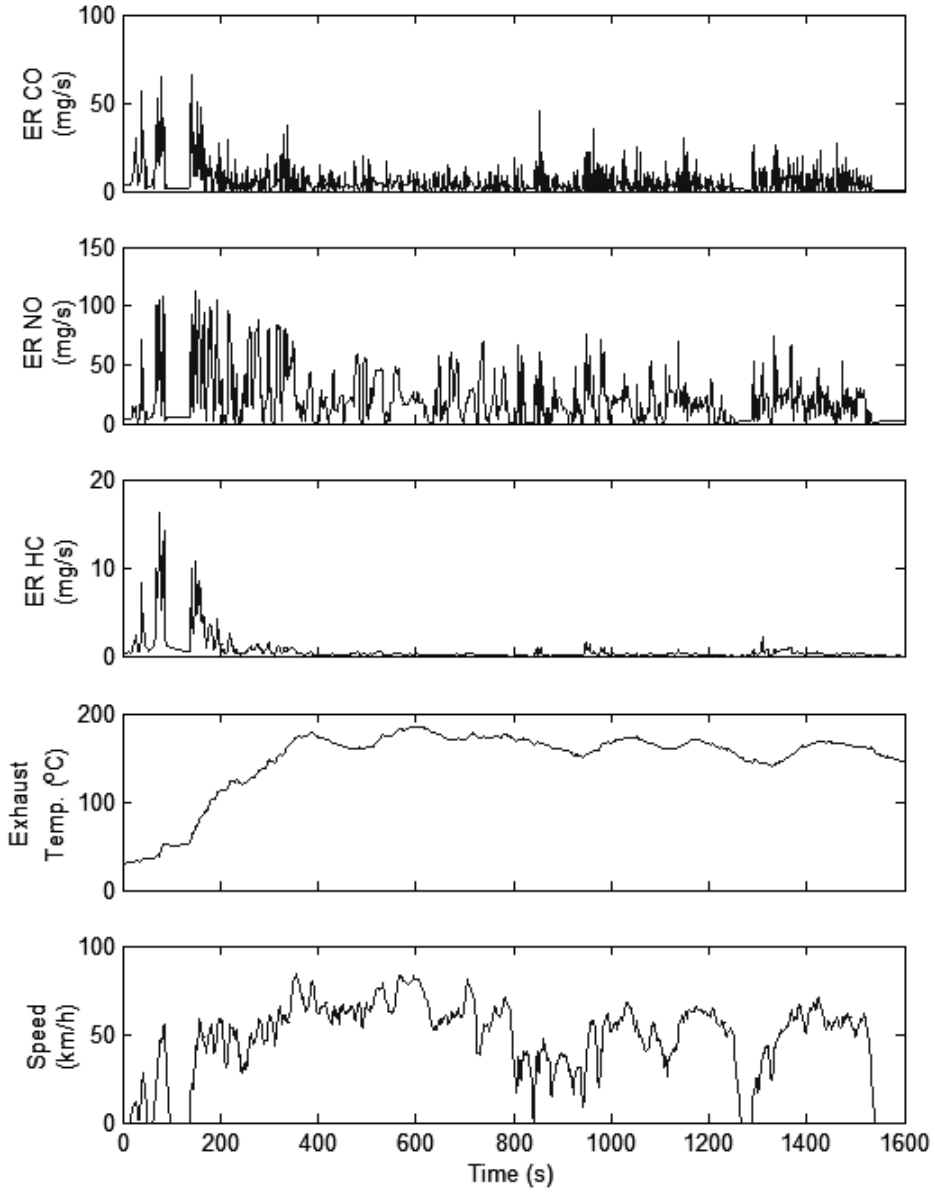

b)

Fig. 3.10 Instantaneous emissions from a) LGV 3 and b) LGV 4 at the beginning of a test run

3.5.1 Vehicle speed and its effect on emissions

Fig. 3.11 shows the CO, NO, and HC emission indices of LGVs, computed from Eqs. 3.1-3.3. Large fluctuations in CO emission indices of LGV 3 can be observed when vehicle speed is between 50 and 90km/h. NO emission index is generally high when a

vehicle is idle or travelling low speed. As vehicle speed increases, NO emission index decreases. The relationship between CO and HC emission indices of LGVs and vehicle speed is generally weak. This can be illustrated by Fig. 3.11a, which shows that there is no clear, uniform relationship between CO emission indices and vehicle speed. Likewise, Fig. 3.11c shows that no common pattern can be observed from HC emission of various vehicles in relation to speed. This can be attributed to the small number of vehicles being tested.

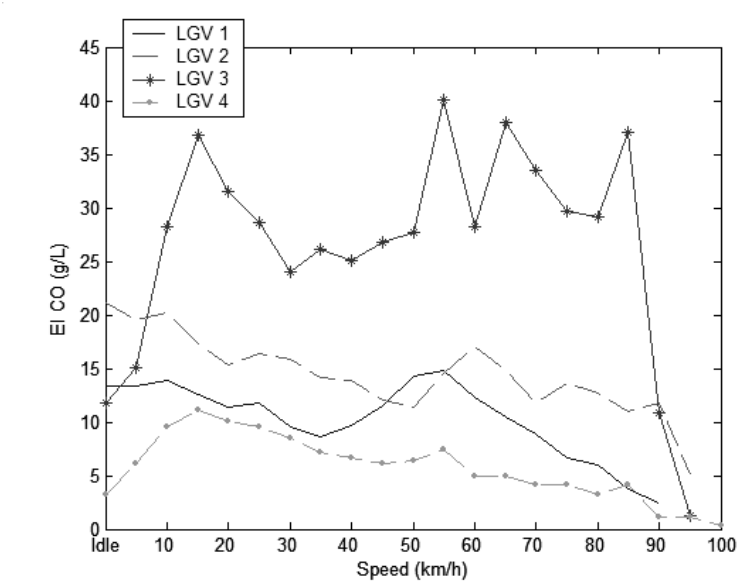

a)

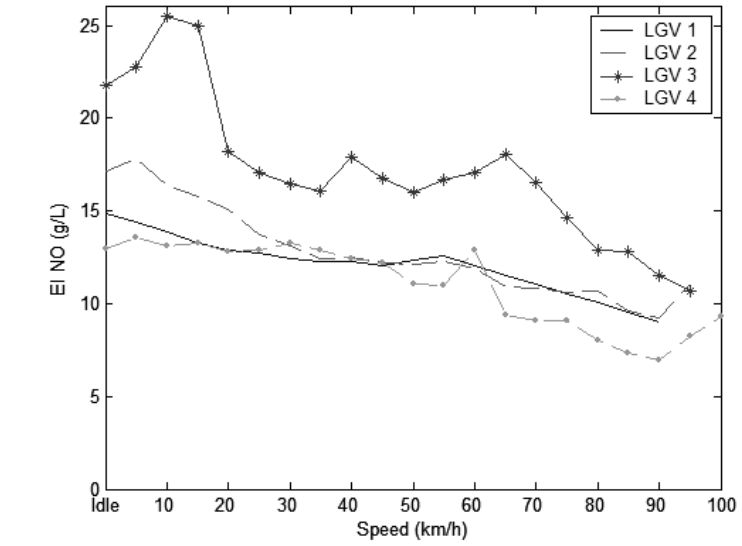

b)

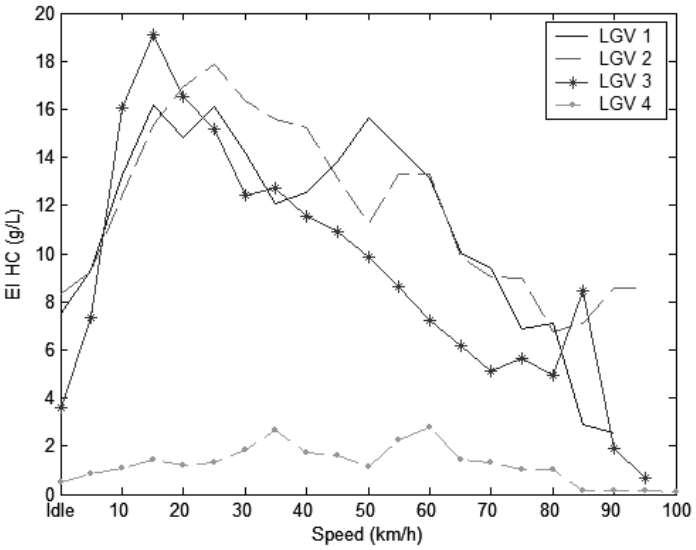

c)

Fig. 3.11 a) CO, b) NO, and c) HC emission indices of diesel LGVs

Fig. 3.11a shows that there is a large fluctuation in CO emission of LGV 3 indices at speeds of 50-90km/h while Fig. 3.11b shows that LGVs generally have higher NO emission indices while travelling below 20km/h. Fig. 3.12 shows the instantaneous emissions of LGV 3 under high (>50km/h) and low speed driving conditions.

Fig. 3.12a shows the variations in instantaneous emissions of LGV 3 while travelling between 50-90km/h. The plot shows that minimal amount of CO_2 is emitted when the vehicle underwent hard deceleration. This period corresponds to the time when CO emission index was high (Eq. 3.1). This suggests that little to no fuel is injected to the engine when the vehicle undergoes hard deceleration. Thus large fluctuations in CO emission index of LGV 3 during high-speed travel appear to be related to heavy deceleration.

Fig. 3.12b shows variations in instantaneous gaseous concentrations and emission indices of LGV 3 under low speed driving conditions. High NO emission indices can be

observed while the vehicle speed decreases, during which very low levels of CO and CO_2 are emitted by the vehicle. Low CO_2 concentrations indicate that minimal amount of fuel is being consumed at the time. Similar variations in NO emission index can be observed from the other LGVs as the vehicle decelerates to a stop. Thus it appears that NO emission indices during low speed driving are skewed by high values observed from times when the vehicle undergoes aggressive deceleration.

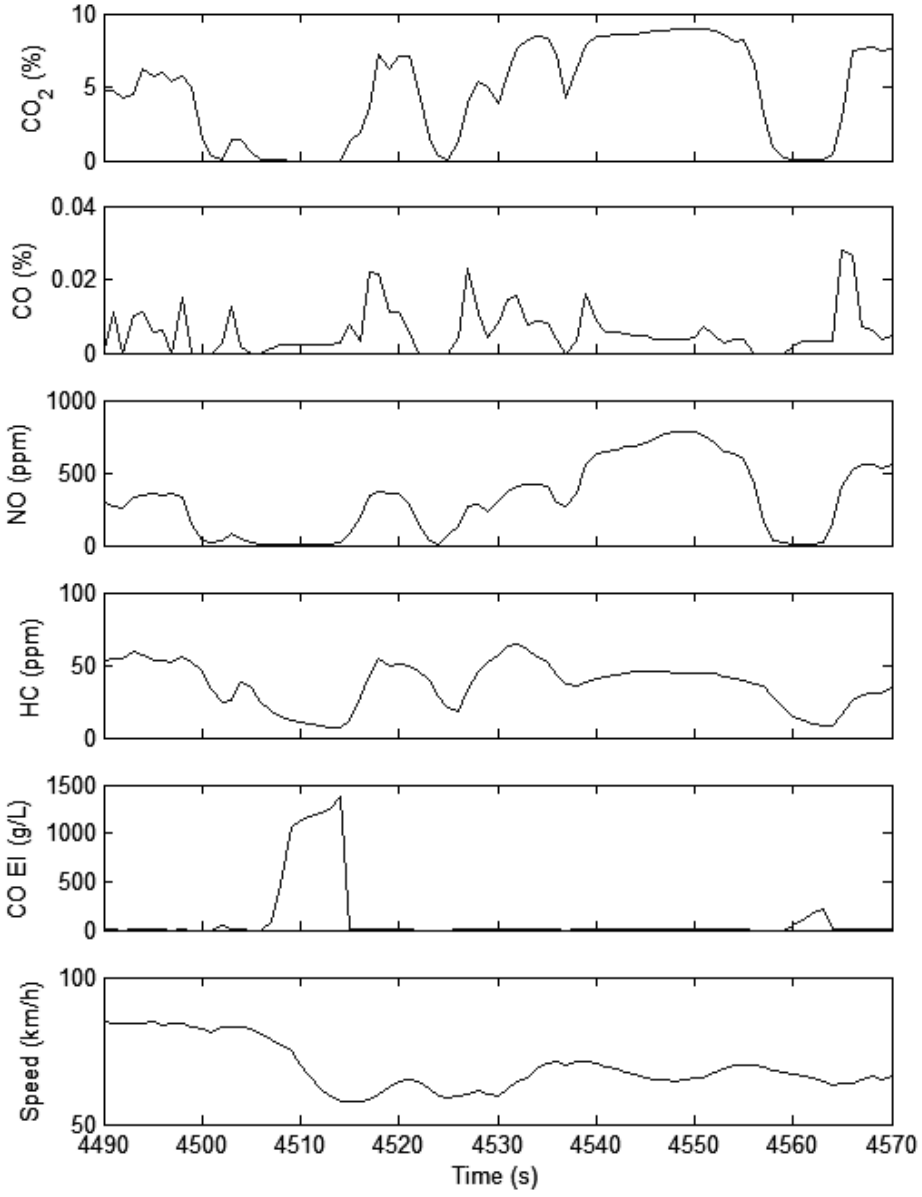

a)

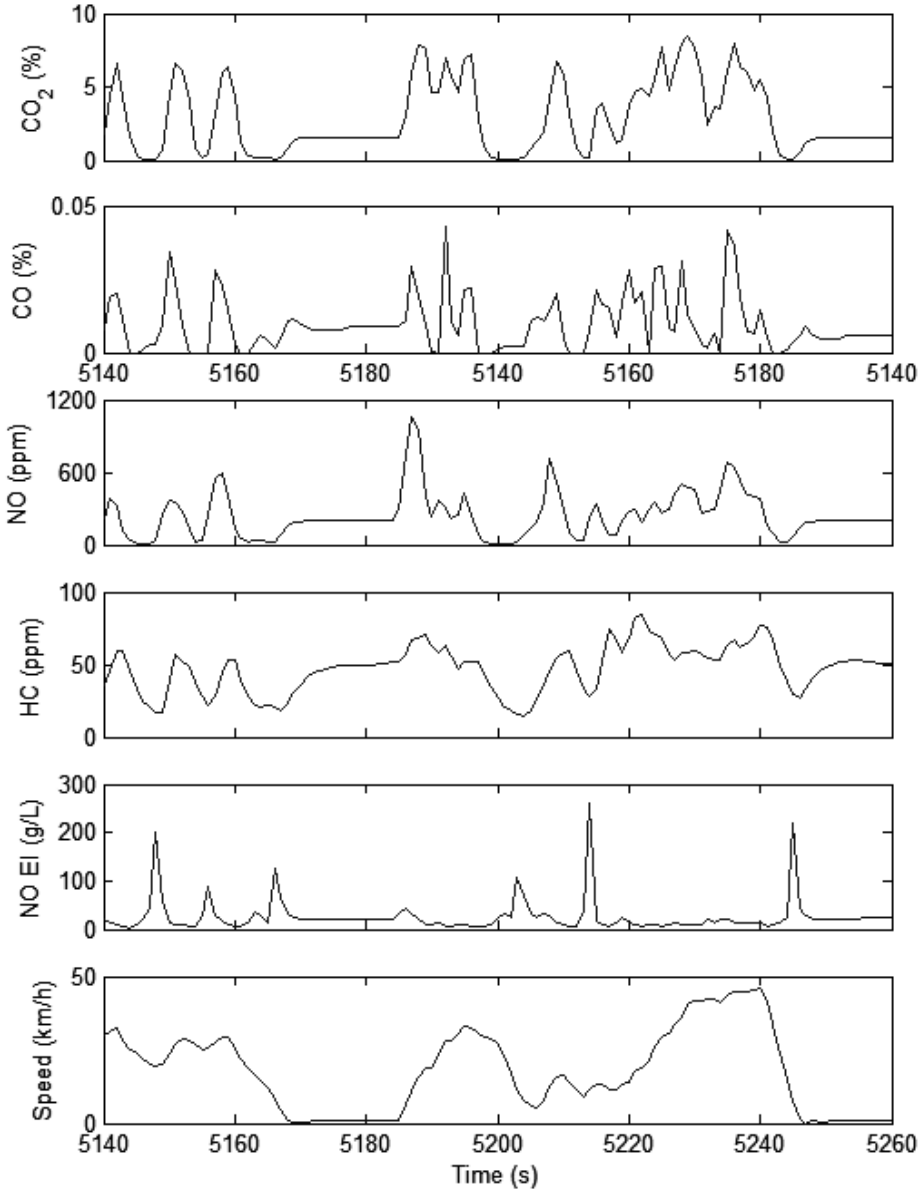

b)

Fig. 3.12 Instantaneous emissions from LGV 3 while travelling at a) high and b) low speeds

The CO, NO, and HC emission factors for the four LGVs, computed using Eq. 3.5 are shown in Fig. 3.13. It shows that gaseous emission factors of CO and HC are inversely related to instantaneous vehicle speed. The plot shows that LGV 4 emits the lowest amount of gaseous pollutants and LGVs 3 and 4 have lower HC emission factors than

LGVs 1 and 2. The relationship between emission factor and vehicle speed can be attributed to the way emission factors are derived from on-road measurements—from Eq. 3.5 it can be observed that gaseous emission factors and vehicle speed are inversely related.

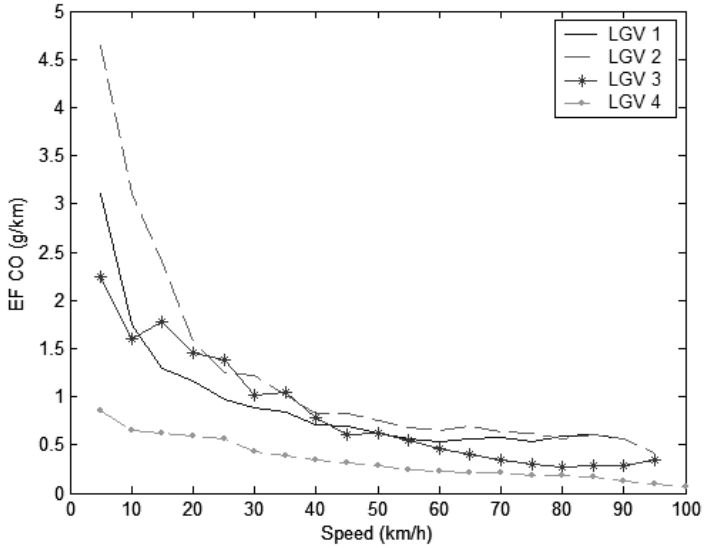

a)

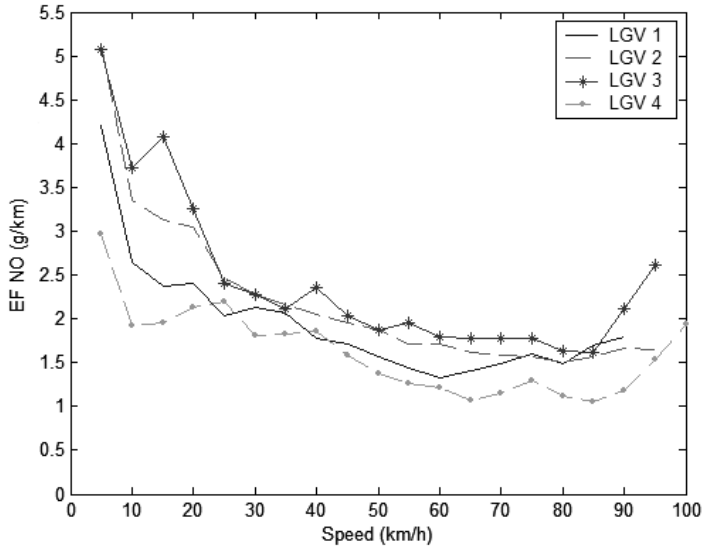

b)

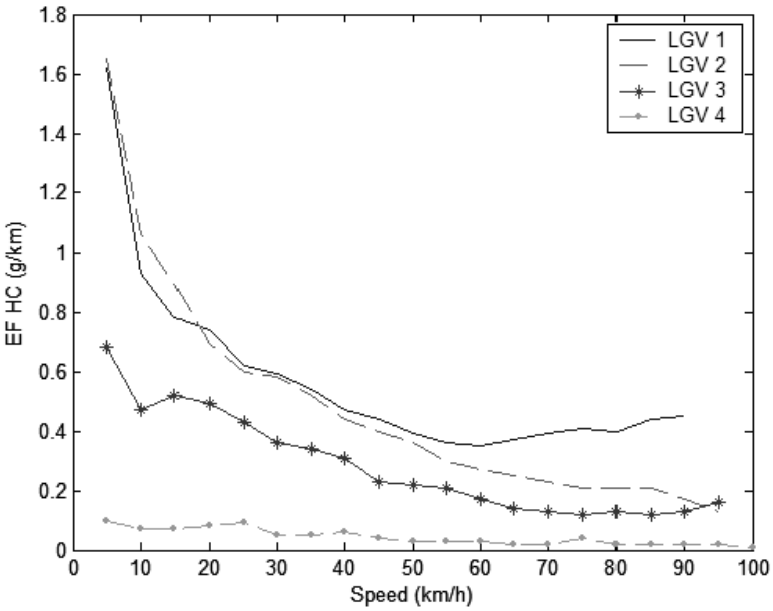

c)

Fig. 3.13 a) CO, b) NO, and c) HC emission factors of LGVs

Emission rates of LGVs are shown in Fig. 3.14. The figure shows that, as vehicle speed increases, NO emission rates of LGVs climb upward. CO emission rates of the LGVs 1 and 2 also increase as vehicle speed increases. Meanwhile, CO emission rate of LGV 3 exhibits large fluctuations and there is little variation in CO emission rate of LGV 4 in the range of 35-85km/h. The decrease in CO emission rate of LGV 3 at higher speeds (>50km/h) is probably related to rapid deceleration of the vehicle under high speed driving conditions, as shown in Fig. 3.12a. HC emission rate at low speed increases as vehicle speed increases. At higher speeds, there is little variation in emission rate as vehicle speed increases, with the exception of LGV 1. On-road measurements show that vehicles travelling at higher speeds generally have higher gaseous emission rates, similar to previous results (El-Shawarby et al., 2005). The small variation in CO emission rate and low HC emission rate of LGV 4 at high speeds can be attributed to the more efficient operation of the oxidation catalytic converter. Since the oxidation catalytic converter has very little effect on NO emissions, NO emission rate of LGV 4

exhibits similar patterns as other LGVs.

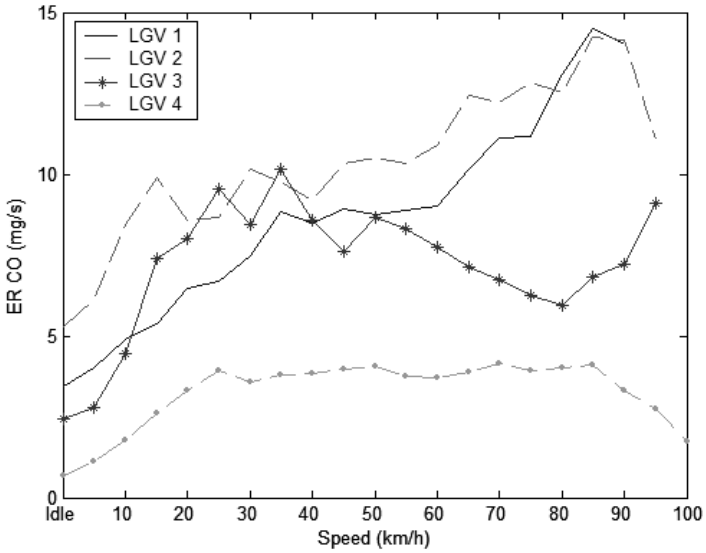

a)

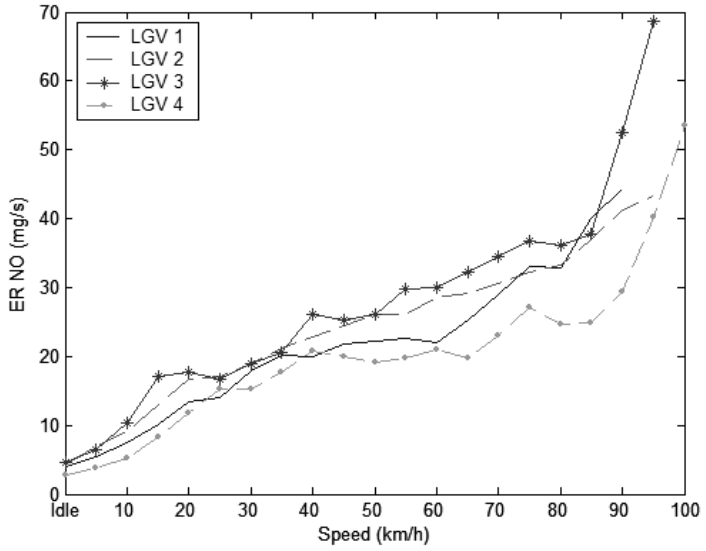

b)

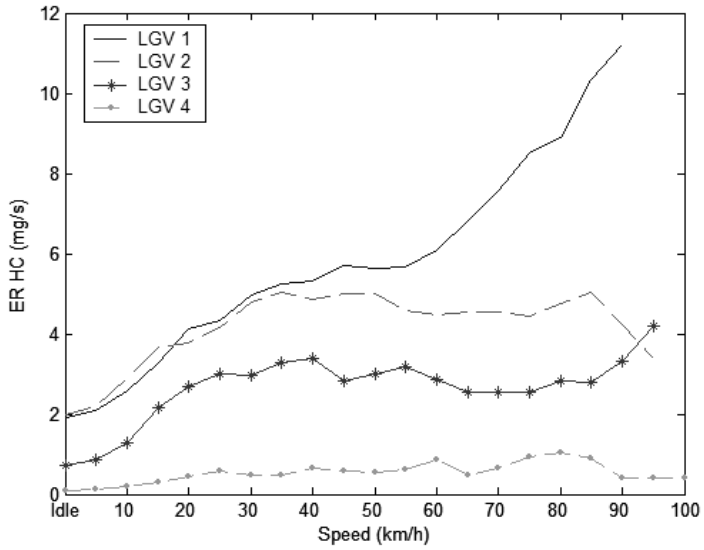

c)

Fig. 3.14 a) CO, b) NO, and c) HC emission rates of LGVs

3.5.2 Effect of acceleration on vehicle emissions

To examine the effect of acceleration on emissions of LGVs, exhaust flow and emission rates of the four LGVs under idling, acceleration, cruising, and deceleration modes, defined in Table 3.2, are listed in Table 3.7. The emission rate of each mode is obtained by taking the average of the instantaneous emission rates under that particular mode.

Flow Rate (L/s)	Idle	Deceleration	Cruising	Acceleration
LGV 1	18.40±0.02	37.88±0.16	50.83±0.28	49.36±0.18
LGV 2	27.14±0.03	51.14±0.16	62.15±0.31	66.37±0.23
LGV 3	19.53±0.01	46.52±0.12	60.37±0.23	65.79±0.16
LGV 4	23.16±0.03	62.97±0.17	77.91±0.34	85.51±0.24
CO (mg/s)				
LGV 1	3.46±0.01	4.40±0.04	7.99±0.08	9.33±0.06
LGV 2	5.29±0.02	6.51±0.06	11.05±0.11	12.47±0.08
LGV 3	2.43±0.01	3.65±0.03	7.57±0.07	10.35±0.05
LGV 4	0.67±0.01	1.42±0.02	2.92±0.05	5.40±0.04
NO (mg/s)				
LGV 1	3.97±0.01	9.40±0.10	19.01±0.21	21.33±0.12
LGV 2	4.35±0.02	12.35±0.12	21.72±0.26	28.06±0.18
LGV 3	4.60±0.02	10.95±0.10	22.48±0.20	29.67±0.13
LGV 4	2.76±0.01	8.67±0.06	15.92±0.15	23.73±0.11
HC (mg/s)				
LGV 1	1.92±0.01	3.45±0.02	5.27±0.04	5.36±0.02
LGV 2	1.99±0.01	3.29±0.02	4.38±0.03	4.91±0.02
LGV 3	0.72±0.01	1.80±0.01	2.76±0.02	3.05±0.01
LGV 4	0.10±0.01	0.30±0.01	0.53±0.03	0.73±0.02

Table 3.7 Exhaust flow and emission rates of LGVs under various operating modes

Table 3.7 shows that exhaust flow rate of LGVs do not correlate well with engine power or size. Exhaust flow rates of LGVs are considerably lower while idling than any other operating modes. However, the difference between exhaust flow rates under cruise and acceleration modes is rather small. All LGVs emit the lowest amounts of gaseous pollutants when the vehicle is operating at idling mode, followed by decelerating and cruising modes. A LGV emits the highest amounts of gaseous pollutants while accelerating. The high amount of gaseous pollutants being emitted during acceleration may be related to fuel consumption rate and engine speed, which is the lowest at idle and highest at acceleration.

Compared to taxis (Table 3.5), a more uniform relationship can be observed between operation mode of LGVs and gaseous emissions can be observed. Emission rate of a LGV under cruising conditions is approximately twice the emission rate during deceleration. Meanwhile, the difference in emission rates during cruising and acceleration modes is generally small. This is in contrast to previous studies, where large difference in emission rates of vehicles operating in cruising and acceleration modes can be observed (Chen et al., 2007). As shown in Table 3.7, flow rates of LGVs under cruising and acceleration modes are similar, this can result in vehicles having similar emission rate while travelling under cruising and acceleration conditions.

Gaseous emissions from LGV 2 at various speed and acceleration rates are shown in Fig. 3.15. The relationship between gaseous emission rates and acceleration of other LGVs are similar. When LGV 2 accelerates aggressively, it emits 8-29, 9-57, and 3-11 mg of CO, NO, and HC per second, respectively; when a LGV undergoes rapid deceleration, the amount of CO, NO, and HC emitted are 1.4-9.2, 3-27, and 1.3-5.3 mg/s, respectively. At various acceleration rates, CO and NO emissions generally are higher when the vehicle travels at a higher speed while HC emissions tend to be the highest when the vehicle is travelling between 30 and 50km/h.

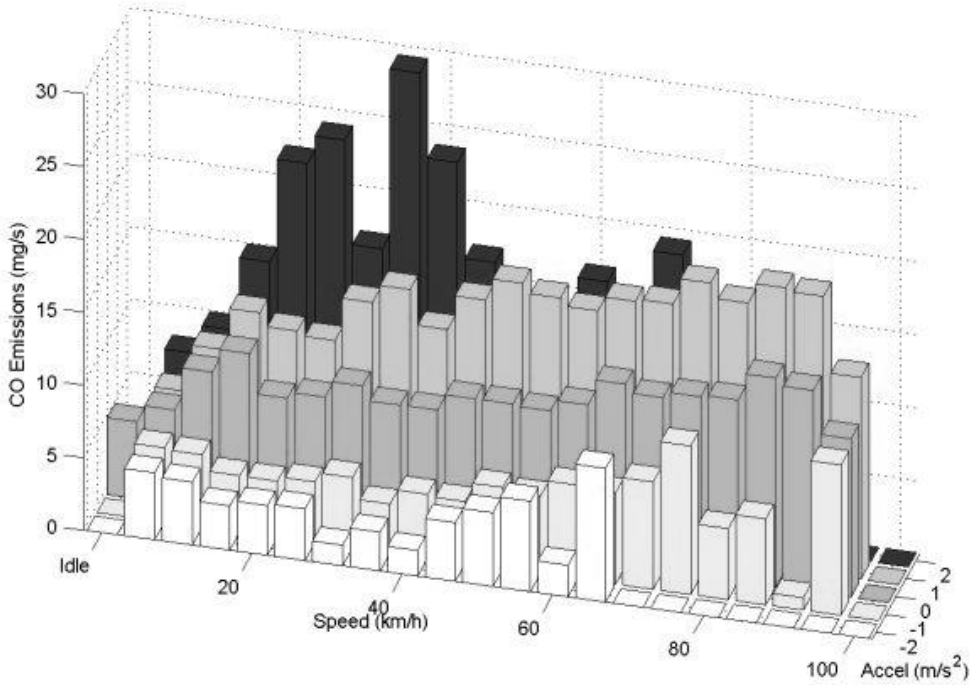
CO Emissions (mg/s)
30
25
20
15
10
5
0
Idle
20
40
60
80
100
Speed (km/h)
2
1
0
-1
-2
Accel (m/s^2)

a)

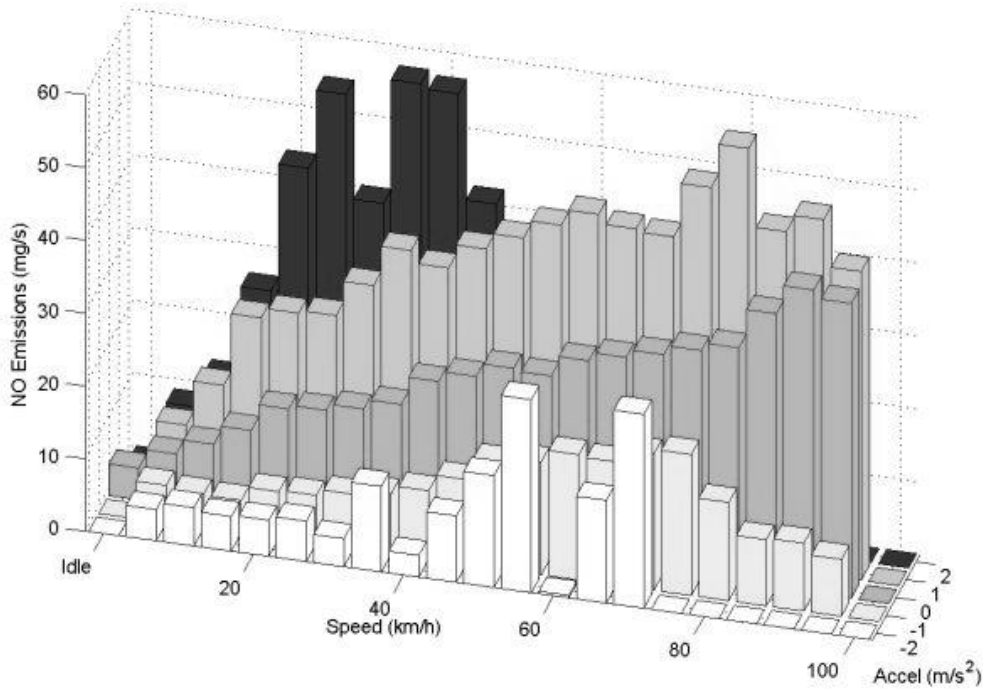
NO Emissions (mg/s)
60
50
40
30
20
10
0
Idle
20
40
60
80
100
Speed (km/h)
2
1
0
-1
-2
Accel (m/s^2)

b)

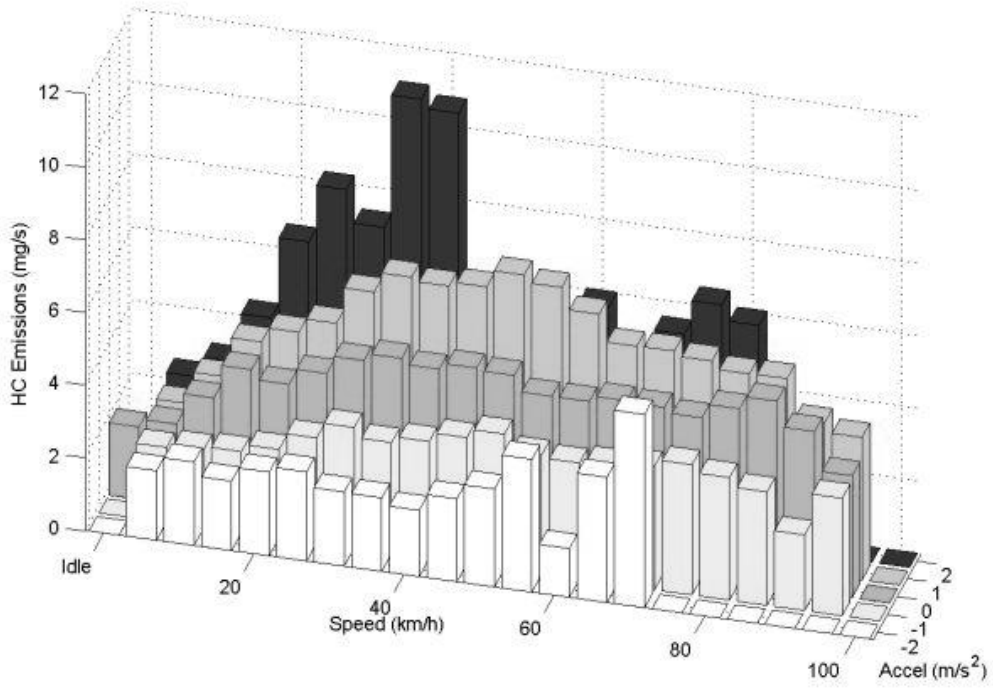

c)

Fig. 3.15 a) CO, b) NO, and c) HC emission rates of LGV 2 under acceleration, cruising, and deceleration modes

3.6 Chapter Summary

Intensive on-road gaseous emissions measurements of four LPG taxis and four diesel light goods vehicles (LGVs), using a portable emission measurement system (PEMS), were carried out and in-depth data analysis was performed. The vehicles tested were carefully selected based on model year so as to represent different generation of technology of the in-use vehicle fleet. This dataset contains second-by-second vehicle emission, fuel consumption, air/fuel ratio and speed information and thus enables analysis of on-road vehicle emission characteristics in relationship with driving speed and engine operating conditions.

The results show that, for taxis adhering to Euro 2 and 3 emission standards, newer vehicles emit less, due to improvements in engine technology and emission control.

Extraordinarily high levels of CO and HC emissions from the Euro 4 taxi can be observed while idling, during which large fluctuations in air-fuel ratio can be observed. This can be attributed to malfunction of fuel injection control, indicating that the engine management system is not operating properly. CO and HC emission indices of taxis tend to decrease as vehicle speed increases while NO emission index increases as vehicle speed becomes higher. Gaseous emission rates increase as vehicle speed increases, with the exception of HC from taxis, while emission factors are inversely related to vehicle speed. Vehicles generally have the lowest gaseous emission rates while idling. A moving vehicle emits higher amounts of gaseous pollutants while accelerating.

The LGV with the lowest amounts of gaseous emissions is equipped with a warmed up catalytic converter while the other vehicles are not equipped with any type of emission control. High air/fuel ratios and emission indices are observed from LGVs during deceleration, indicating little fuel is being burnt while the vehicle decelerates, resulting in higher levels of HC, within the exhaust.

The above revealed on-road instantaneous vehicle emission characteristics further enable the possibility of validating the vehicle emission measurements obtained by roadside remote sensing technique to be discussed in the next chapter.

Chapter 4

Remote Sensing of Emissions from On-Road Vehicles

4.1 Introduction

In the previous chapter, collection and analysis of on-road emissions from taxis and light goods vehicles (LGVs) under a number of operating conditions were discussed. One major shortcoming of on-road measurement techniques is that, similar to dynamometer testing, the number of vehicles tested is limited by time and cost constraints. To overcome this limitation, continuous monitoring of roadside air quality and remote sensing techniques are developed to study on-road emissions from a large number of vehicles (Bishop and Stedman, 2008).

To investigate gaseous emissions from a wide range of vehicles, remote sensing techniques is employed to measure vehicle emissions from the roadside. Gaseous emission from vehicles of different vehicle and fuel types are examined. In particular, emissions of vehicles of the same vehicle type but different fuel types are investigated. The emission indices and factors of light-duty vehicles are examined. The effect vehicle model year and road grade have on vehicle emissions is also studied. The emission factors of taxis and LGVs derived from on-road and remote sensing measurements are compared and the discrepancies between the two sets of emission factors are investigated.

4.2 Remote Sensing Measurement Campaign

Remote sensing measurements were carried out by the Hong Kong Environmental Protection Department at 35 sites on weekdays between March 2007 and April 2008.

The gradients of the road segments, consisting mostly of highway on-ramps and intersections, range between -0.02 and 0.17. At the measurement sites, it is assumed that the majority of vehicles are undergoing acceleration. The vehicles travelling past the remote sensing site are assumed to be sufficiently warmed up, thus it is assumed that no vehicles operated under cold-start conditions, under which emissions are higher (Mazzoleni et al., 2004a).

A vehicle's emission is measured by remote sensing using a laser beam that contains an infrared and an ultraviolet beam. Concentrations of carbon monoxide (CO), carbon dioxide (CO_2), and hydrocarbons (HC) are measured with a non-dispersive infrared (NDIR) beam while concentration of nitric oxide (NO) is measured using a non-dispersive ultraviolet (NDUV) beam. The two beams are released from a source detector module, located on one side of a traffic lane, and reflected back to the module by a mirror located on the other side of the lane. The strength of the beams is measured continuously. When a vehicle travels past the test site, its exhaust absorbs some of the light emitted. Concentrations of gaseous emissions are determined by comparing the strength and waveform of the beams exiting and returning to the source detector module. A vehicle's emission is determined based on gaseous concentration measurements immediately before and after the vehicle's passage through the remote sensing site. Measurement instruments are calibrated at least once daily (Ko and Cho, 2006).

Speed measurements are collected from a speed sensor, which contains a detector bar and an emitter bar that emits two lasers. The two lasers are separated by a fixed distance. As a vehicle travels past the measurement site, the beam's path to the mirror is obstructed. The vehicle's speed at the time when the vehicle passes each of the laser beams is derived and the speed and acceleration, defined to be the difference between

the speeds measured by the two lasers, of the vehicle are recorded. The license plate information of each vehicle travelling past the test site is recorded by a video camera. The vehicles' model year, vehicle type, and fuel type are retrieved from the vehicle registration database.

4.3 Collation of remote sensing data

The CO, NO, and HC emission indices of each vehicle are derived from remote sensing measurements using the following equations (Ning and Chan, 2007):

$$EI_{CO} = \frac{[CO]}{[CO]+[CO_2]+3\cdot[HC]/0.5}\cdot\frac{28}{MW_{fuel}}\cdot D_{fuel} \quad (4.1)$$

$$EI_{NO} = \frac{[NO]}{[CO]+[CO_2]+3\cdot[HC]/0.5}\cdot\frac{30}{MW_{fuel}}\cdot D_{fuel} \quad (4.2)$$

$$EI_{HC} = \frac{[HC]/0.5}{[CO]+[CO_2]+3\cdot[HC]/0.5}\cdot\frac{44}{MW_{fuel}}\cdot D_{fuel} \quad (4.3)$$

where [*P*] is the measured concentration of a pollutant *P*, expressed in terms of %, MW_{fuel} and D_{fuel} are the molecular weight and density of the fuel, respectively. The molecular weight of petrol, diesel, and LPG fuels are 13.86g/(mol C), 13.85g/(mol C), and 14.54g/(mol C) respectively while the density of petrol, diesel, and LPG fuels are 750g/L, 850g/L, and 558.6g/L respectively (Holmén and Niemeier, 1998; Kean et al., 2001; Ning and Chan, 2007). HC measurements are multiplied by a factor of 2 as it has been observed that HC measurements obtained from a flame ionization detector and those obtained from NDIR differ by this factor (Unal et al., 2004; Tang and Wang, 2006). This conversion is made so that emission factors derived from remote sensing

measurements and those derived from on-road tests, whose results are discussed in Chapter 3, can be compared. Such comparisons will be discussed later.

The vehicles are classified into the following vehicle types: passenger cars (petrol/diesel), light buses (diesel/LPG), light goods vehicles (petrol/diesel), heavy goods vehicles (diesel), taxis (LPG), private buses (diesel), public buses (diesel), and franchised buses (diesel). Diesel vehicles are also classified into two classes by vehicle weight—light-duty (passenger cars, light buses, and LGVs) and heavy-duty (HGVs and buses). All petrol and LPG vehicles are considered light-duty.

Gaseous emission factors of a vehicle are computed from its emission indices using the following:

$$EF_{P,fuel} = EI_{P,fuel} \cdot FC_{fuel} \quad (4.4)$$

where FC_{fuel} is the fuel consumption rate in L/km (Ning and Chan, 2007). A vehicle's fuel consumption rate is often expressed as a function of speed and acceleration (Kent and Mudford, 1979; Panis et al., 2006). Fuel consumption can be estimated from gaseous emission factors using the following (Kent and Mudford, 1979; Song et al., 2009):

$$FC_{Fuel} = \left(\frac{EF_{CO2}}{44} + \frac{EF_{CO}}{28} + \frac{EF_{HC}}{MW_{Fuel}} \right) \cdot \left(\frac{MW_{Fuel}}{D_{fuel}} \right) \quad (4.5)$$

The relationship between fuel consumption rate and vehicle speed and acceleration for different vehicle types are expressed as Eq. 4.6. The fuel consumption equation for petrol vehicles (Eq. 4.6a) is derived from dynamometer measurements of a passenger car's fuel consumption (Post et al., 1984). The R^2 value of the equation is 0.844. Fuel

consumption equations of diesel and LPG vehicles (Eqs. 4.6b and c) are derived from instantaneous CO_2, CO, and HC emission factors (Eq. 4.5), which are computed from on-road emission measurements discussed in Chapter 3. The R^2 values of the equations are 0.662 and 0.948 respectively. Here fuel consumption rates of light- and heavy-duty diesel vehicles are assumed to be the same. In practice fuel consumption rate of heavy-duty diesel vehicles is vastly higher than that of light-duty diesel vehicles (Pierson et al., 1996).

$$FC_{Petrol} = 0.135 + \frac{2.017}{v} + 0.029 \cdot a \quad (4.6a)$$

$$FC_{Diesel} = 0.066 + \frac{1.034}{v} + 0.042 \cdot a \quad (4.6b)$$

$$FC_{LPG} = 0.153 + \frac{3.296}{v} + 0.025 \cdot a \quad (4.6c)$$

4.4 Emissions from On-road Vehicles

4.4.1 Fuel effect on emissions

The gaseous emission indices and factors of various vehicle types are shown in Table 4.1. It shows that vehicles fuelled by diesel have lower levels of CO and HC emissions compared to those fuelled by petrol and LPG. NO emission of petrol and LPG vehicles is lower compared to diesel vehicles. In particular, LGVs fuelled by petrol emit lower amount of NO and higher amounts of CO and HC compared to the vehicles fuelled by diesel. Meanwhile, diesel light buses have lower CO and HC emissions and higher NO emission compared to LPG light buses. The differences in emission indices and factors are significant at the 95% level. This is likely due to differences in operating

characteristics of petrol/LPG engines and diesel engines—petrol and LPG engines typically operate at rich conditions, under which CO and HC emissions increase and NO emission decrease, while diesel engines typically operate at lean conditions, under which higher level of NO and lower levels of CO and HC are emitted (Ferguson and Kirkpatrick, 2001; Ceviz and Yüksel, 2005).

Table 4.1 shows that LPG taxis have higher NO and HC emission indices compared to passenger cars, which generally have similar engine size and power as taxis. CO emission indices of petrol passenger cars are lower than taxis, but the opposite holds for CO emission factors. Result showing that petrol vehicles emit less NO than LPG vehicles agrees with previous work (Ceviz and Yüksel, 2005; Yang et al., 2007). However, results showing that LPG taxis emitting higher levels of HC compared to petrol passenger cars are opposite of the conclusion found in previous work (Ning and Chan, 2007; Yang et al., 2007).

As shown in Table 4.1, petrol LGVs generally emit higher amounts of gaseous pollutants than passenger cars. Meanwhile, motorcycles have higher gaseous emission factors compared to other types of petrol-powered vehicles, indicating that emissions from motorcycles are released directly into the atmosphere without any treatment (Tsai et al., 2000).

Heavy-duty goods vehicles generally have the highest gaseous emission indices and factors among diesel vehicles. Franchised buses have lower CO and HC emission indices compared to other types of vehicles running on diesel while passenger cars have the lowest NO emission index among diesel vehicles. Light buses generally have higher gaseous emission indices than other types of light-duty diesel vehicles.

		EI (g/L)			EF (g/km)		
Petrol	*N*	CO	NO	HC	CO	NO	HC
PC	88733	35.82±0.24	4.59±0.02	3.30±0.03	7.32±0.05	0.98±0.01	0.69±0.01
LGV	1131	95.78±3.90	5.77±0.20	7.08±0.46	19.31±0.57	0.84±0.04	1.39±0.04
MC	556	151.35±8.63	7.67±0.27	22.44±1.87	36.82±2.21	1.82±0.08	5.54±0.51
Diesel							
PC	899	4.93±0.29	5.22±0.12	2.91±0.12	0.63±0.08	0.56±0.02	0.37±0.02
Private LB	2210	4.98±0.30	10.55±0.13	4.33±0.10	0.54±0.03	1.22±0.02	0.47±0.01
Public LB	3299	5.79±0.39	11.82±0.08	3.78±0.07	0.60±0.03	1.42±0.02	0.42±0.01
LGV	58930	4.43±0.04	7.74±0.02	3.30±0.02	0.52±0.01	0.91±0.01	0.38±0.01
HGV	6916	6.51±0.24	13.30±0.08	5.47±0.08	0.69±0.05	1.39±0.02	0.54±0.02
Private Bus	248	4.11±0.44	10.31±0.35	3.05±0.16	0.43±0.05	1.15±0.06	0.32±0.02
Public Bus	9561	5.90±0.19	10.82±0.06	3.99±0.04	0.71±0.04	1.24±0.01	0.43±0.01
FB	3325	3.73±0.11	12.44±0.08	2.33±0.03	0.55±0.03	1.80±0.03	0.35±0.01
LPG							
Private LB	171	24.20±3.06	3.13±0.49	1.90±0.25	6.22±0.76	0.92±0.15	0.54±0.08
Public LB	3716	85.87±1.65	3.50±0.10	5.62±0.26	22.01±0.44	0.91±0.03	1.43±0.07
Taxi	99838	27.43±0.10	10.04±0.02	6.98±0.02	7.76±0.03	2.91±0.01	1.99±0.01

Table 4.1 Emissions from major types of vehicles. (*N*—number of vehicles, PC—passenger car, LGV—light goods vehicle, HGV—heavy goods vehicle, MC—motorcycle, LB—light bus, FB—franchised bus)

Among LPG vehicles, light buses emit the highest amount of CO while taxis emit the highest amounts of NO and HC. Since light buses have higher vehicle load and engine size than taxis, this suggests that gaseous emissions from taxis may be the result of their heavy usage, as taxis are often on-road throughout the day. The long operation period of taxis may result in faster deterioration of engine performance and effectiveness of emission control devices such as catalytic converters. The operational period of taxis also prevents proper maintenance from taking place.

To study the emission distribution of various types of vehicles, remote sensing measurements of each vehicle type are sorted by increasing concentration. They are then classified into ten classes of equal size, or deciles, each representing 10% of the vehicles. Decile 1 consists of vehicles emitting the lowest amount of a pollutant and

decile 10 consists of vehicles emitting the highest amount of a pollutant. The contribution of each decile towards gaseous emissions of petrol, light-duty diesel, and LPG vehicles are shown in Fig. 4.1. Each bar represents the contribution of a pollutant from one decile of vehicles running on one type of fuel (Mazzoleni et al., 2004a; Ko and Cho, 2006).

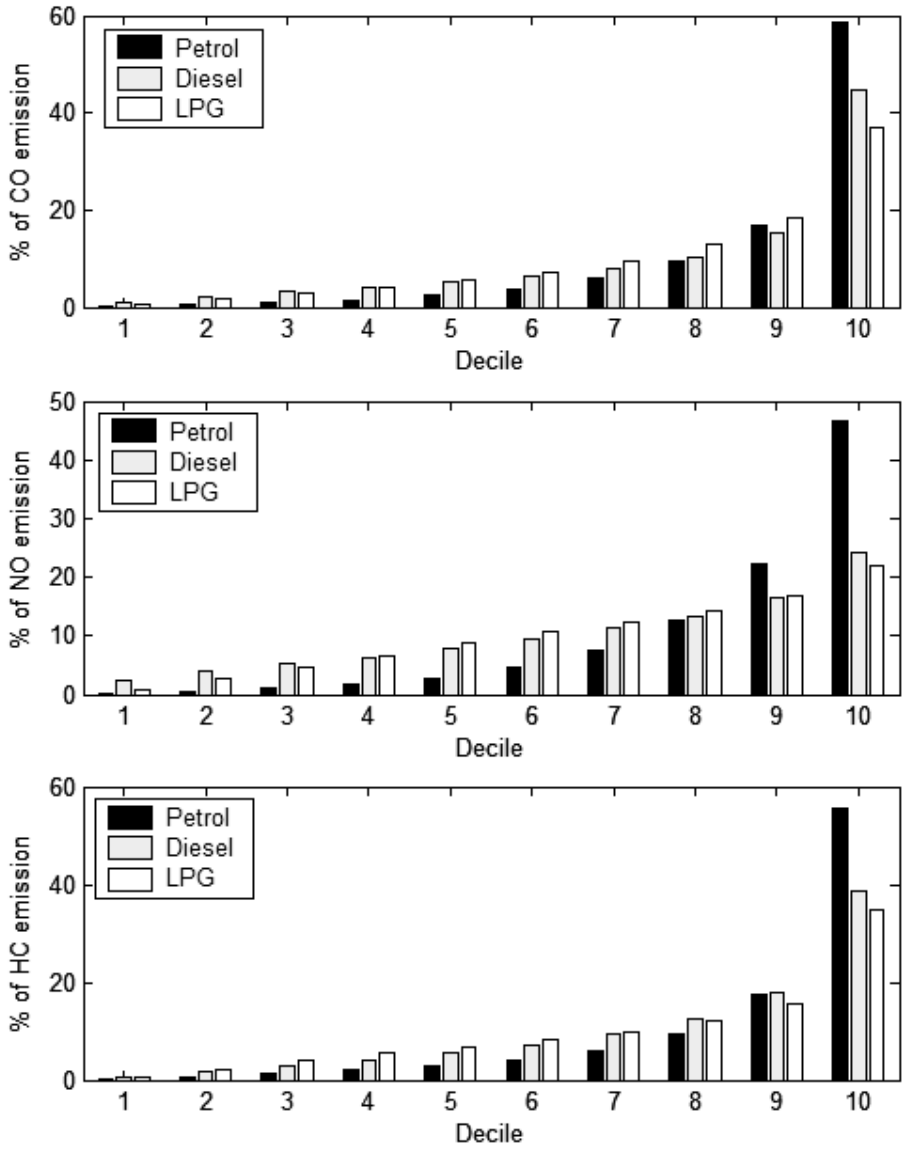

Fig. 4.1 Distribution of gaseous emissions from petrol, light-duty diesel and LPG vehicles

Fig. 4.1 shows that CO emissions of petrol vehicles are more skewed towards high-emitting vehicles while the CO emission distribution of diesel and LPG vehicles are generally similar. NO emissions of diesel and LPG vehicles are evenly distributed between different deciles. Meanwhile, a small number of vehicles contribute greatly towards NO emissions from petrol vehicles. High-emitting vehicles contribute more towards HC emissions from petrol vehicles than diesel and LPG vehicles. The figure shows that NO emissions of various types of vehicles tend to be more evenly distributed compared to CO and HC emissions. This suggests that emissions from petrol vehicles are highly influenced by how well these vehicles are maintained. However, emission from vehicles can also be affected by other factors such as traffic conditions and vehicle age.

4.4.2 Vehicle age and emissions

To examine the relationship between a vehicle's age and gaseous emission, vehicles are classified by their model year and emissions of light-duty petrol, diesel, and LPG vehicles of different model years are shown in Fig. 4.2. The emission standards of vehicles of different years of model are listed on Table 4.2, which shows that newer model vehicles are subject to increasingly stringent emission standards.

Fig. 4.2 shows that newer model petrol vehicles have vastly lower gaseous emissions compared to older vehicles—CO, NO, and HC emission factors of Euro 4 vehicles (vehicles with model years 2006 or later) are 68%, 72%, and 55% lower than those of Euro 2 vehicles. Meanwhile, Euro 4 LPG vehicles emit 62%, 87%, and 87% less CO, NO, and HC compared to Euro 2 vehicles respectively. A decreasing trend in gaseous emissions from light-duty diesel vehicles can also be observed as vehicle model year increases, but the reduction is smaller—CO, NO, and HC emission factors of Euro 4

vehicles are 6%, 10%, and 27% lower than those of Euro 2 vehicles respectively.

Fig. 4.2 also shows that gaseous emission factors of earlier model LPG vehicles are higher than those of petrol and diesel vehicles of the same model year. CO emissions from more recent model LPG vehicles are also higher than petrol and diesel vehicles. NO and HC emission factors of petrol vehicles are the lowest among vehicles with model year 2000 and later.

The reduction in gaseous emissions from vehicles as model year increases may be due to the increasingly stringent emission standards imposed on vehicles. Emission control devices such as catalytic converters are installed to newer-model vehicles in order to meet such standards (Tables 4.2b and c).

Fig. 4.2 shows that NO and HC emission factors of older model LPG vehicles are considerably higher than petrol and diesel vehicles of the same model year. This suggests that engine performance and effectiveness of emission control devices of LPG vehicles deteriorate at a faster rate than petrol and diesel vehicles. This may be due to that LPG vehicles, which consist mainly of public transport vehicles, are on road of long consecutive periods each day, which can hasten engine wear and deterioration of engine performance.

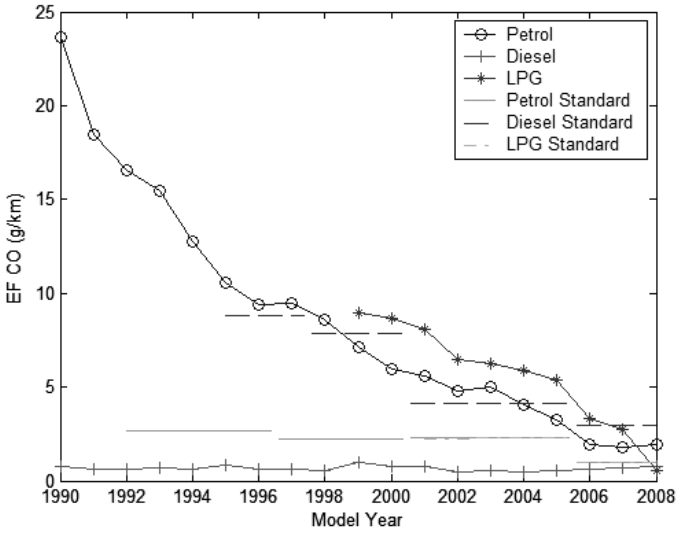
Petrol
Diesel
LPG
Petrol Standard
Diesel Standard
LPG Standard
EF CO (g/km)
Model Year
0
5
10
15
20
25
1990
1992
1994
1996
1998
2000
2002
2004
2006
2008

a)

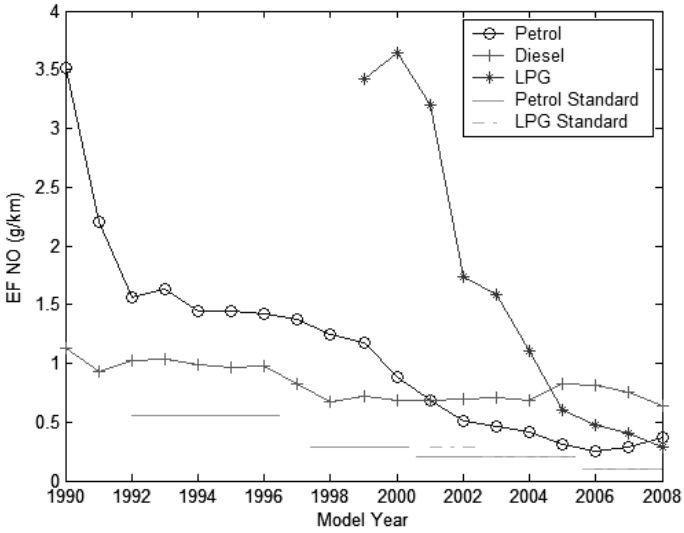
Petrol
Diesel
LPG
Petrol Standard
LPG Standard
EF NO (g/km)
Model Year
0
0.5
1
1.5
2
2.5
3
3.5
4
1990
1992
1994
1996
1998
2000
2002
2004
2006
2008

b)

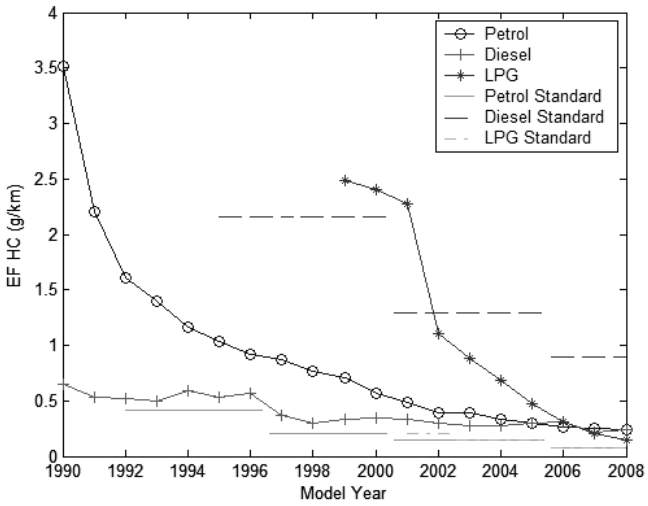

c)

Fig. 4.2 Gaseous emission factors of light-duty vehicles and emission standards in relation to model year (Mean NO emission from light-duty diesel vehicles of all model years satisfy corresponding emission standards and thus not shown)

Comparing emission factors derived from remote sensing measurements with emission standards (Table 4.2) show that on-road emissions of LPG vehicles generally exceed values outlined by emission standards. Gaseous emissions of petrol vehicles of various model years tend to exceed the corresponding emission standard values. Gaseous emission factors of light-duty diesel vehicles, meanwhile, generally comply with the emission standard values.

On-road emission tests, discussed in Chapter 3, show that CO and HC emission factors of an Euro 4 LPG vehicle are similar to those of Euro 2 vehicles. This is opposite of what is observed from remote sensing measurements, where, among LPG vehicles, Euro 4 vehicles have lower emission factors compared to older vehicles.

a)	Pre-Euro	Euro 1	Euro 2	Euro 3	Euro 4
Petrol	Before 1992	1992	1997	2001	2006
Diesel	Before 1995	1995	1998	2001	2006
LPG	N.A.	N.A.	2001	2003	2006

b)	Euro 1	Euro 2	Euro 3	Euro 4
CO (g/km)	2.7	2.2	2.3	1
NO (g/km)	0.55	0.29	0.2	0.1
HC (g/km)	0.42	0.21	0.15	0.08

c)	Euro 1	Euro 2	Euro 3	Euro 4
CO (g/km)	8.82	7.84	4.12	2.94
NO (g/km)	15.69	13.73	9.8	6.86
HC (g/km)	2.16	2.16	1.29	0.9

Table 4.2 a) Emission standards of vehicles of different model years; b) Gaseous emission standards of petrol passenger cars and LPG taxis (Li et al., 2008); c) Gaseous emission standards of diesel LGVs. Emission standards are converted from g/kWh by a factor of 1.96kWh/km (Lenaers, 1996)

4.4.3 Effect of vehicle speed and acceleration on emission

The relationship between vehicle speed and emissions of light-duty vehicles fuelled by petrol, diesel, and LPG are shown in Fig. 4.3 and 4.4. Fig. 4.3 shows the relationship between emission indices and vehicle speed while Fig. 4.4 shows emission factor of vehicles under different speeds.

Fig. 4.3 shows that the CO emissions index of petrol vehicles increases as vehicle speed increases. The increase in CO emission is more pronounced when vehicles travel at speed of over 50 km/h. CO emission indices of diesel and LPG vehicles travelling below 60km/h, meanwhile, show a slightly decreasing trend. In general, NO emission indices of petrol and LPG vehicles increases as vehicle speed increases while diesel vehicles travelling between 25 and 70km/h have mostly similar NO emission indices. There is generally little variation in HC emission index of petrol vehicles travelling below 70km/h while HC emission indices of diesel and LPG vehicles are inversely related to vehicle speed. At speeds of 70km/h or higher, large variations in emission

indices can be observed. This can be due to large variations of emissions from vehicles travelling at such speeds.

Fig. 4.4 shows that CO emission factors of petrol light-duty vehicles follow a U-shape pattern. CO emission factor for such vehicles is the lowest at 50km/h. Meanwhile, CO emission factors of light-duty diesel and LPG vehicles decrease as vehicle speed increases. At different speeds, diesel vehicles have the lowest CO emission factors. LPG vehicles have higher CO emission factors than petrol vehicles when travelling at low speed while the opposite holds at speeds above 60km/h. As vehicle speed increases, NO and HC emissions of light-duty vehicles decrease, regardless of fuel type. LPG vehicles have higher NO and HC emission factors than petrol and diesel vehicles regardless of speed. NO and HC emission factors of petrol and diesel vehicles are mostly similar.

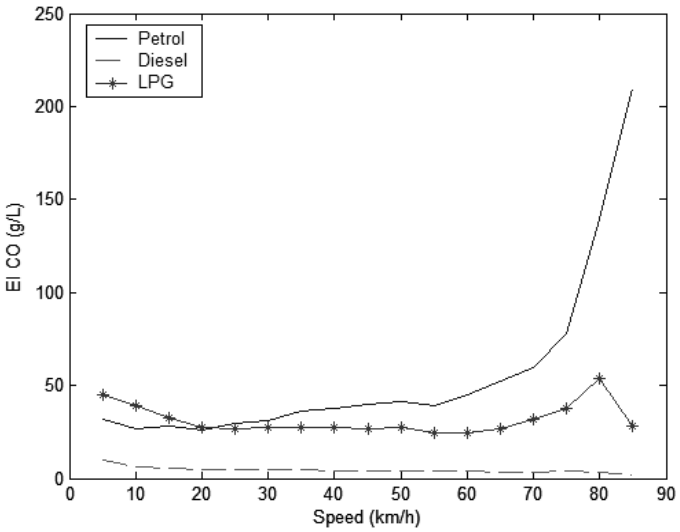

a)

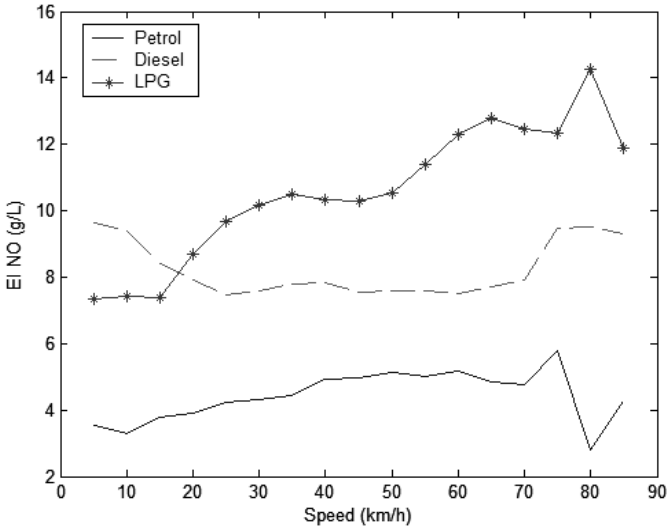

b)

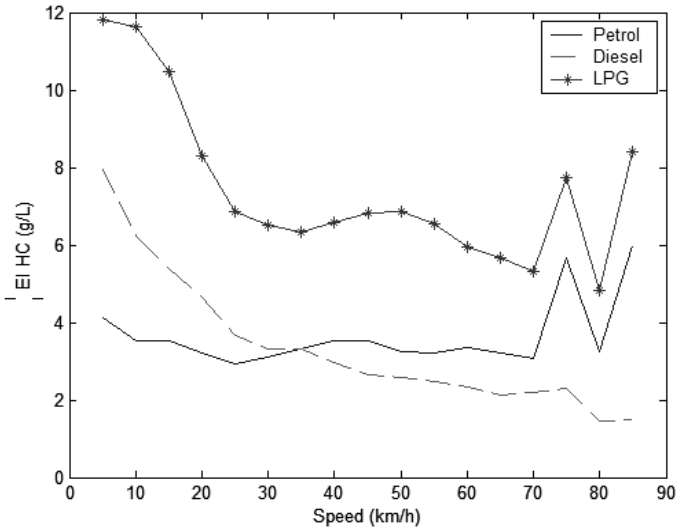

c)

Fig. 4.3 a) CO, b) NO, and HC emission indices of light-duty vehicles under various vehicle speeds

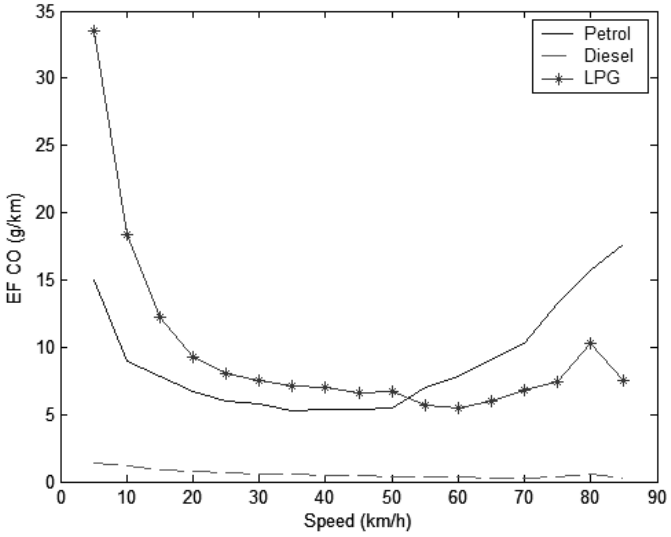
Petrol
Diesel
LPG
EF CO (g/km)
Speed (km/h)
0
5
10
15
20
25
30
35
0
10
20
30
40
50
60
70
80
90

a)

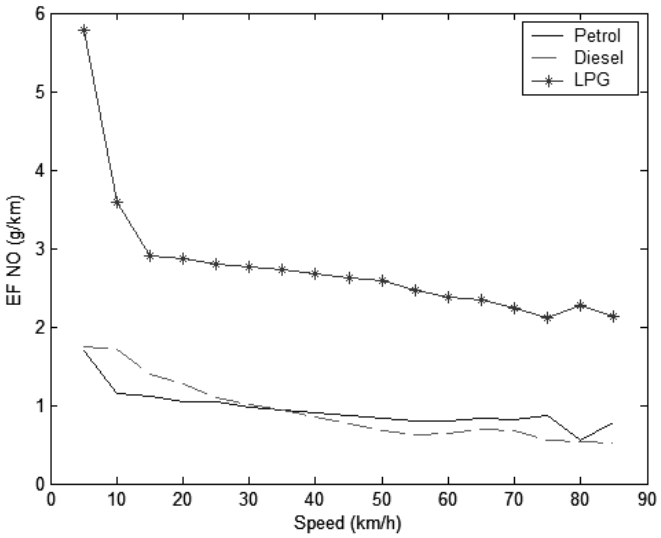
Petrol
Diesel
LPG
EF NO (g/km)
Speed (km/h)
0
1
2
3
4
5
6
0
10
20
30
40
50
60
70
80
90

b)

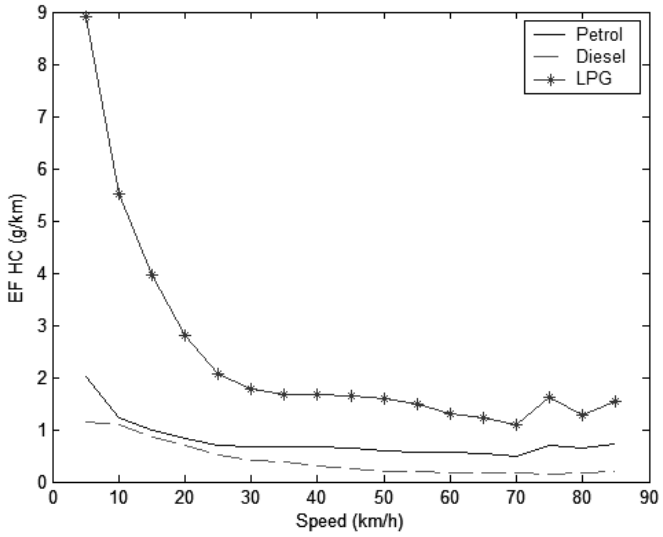

c)

Fig. 4.4 a) CO, b) NO, and c) HC emission factors of light-duty vehicles in relation to vehicle speed

Fig. 4.5 shows the effect vehicle acceleration has on gaseous emissions of light-duty petrol, diesel, and LPG vehicles. It shows that, in general, emission factors of vehicles increase as acceleration rate increases. Gaseous emissions of vehicles undergoing aggressive acceleration are 3 to 4 times greater compared to cruising vehicles. Meanwhile, gaseous emission factors of diesel vehicles undergoing rapid acceleration are 5 to 8 times greater higher than those undergoing cruising. CO and HC emission factors of LPG vehicles undergoing mild acceleration and deceleration are similar to those of cruising vehicles. At a given acceleration rate, emission factors of LPG vehicles are generally higher compared to petrol and diesel vehicles. The result shown in Fig. 4.5 are mostly similar to results found in on-road emission measurements, discussed in Chapter 3.

From this it can be observed that, in general, gaseous emission factors of a vehicle are the lowest when it is decelerating and the highest when it undergoes aggressive acceleration. The high gaseous emission factors of vehicles undergoing rapid

acceleration may be a result of high concentration of gaseous pollutants within the tailpipe exhaust and the vehicle having higher exhaust flow rate, resulting from heavier engine work, during acceleration (Ko and Cho, 2006; Chen et al., 2007).

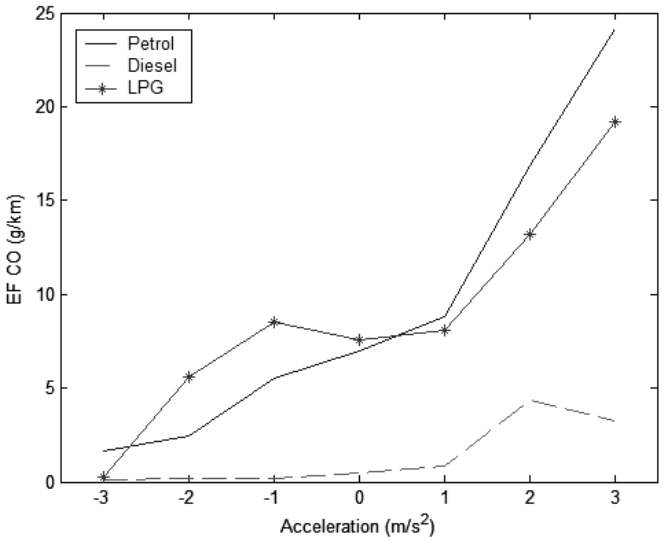

a)

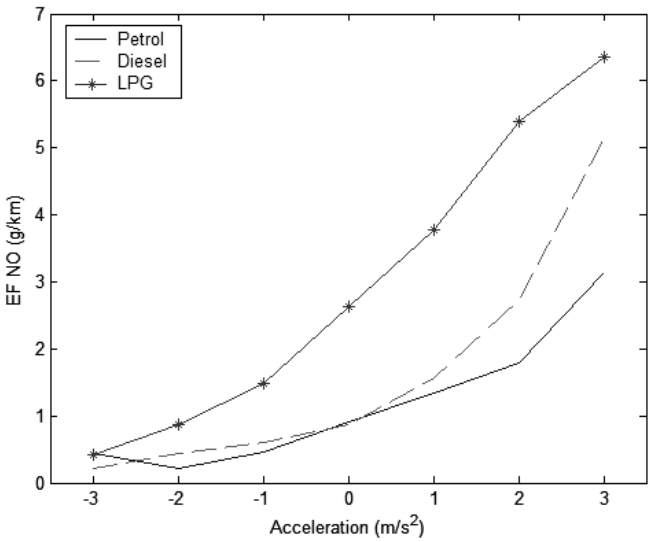

b)

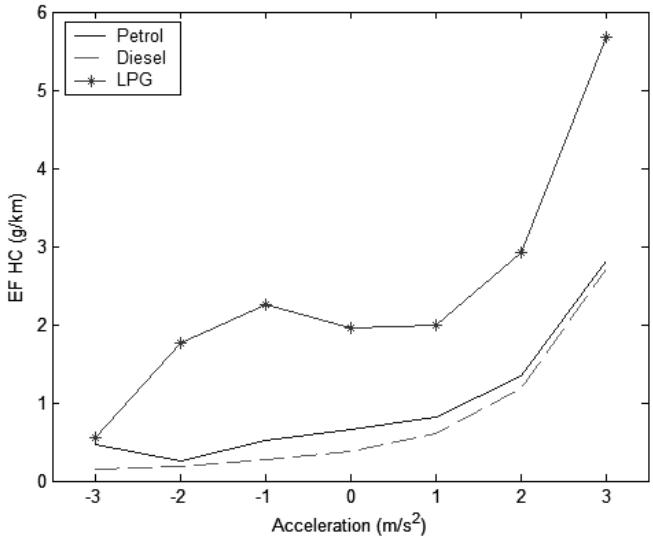

c)

Fig. 4.5 a) CO, b) NO, and c) HC emission factors of petrol, light-duty diesel, and LPG vehicles under various acceleration rates

4.4.4 Road grade and vehicle emissions

A vehicle's engine load is higher when travelling uphill compared to the engine load of a vehicle travelling on a roadway with zero or negative road grade (Kean et al., 2003; Li et al., 2007). At a given speed, engine load is higher and thus a vehicle consumes more fuel and emits higher level of pollutants, when travelling at steeper grades (Park and Rakha, 2006). To examine the effect of road gradient on vehicle emission in Hong Kong, gaseous emission factors of vehicles travelling on three road segments of varying gradients are investigated. The average vehicle speed and acceleration of the road segments are 40-50km/h and 1.5m/s^2 respectively.

Table 4.3 shows the relationship between road grade and gaseous emissions from petrol passenger cars and LPG taxis. The table shows that taxis travelling on a roadway with a large uphill gradient emit higher levels of CO and NO than vehicles travelling downhill while the opposite holds for HC emissions. Passenger cars travelling uphill emit higher

amounts of NO than those travelling downhill. Meanwhile, the relationship between road gradient and emissions of CO and HC from petrol vehicles is not clear.

Site No.	23	27	35
Road Grade (%)	6.9	1.7	-0.9
Taxi			
CO (g/km)	9.50±0.34	8.80±0.21	8.30±0.22
NO (g/km)	3.15±0.06	2.81±0.05	2.73±0.04
HC (g/km)	1.32±0.04	2.06±0.06	2.79±0.10
Passenger Car			
CO (g/km)	7.67±0.52	12.52±0.53	9.02±0.87
NO (g/km)	1.44±0.07	0.98±0.03	0.89±0.04
HC (g/km)	0.62±0.04	0.98±0.06	0.73±0.08

Table 4.3 Gaseous emission factors on roadways of varying gradient

While vehicles travelling uphill generally emit vastly higher levels of gaseous pollutants than those travelling on roadways with zero or negative gradients (Park and Rakha, 2006; Li et al., 2007), negative relationship between HC emission and road grade has been observed in past remote sensing studies (Zhang et al., 1993). The higher CO and NO emissions observed from taxis travelling uphill can be attributed to the higher power demands for the engine and thus greater fuel consumption (Kean et al., 2003; Li et al., 2007). Meanwhile, high HC emission factor observed from taxis travelling downhill can be attributed to such vehicles consuming minimal amount of fuel (Zhang et al., 1993). This results in lower CO_2 emissions and, by Eqs. 4.3 and 4.4, higher HC emission indices and thus emission factors. Table 4.3 shows that while road grade greatly affect gaseous emissions of a single vehicle (Park and Rakha, 2006), variability between different vehicles can result in large variations in gaseous emissions from vehicles travelling on a single road segment (Mazzoleni et al., 2004b). This can result in gaseous emission factors not being positively correlated with road grade, as found here

and in Colberg et al. (2005).

4.5 Comparison of On-road and Remote Sensing Emission Measurements

To compare the vehicle emission measurements collected using different methods, gaseous emission factors of taxis and LGVs obtained from on-road and remote sensing measurements, discussed in Chapter 3 and this chapter respectively, are examined.

Gaseous emission factors of taxis and LGVs derived from on-road measurements, discussed in Chapter 3, and remote sensing techniques, discussed in this chapter, are shown in Table 4.4. Emission factors, derived from on-road measurements, are compared with emission factors, derived from remote sensing measurements, of vehicles with the same model year. The comparison is made to determine whether one measurement method yields higher emission factors compared to the others.

a)	Model Year	CO (g/km)	NO (g/km)	HC (g/km)
RS	2001	7.71±0.02	2.06±0.01	1.35±0.02
	2003	6.17±0.12	1.17±0.02	0.87±0.02
	2005	5.36±0.28	0.60±0.04	0.47±0.04
	2007	2.76±0.27	0.30±0.06	0.20±0.02
On-road	2001	12.40±0.11	2.51±0.01	2.17±0.05
	2003	7.77±0.07	1.31±0.01	1.23±0.02
	2005	2.73±0.04	0.30±0.01	0.32±0.01
	2007	14.52±0.19	0.24±0.01	1.26±0.04

b)	Model Year	CO (g/km)	NO (g/km)	HC (g/km)
RS	2001	0.55±0.04	0.78±0.02	0.33±0.01
	2003	0.47±0.02	0.79±0.02	0.28±0.01
	2005	0.48±0.02	1.21±0.01	0.31±0.01
	2007	0.65±0.03	1.05±0.02	0.21±0.01
On-road	2001	1.07±0.01	2.13±0.02	0.64±0.02
	2003	1.47±0.02	2.45±0.03	0.59±0.01
	2005	1.06±0.01	2.67±0.02	0.35±0.01
	2007	0.41±0.01	1.71±0.01	0.05±0.01

Table 4.4 Emissions factors of a) taxis; and b) LGVs using on-road and remote sensing measurements (10-80 km/h)

The table shows that emission factors of LGVs derived from on-road measurements tend to be higher than emission factors of LGVs of the same model years derived from remote sensing measurements, with HC emissions factors of model year 2007 LGVs being the exception. Gaseous emissions of taxis are generally higher when measurements were obtained on-road in comparison with remote sensing methods, with the exception of CO and HC emissions from model year 2005 taxis. As shown in Fig. 4.6, a majority of vehicles travelled past the remote sensing system at speeds above 30km/h. Comparing Fig. 4.6 with Fig. 3.3 shows that remote sensing methods sampled emissions from vehicles travelling at higher speeds. Since emission factors are inversely related to vehicle speed, the speed at which vehicles generally travel past remote sensing instruments would result in lower emission factors.

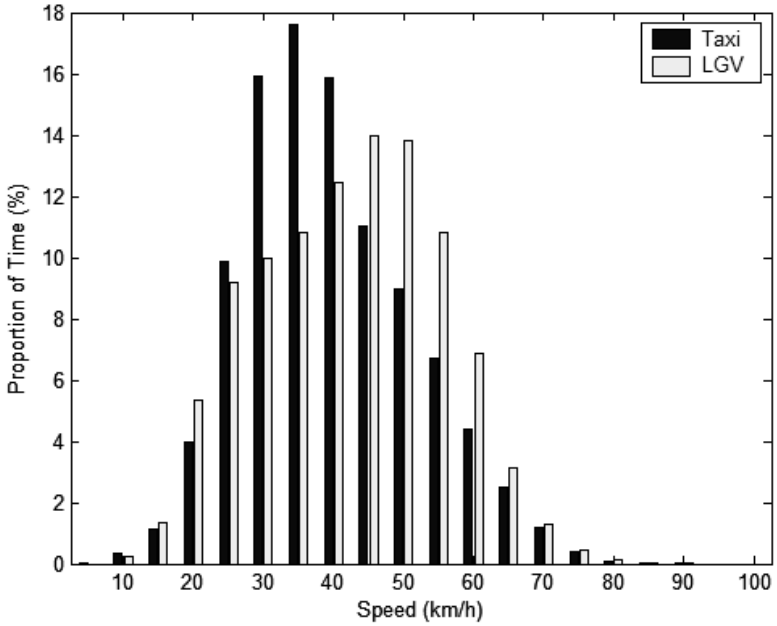

Fig. 4.6 Speed distribution of taxis and LGVs travelling past remote sensing instruments

To examine emissions of vehicles travelling at similar speeds, emission factors of taxis and LGVs, derived from remote sensing and on-road measurements, of various speeds and model years are shown in Fig. 4.7 and 4.8 respectively. Fig 4.7 shows that, at different speeds, on-road measurements of taxi emissions yielded higher CO emission factors than remote sensing measurements. NO emissions from older model taxis (vehicles with model years 2001 and 2003) measured using the PEMS tend to be higher than those obtained using remote sensing measurements. There are more discrepancies between HC emission factors of taxis derived from on-road and remote sensing measurements.

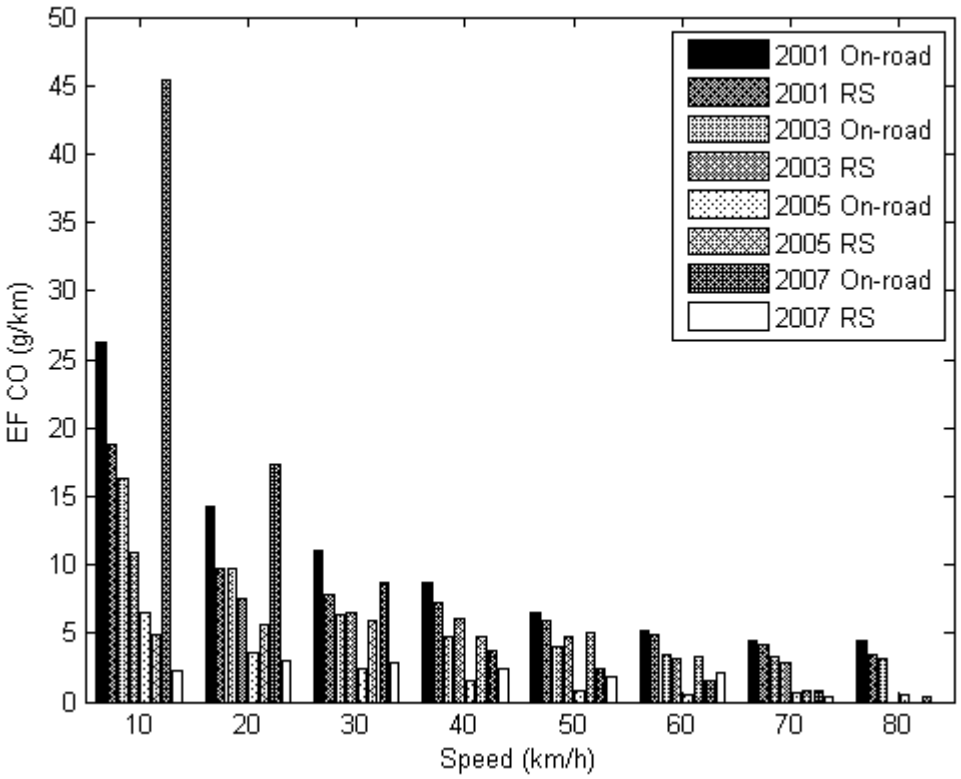
EF CO (g/km)
Speed (km/h)
2001 On-road
2001 RS
2003 On-road
2003 RS
2005 On-road
2005 RS
2007 On-road
2007 RS

a)

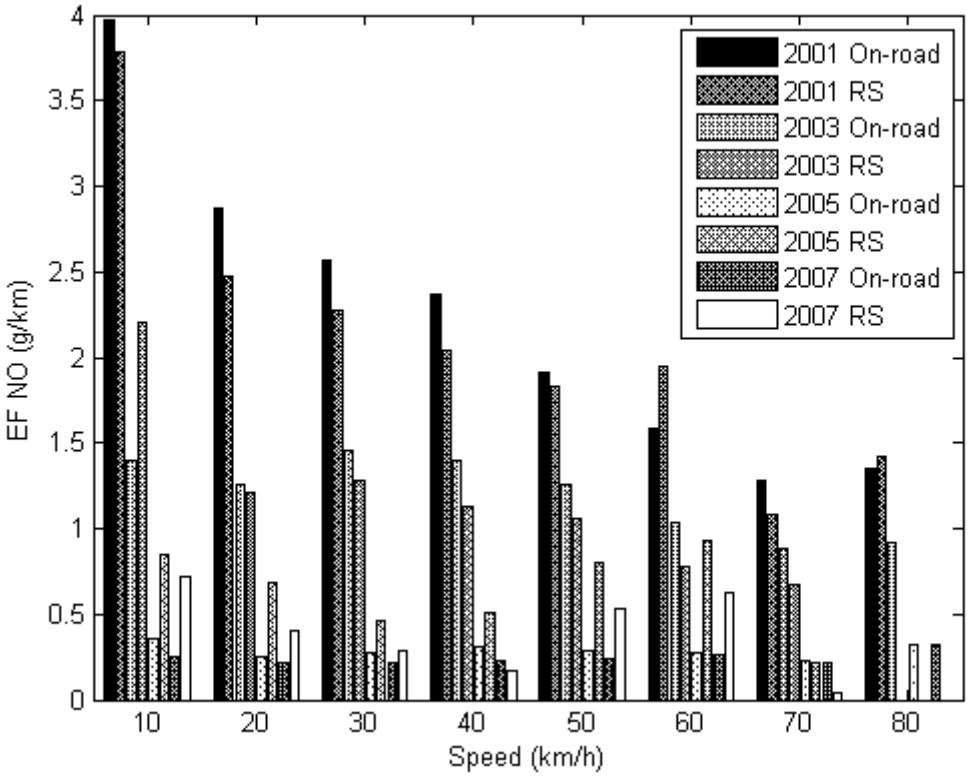
EF NO (g/km)
Speed (km/h)
2001 On-road
2001 RS
2003 On-road
2003 RS
2005 On-road
2005 RS
2007 On-road
2007 RS

b)

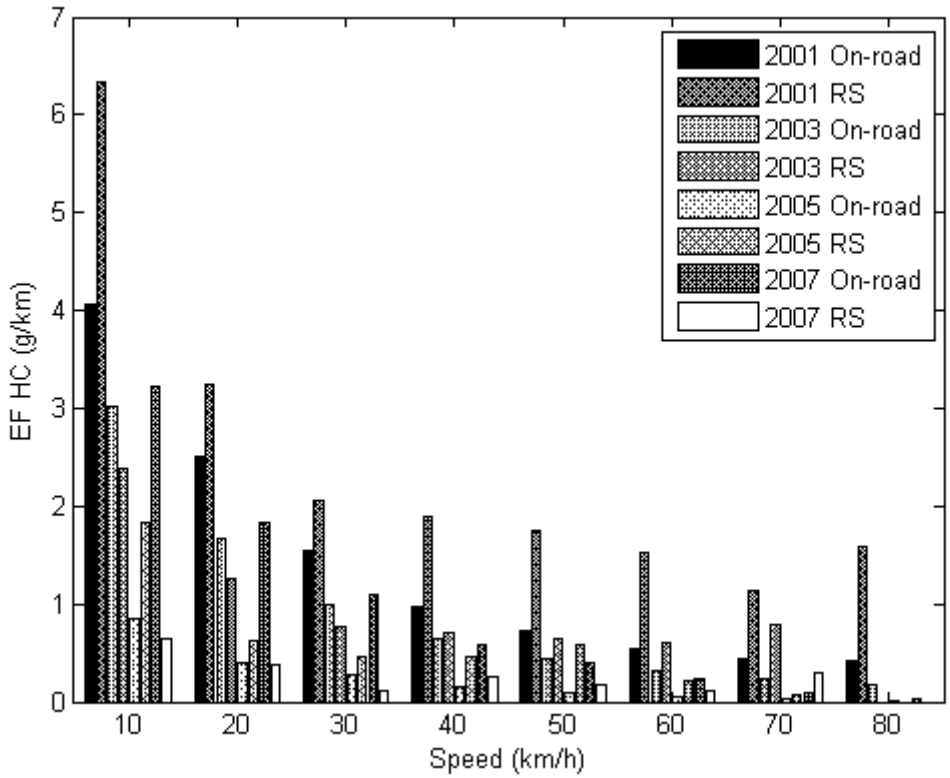

c)

Fig. 4.7 Emission factors of taxis obtained from remote sensing and on-road measurements

Fig. 4.8 shows the gaseous emission factors, derived from on-road and remote sensing measurements, of LGVs travelling between 10 and 80 km/h. It shows that CO and HC emission factors of LGVs with model years 2001 and 2003 are higher when measurements are collected using on-road equipment. LGVs with model year 2007 have higher CO and HC emission factors when measurements are made using remote sensing techniques. NO emission factors of different model years, derived from on-road measurements, are higher than those derived from remote sensing measurements.

The discrepancies in gaseous emission factors of older model (2001-2005) LGVs may be due to the lack of emission treatment devices such as catalytic converters in the LGVs used for on-road testing (Table 3.1). Likewise, a number of model year 2007 LGVs sampled by remote sensing measurements may not be equipped with emission

treatment devices. This can result in remote sensing measurements yielding higher gaseous emission factors of LGVs with model year 2007 in comparison to the vehicle used for on-road measurements, which is equipped with an oxidation catalytic converter.

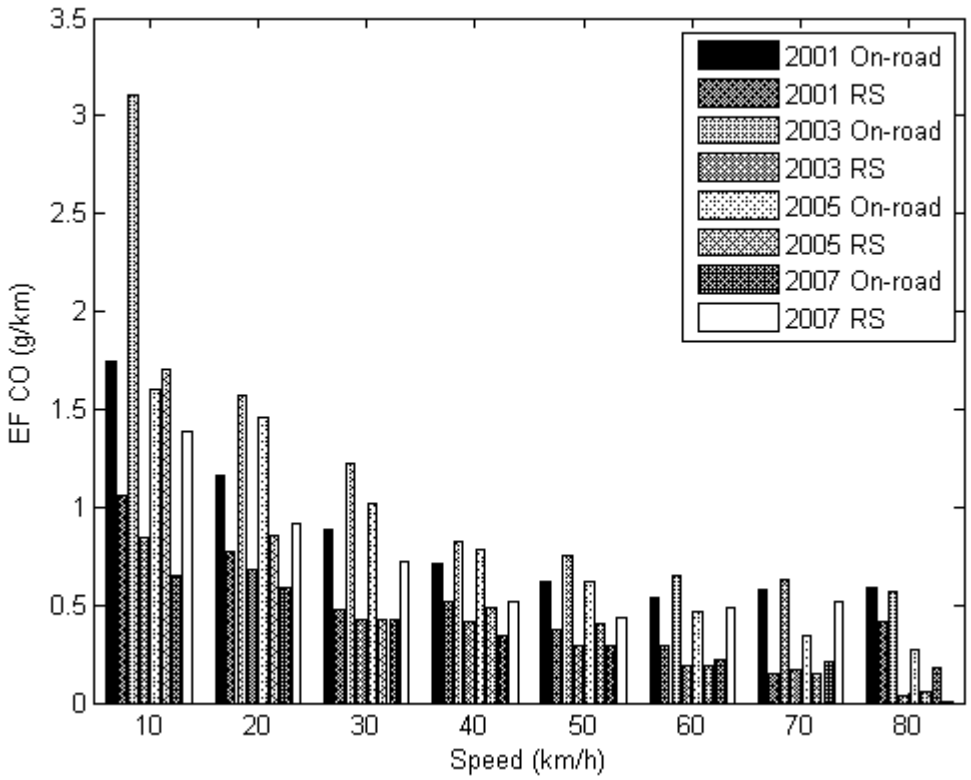

a)

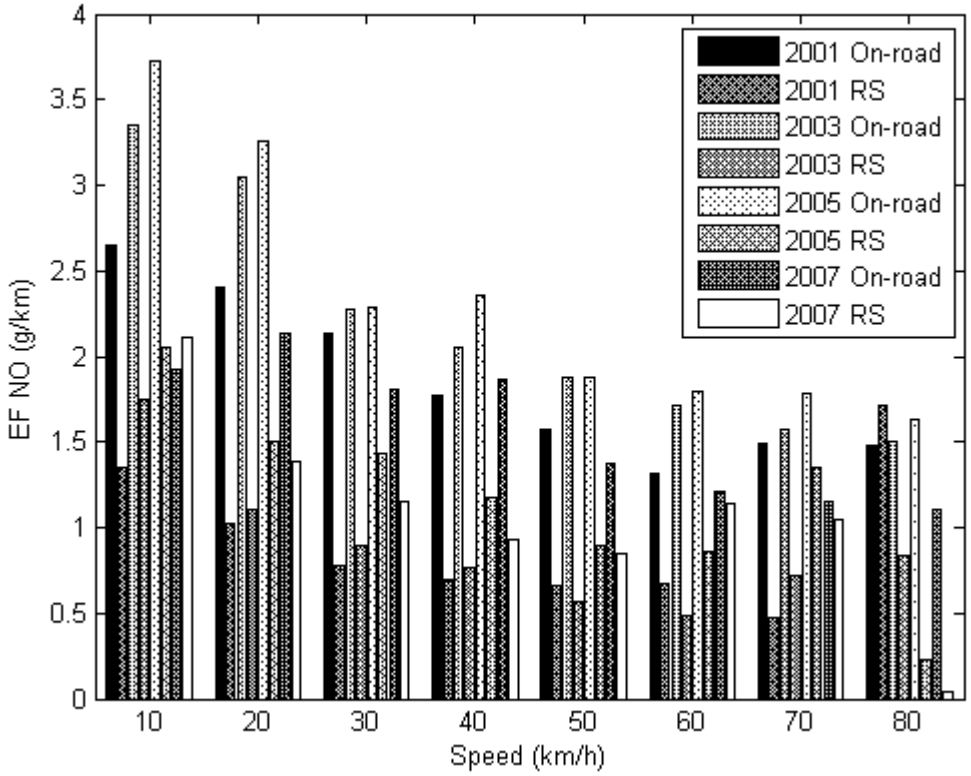

b)

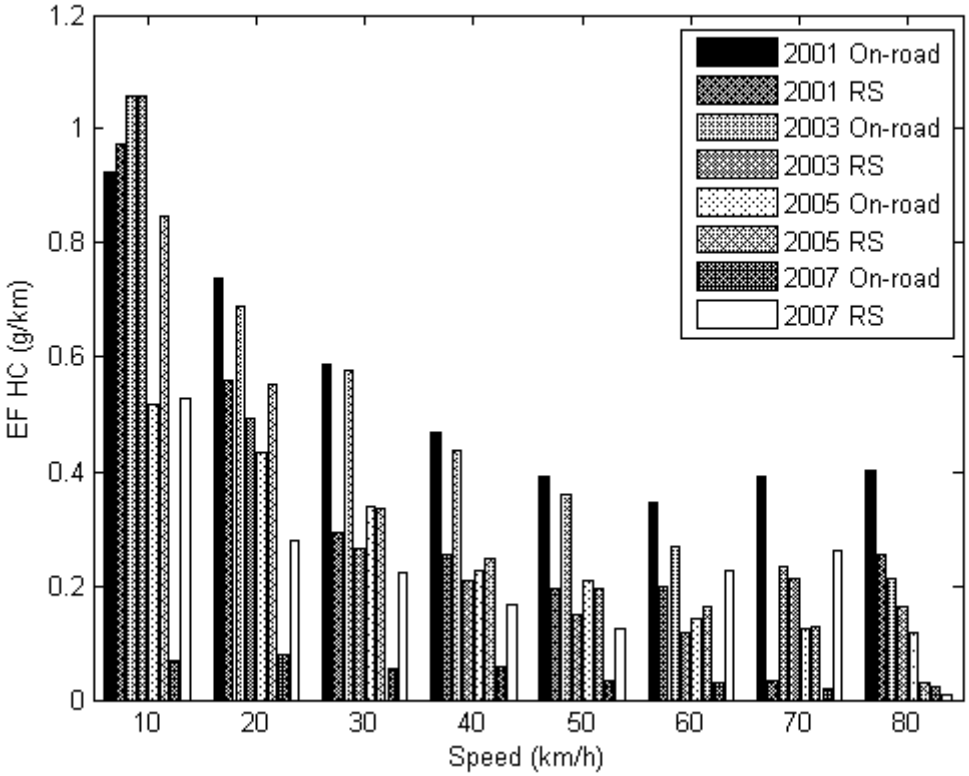

c)

Fig. 4.8 Emission factors of diesel LGVs derived from on-road and remote sensing measurements

Fig. 4.9 shows the linear relationship between gaseous emission factors, derived from on-road and remote sensing measurements, of taxis of various model years under different speeds. Since the engine management system of the vehicle selected for on-road tests appears to be malfunctioning, emission factors of taxis with model year 2007 are omitted in the computation of correlation between emission factors derived from on-road and remote sensing measurements. The figure shows that the slopes of regression lines for CO and NO emission factors are smaller than 1, indicating that emission factors derived from on-road measurements are higher than those derived from remote sensing measurements. Meanwhile, the slope of the regression line for HC emission factors is greater than 1, indicating that remote sensing measurements yield higher emission factors. The R^2 values of the fitted lines are larger than 0.8, suggesting that the equations can be considered an adequate baseline for correlating taxi emission factors derived from different measurement methods.

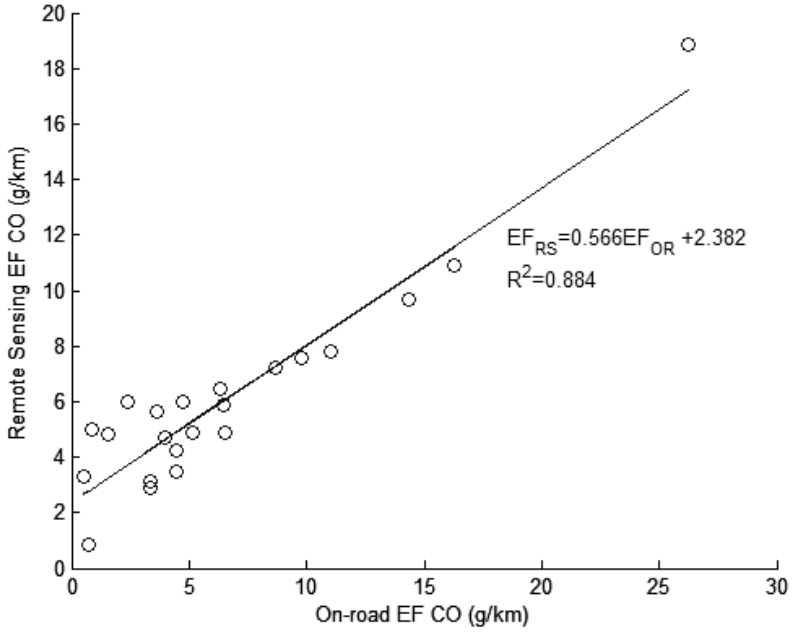

a)

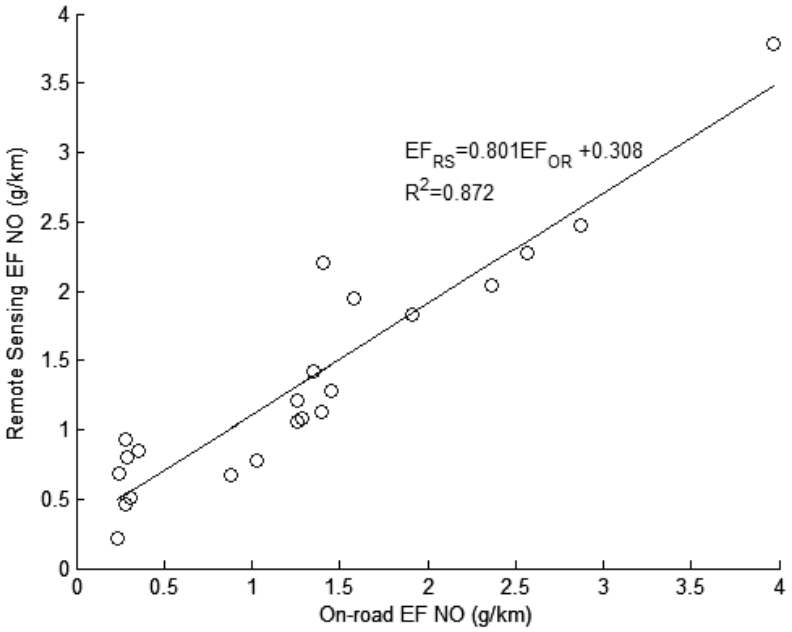

b)

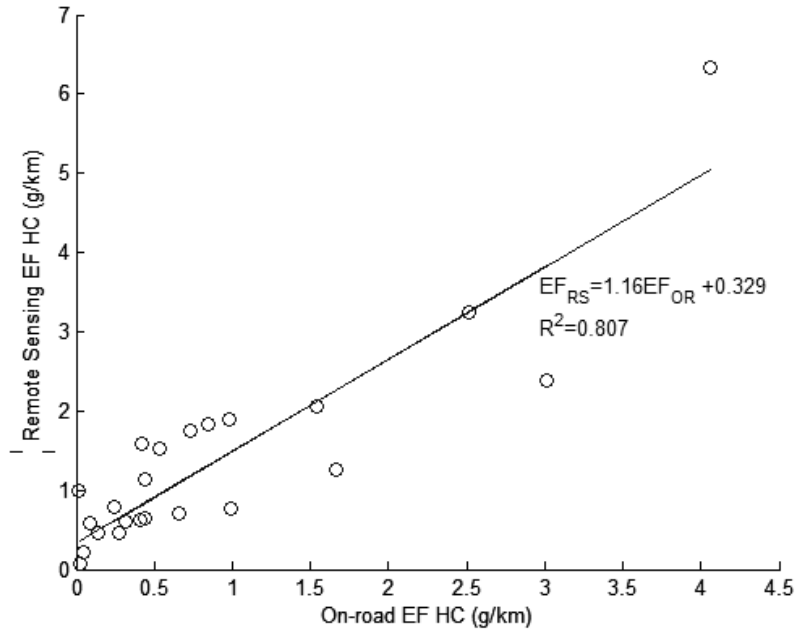

c)

Fig. 4.9 Linear relationship between a) CO, b) NO, and c) HC emission factors of taxis derived from on-road (OR) and remote sensing (RS) measurements

Fig. 4.10 shows that regression lines of CO, NO, and HC emission factors have slope smaller than 1, indicating that emission factors are higher when measurements are collected on-road. The correlations between emission factors derived from on-road and

remote sensing measurements are stronger for taxis than for LGVs. Larger variations in gaseous emission factors of LGVs can be attributed to LGVs having different engine size and power and vehicle weight.

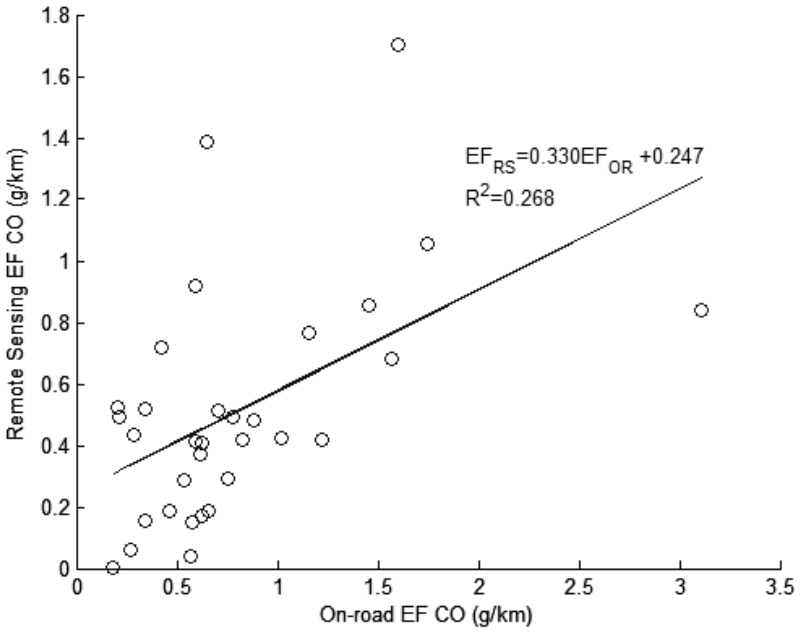

a)

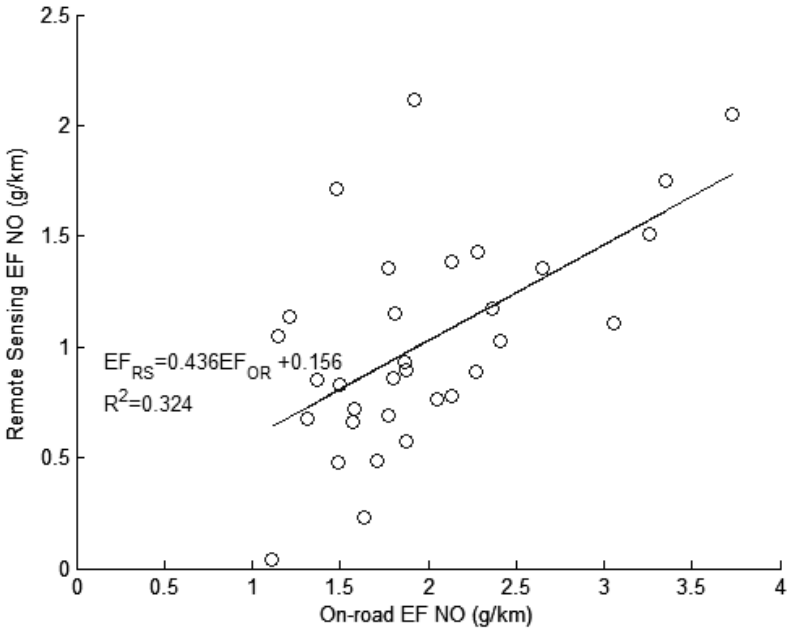

b)

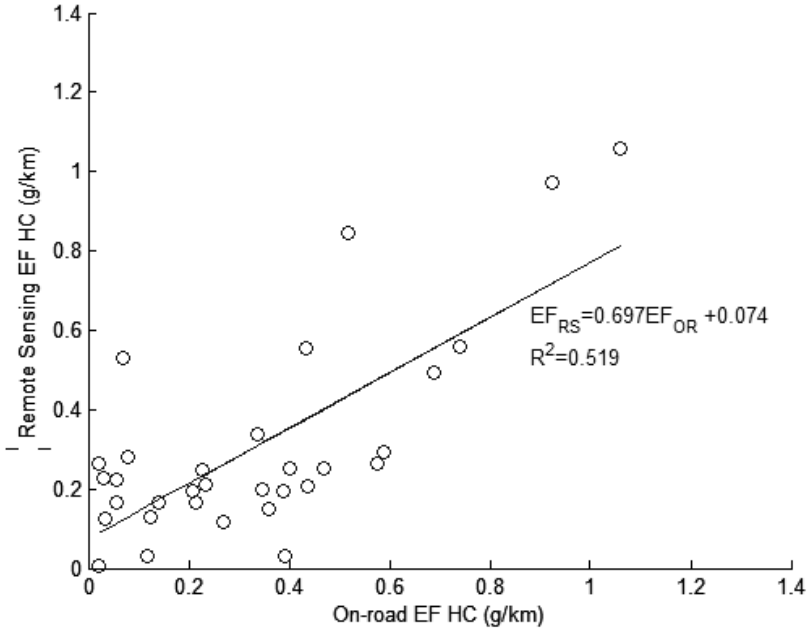

c)

Fig. 4.10 Linear relationship between a) CO, b) NO, and c) HC emission factors of LGVs derived from on-road (OR) and remote sensing (RS) measurements

Table 4.4 and Figs. 4.7-10 show that gaseous emission factors of vehicles derived from on-road measurements are generally higher compared to those derived from remote sensing measurements. This may be due to that on-road measurements collect a vehicle's exhaust from within the vehicle's exhaust pipe while remote sensing techniques measure the content of a vehicle's exhaust after it is expelled into the atmosphere. The source detector module is generally set at a height matching that of a typical vehicle exhaust pipe. However, the height of a vehicle's exhaust pipe may not match that of the source detector module. This can lead to larger dilution of the vehicle's exhaust taking place, which lowers the concentrations of gaseous pollutants being measured by the remote sensing unit. Furthermore, the exhaust pipe of many goods vehicles is located at the centre of the vehicle, rather than at the back. Thus emissions of such vehicles may have been further diluted, which results in lower emission factors, as

it travels past the remote sensing unit.

Bishop and Stedman (1996) showed that, when travelling at similar speeds, remote sensing measurements of a vehicle's emission could vary greatly between tests. The variation in emission from high-emitting vehicles was greater (Bishop and Stedman, 1996; Samuel et al., 2005). This suggests that test duration is too short for the remote sensing system to measure a vehicle's emission accurately. Thus remote sensing measurements may not accurately reflect a vehicle's emission at the time the vehicle travels past the remote sensing instruments. That is why it is vital to validate the remote sensing measurements and carefully planned on-road emission measurements on sampled vehicles provide a good opportunity of such validation exercise.

Transformation of NO in the vehicle exhaust after its release into the atmosphere can also result in lower NO emission factors being derived from remote sensing measurements. Previous work has found that over 90% of NO_x emitted by vehicles is in the form of NO (Carslaw and Beevers, 2004; Alvarez et al., 2008). Meanwhile, field measurements show that 65-80% of NO_x measured in close proximity of a roadway is in the form of NO (Väkevä et al., 1999; Pandey et al., 2008). This indicates that rapid transformation of NO into NO_2 takes place as the vehicle's exhaust exits the tailpipe, due to the presence of oxidants such as ozone and free radicals near the road surface (Shi and Harrison, 1997; Kenty et al., 2007). Such transformations can result in lower levels of NO detected by the source detector module and thus lower NO emission factors being derived from remote sensing measurements. Since remote sensing techniques are not capable of measuring NO_2 concentrations, the NO/NO_x ratio of the vehicles' emission detected by the remote sensing instrument is not known.

The above observations on emission factors derived from on-road and remote sensing

emission measurement should be considered preliminary, due to the small number of vehicles considered for on-road measurements. In particular, gaseous emission factors from the Euro 4 LPG vehicle (Table 3.4) used for on-road testing are vastly higher compared to average emission factors of vehicles with the same emission standards, as shown in Fig. 4.2 and Table 4.5. This can greatly skew the correlation between on-road and remote sensing emission factors. Thus Euro 4 LPG vehicles are not considered in the computation of correlation between on-road and remote sensing emission factors. Nevertheless, such comparisons can help establish a correlation between on-road and remote sensing emission measurements and improve capabilities of high-emitting vehicle identification programs, where measurements are collected using remote sensing techniques.

4.6 Chapter Summary

In this chapter on-road gaseous emissions from a number of vehicle types, measured using remote sensing techniques, are investigated. The results show that the distribution of vehicle emission is more skewed among petrol vehicles than diesel or LPG vehicles. Meanwhile, NO emissions from vehicles of different fuel types tend to be more evenly distributed than CO and HC emissions. A reduction in gaseous emissions from petrol, diesel, and LPG vehicles can be observed as model year of vehicles increases, likely a result of better engines complying with more stringent emission standards.

In general, diesel vehicles emit higher levels of NO and lower amounts of CO and HC compared to petrol vehicles of the same vehicle type. LPG taxis and light buses have higher gaseous emission factors compared to petrol passenger cars and diesel light buses, respectively. The high emission from LPG vehicles may be due to that such vehicles are often operated for long consecutive periods of time, which can hasten

deterioration of engine performance of these vehicles.

For vehicles of different fuel type, there appears to be no clear correlation between vehicle speed and gaseous emission indices of light-duty vehicles. Meanwhile, vehicle speed and gaseous emission factors are inversely correlated. Light-duty vehicles of different fuel types generally emit the least amount of gaseous pollutants while decelerating. High emission levels are observed when vehicles undergo heavy acceleration. CO and NO emissions from taxis increase as road gradient increases while the relationship between road grade and emissions from petrol passenger cars appears to be weak.

Gaseous emission factors of taxis and diesel LGVs, derived from on-road and remote sensing measurements, are compared. The results show that on-road measurements yielded higher gaseous emission factors from vehicles as dispersion reduce gaseous concentrations detected by remote sensing instruments. Reaction of NO in the atmosphere can also result in lower concentrations of NO detected by remote sensing equipment compared to on-board measurements, thus reducing emission factors derived from remote sensing measurements. The limitations of such comparisons, arising from differences in sample size and computation methods, are also discussed.

Chapter 5

On-road Emissions and Air Quality in the Urban Setting

5.1 Introduction

Following the analysis of vehicle emissions characteristics based on the on-road and remote sensing measurements in Chapters 3 and 4, this chapter will look into the impacts of vehicle emissions on the urban microenvironment.

Air quality along busy roadways and adjacent areas of Hong Kong will be examined by studying the temporal variations in air quality at monitoring stations located at different districts within the city. The effect vehicle emission has on air quality at stations in different sections will be estimated by statistical methods. The effect of vehicle emission on urban air quality will be investigated by studying the conditions under which vehicles generally operate in the urban area.

5.2 Air Quality Monitoring Network in Hong Kong

Three air quality monitoring stations are set up near major urban streets in Hong Kong by the Hong Kong Environmental Protection Department to monitor air quality at the roadside. The department also set up monitoring stations in the urban area and new towns, major residential areas located in the suburban sections of the city, to monitor background air quality in various parts of Hong Kong (HKEPD, 2006). Density of high-rise buildings within the urban area is high and street canyons are commonly found. Background stations are located at the rooftop level and monitors the quality of air people living in the area is exposed to. One additional station is set up in a remote location to monitor regional air quality. All stations monitor concentrations of sulphur

dioxide (SO_2) while ozone is monitored at all stations aside from the roadside stations (HKEPD, 2006). The properties of the stations and the pollutants being monitored at each station are listed in Table 5.1. The location of each monitoring station is shown in Fig 5.1.

At each monitoring station, an API 300 monitor tracks CO concentrations by using non-dispersive infra-red absorption with gas filter correlation. NO_2 and NO concentrations are measured using an API 200A Monitor Laboratories 8400 chemiluminescence monitor, while PM_{10} measurements are made using a TEOM 1400 monitor. Such equipment are commonly used for monitoring air quality at permanent monitoring stations (Gramsch et al., 2006; Wang and Lu, 2006; Pandey et al., 2008). Periodic data audits are carried out at each station to maintain measurement accuracy and precision. A system audit reviewing the quality of the quality assurance process on the monitoring network is carried out annually (HKEPD, 2006). Concentrations of air pollutants are recorded hourly.

In the following, CO, NO_2, and PM_{10} measurements collected from each monitoring station between January 2001 and December 2005 are analysed. To examine daily variations in air quality, hourly average concentrations of the three pollutants are computed for each hour of the week by taking the average of concentrations measurements obtained at that particular hour.

Station	Abbreviation	Station Type	Height Above Ground (m)	Distance to nearest Major Roadway (m)	Avg. Daily Traffic at Major Roadway (‘000)	Pollutants Monitored
Causeway Bay	CB	Roadside	3	<5	25	CO, NO, NO_2, PM_{10}
Central	C	Roadside	4.5	<5	35	CO, NO, NO_2, PM_{10}
Mong Kok	MK	Roadside	3	<5	50	CO, NO, NO_2, PM_{10}
Central-Western	CW	Urban	18	150	12	NO, NO_2, PM_{10}
Eastern	E	Urban	15	150	25	NO_2, PM_{10}
Sham Shui Po	SSP	Urban	17	20	40	NO, NO_2, PM_{10}
Kwai Chung	KC	Urban	13	30	100	NO, NO_2, PM_{10}
Kwun Tong	KT	Urban	25	50	50	NO, NO_2, PM_{10}
Tsuen Wan	TW	Urban	17	50	55	CO, NO, NO_2, PM_{10}
Sha Tin	ST	New Town	21	200	45	NO, NO_2, PM_{10}
Tai Po	TP	New Town	25	80	20	NO_2, PM_{10}
Tung Chung	TC	New Town	27.5	100	40	CO, NO, NO_2, PM_{10}
Yuen Long	YL	New Town	25	50	15	NO_2, PM_{10}
Tap Mun	TM	Rural	11			CO, NO, NO_2, PM_{10}

Table 5.1 Air quality monitoring network in Hong Kong (HKEPD, 2006; HKTD, 2009)

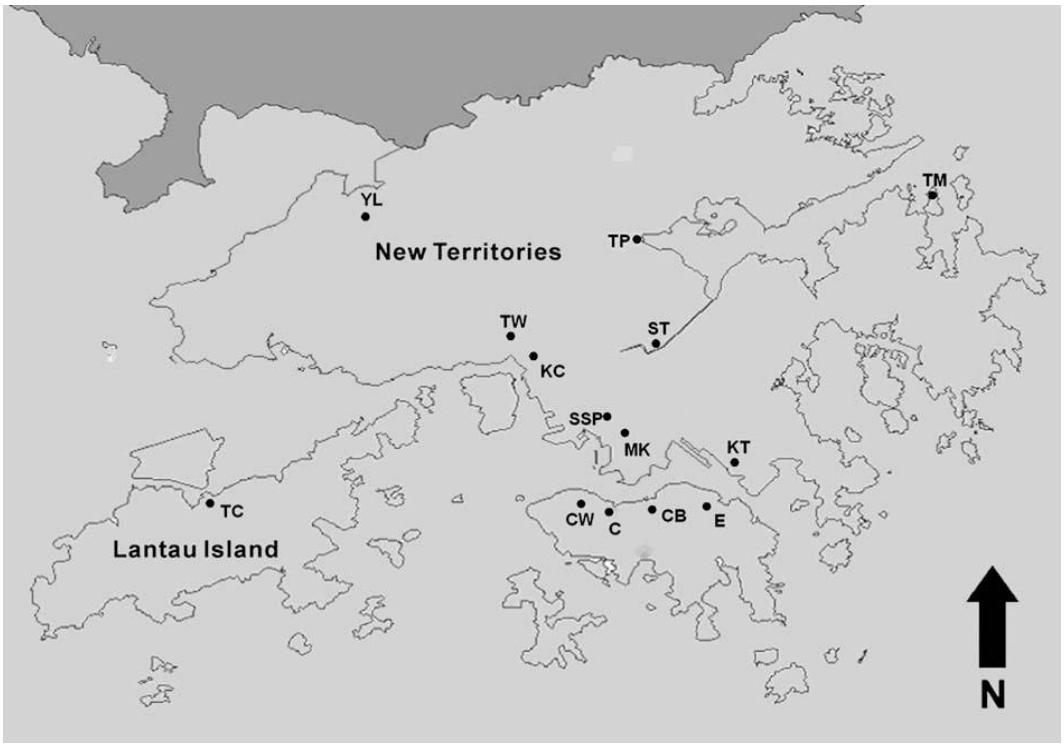

Fig. 5.1 Locations of air quality monitoring stations in Hong Kong

5.3 Urban Air Quality in Relation to Vehicle Emissions

5.3.1 Air quality and its variations in relation to traffic

Fig. 5.2 shows the daily variation in traffic typically observed in the neighbourhood of several monitoring stations, expressed in terms of percentage of average weekly traffic volume (HKTD, 2009). In the urban area, two peaks in traffic, which corresponds to the morning and evening rush hour, can be observed on weekdays. Traffic volume of Saturdays tends to be similar to those observed on weekdays, while traffic volume on Sundays is generally 80% of weekday levels.

Daily variations in CO, NO_2, and PM_{10} concentrations at roadside and background monitoring stations are shown in Fig 5.3. The air quality patterns shown in the figures are representative of those observed at stations of the same type. Daily variations in

concentrations of NO_2 and PM_{10} at stations of the same type are similar, likewise for CO concentrations at the roadside. Air quality at the new town station TC is shown separately as patterns in NO_2 and PM_{10} concentrations observed from the station are different from those observed at other new town stations. This is likely due to the station TC's close proximity to the airport.

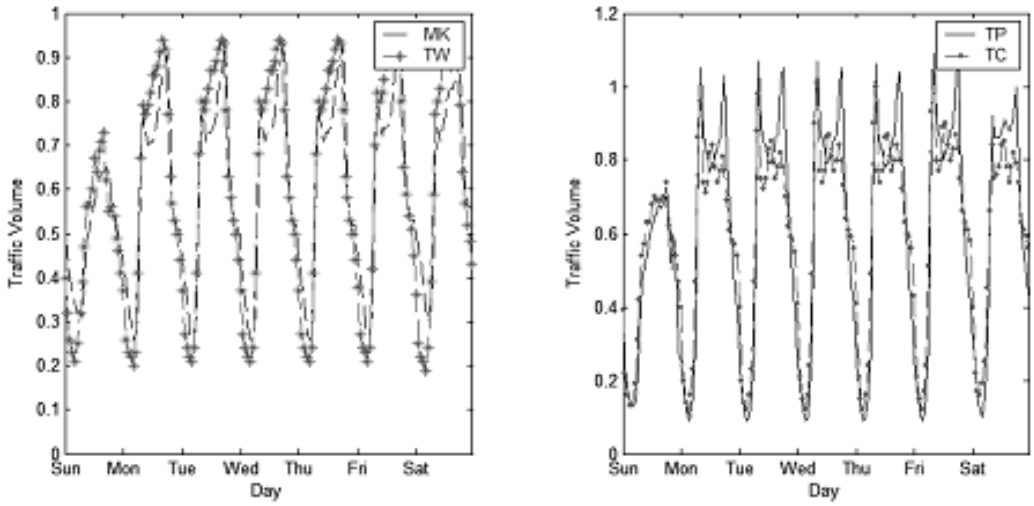

Fig. 5.2 Variations in traffic volume within the urban area and new towns (HKTD, 2009)

Fig. 5.3 shows that the air quality at various parts within the urban area of Hong Kong follow a similar pattern—concentrations of CO, NO_2, and PM_{10} are the lowest at night while peaks in CO, NO_2, and PM_{10} concentrations generally coincide with peaks in traffic, shown in Fig. 5.2. Air quality on Saturdays is generally similar to air quality on weekdays. Concentrations on Sundays are generally lower compared to those observed on weekdays, possibly due to lower traffic volume. During night-time urban background concentrations of CO and PM_{10} are similar to those observed at the rural station. Rural concentrations of CO remain mostly constant throughout the day while concentrations of NO_2 and PM_{10} also show little variation.

A difference of approximately 10 ppb between NO_2 concentrations at urban background and rural stations can be observed at night, suggesting that contribution from local

sources towards NO_2 concentrations remains high during night time. A large difference can be observed between CO concentrations at roadside and background stations at times when traffic volume is light, suggesting that effective dispersion of vehicle emissions may not be taking place in the neighbourhood of roadside monitoring stations. A clear difference between CO concentrations in the urban area and new towns can be observed during daytime, suggesting that dispersion of vehicle emissions within the urban area may be less effective at such times.

Fig. 5.3 shows that there is a larger amplitude of variation, both relative and absolute, in air quality at the roadside stations than at background stations. This is likely the result of the roadside stations' close proximity to the roadway, where air quality is more directly affected by vehicle traffic. Meanwhile, the degree of variation in air quality measurements tend to be larger at background stations within the urban area than those within new towns. This indicates that local emission sources such as vehicle emissions have a larger influence on air quality in the urban area than within new towns. The larger intra-day variation in urban background air quality may also be due to that, as shown in Table 5.1, the distance between a background station and a major roadway is smaller in the urban area compared to new towns.

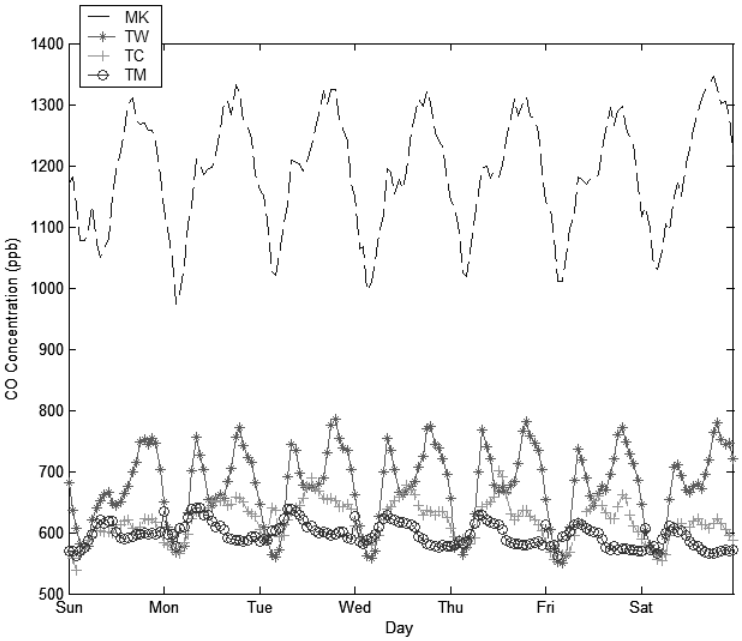
MK
TW
TC
TM
CO Concentration (ppb)
1400
1300
1200
1100
1000
900
800
700
600
500
Sun
Mon
Tue
Wed
Thu
Fri
Sat
Day

a)

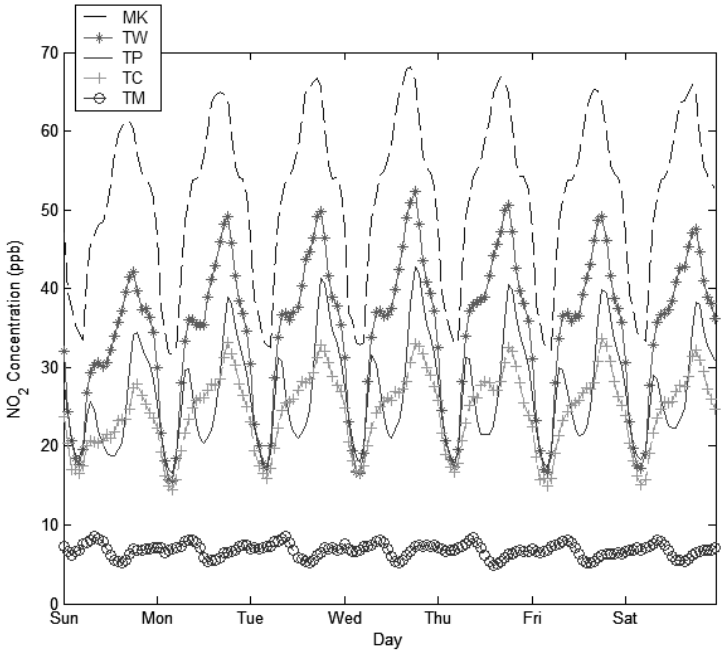
MK
TW
TP
TC
TM
NO2 Concentration (ppb)
70
60
50
40
30
20
10
0
Sun
Mon
Tue
Wed
Thu
Fri
Sat
Day

b)

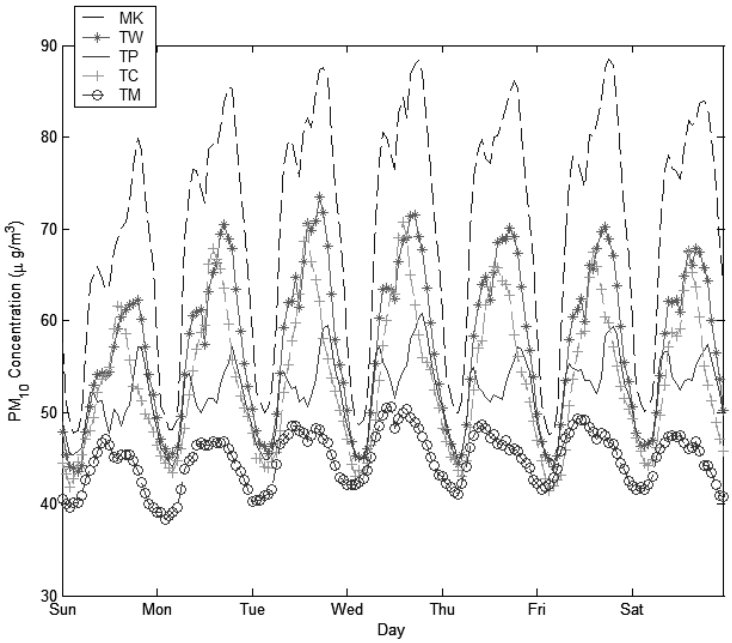

c)

Fig. 5.3 Variations in a) CO; b) NO_2; and c) PM_{10} concentrations at roadside, urban, new town, and rural monitoring stations

The ratio between concentrations at nearby roadside and background stations in the urban area of Hong Kong are computed. This ratio has been used to gauge the importance of vehicle emission towards roadside air quality in a number of cities—a high ratio between roadside and background concentrations is often the result of elevated amount of vehicle emissions near the roadside station, while a low ratio indicates that there is little vehicular traffic at the roadside station (Johansson et al., 2007; Pandey et al., 2008). Conversely, the ratio may also be used to illustrate the effect of roadside emissions on background air quality—a low ratio may indicate that little dispersion of vehicle emission takes place between the roadways in the vicinity of a background monitoring station and the station itself.

The ratios between roadside and background levels of NO_2 and PM_{10} in different areas within Hong Kong are shown in Table 5.2. The station pairs are located in the Central (C/CW), Mong Kok (MK/SSP), and Eastern (CB/E) districts. For each station pair, the

distance between the roadside and background stations is less than 4 km. For comparison, the ratio between concentrations at nearby roadside and background monitoring stations in a number of cities where street canyons are commonplace in the urban area are also shown in Table 5.2. The roadside stations are located within street canyons while the background stations are intended for measurement of general exposure levels. The ratios presented are either the ratio between annual mean concentrations or mean concentrations over the study period.

The lower ratios found in the Mong Kok district is due to higher concentrations of NO_2 and PM_{10} observed at the background station, which is located near a roadway with heavy traffic (Table 5.1). This suggests air quality at the background station in this district may be highly influenced by roadside emissions. The high PM_{10} ratio in the Eastern district is mainly due to elevated PM_{10} level observed at the roadside station, located next to a roadway which is congested for much of the day, resulting in accumulation of pollutants there. In the Central district, the high roadside-background NO_2 ratio may be attributed to that the background station is located along a hill slope, 70 metres above the roadside station. The low PM_{10} ratio, meanwhile, indicates long range transport makes a major contribution towards background particulate concentration.

In Hong Kong, all stations (except CW) are located near sea level. Fig. 5.4 shows the distribution of wind direction at a weather station, maintained by the Hong Kong Observatory, located in the neighbourhood of the SSP station. The figure and measurements at the Hong Kong Observatory (HKO, 2009) shows that, in the urban area of Hong Kong, wind travels mainly from the north-easterly or easterly direction. Thus the low roadside–background PM_{10} ratios observed at Central and Mong Kok

districts, shown in Table 5.2, are likely due to wind carrying more polluted air from the rest of the urban area towards the background station, as the background stations in these districts are located downwind of the roadside station (Fig. 5.1).

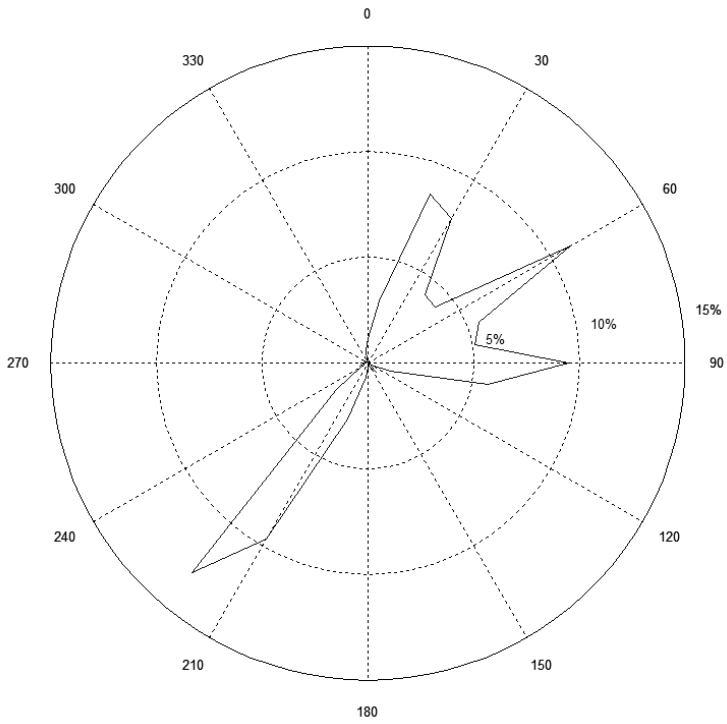

Figure 5.4 Distribution of wind direction near SSP air quality monitoring station

Table 5.2 shows that the ratio between roadside and background concentrations of NO_2 in Hong Kong are similar to that in Seoul and Munich, where background stations are also located on the rooftop (Janssen et al., 2008; Pandey et al., 2008). Meanwhile, the ratios found in the urban area of Hong Kong are higher than that found in central London, where the background station is located upwind of the roadside station (Carslaw and Beevers, 2004).

Ratios between concentrations of PM_{10} at nearby roadside and background stations appear to be lower in heavily trafficked areas in Hong Kong compared to those observed in Stockholm, where the background station is located at rooftop level and

road wear is a major source of particles at the roadside (Johansson et al., 2007). The ratio found in the Camden area of London, meanwhile, is similar to those found at Mong Kok and Central districts. This may be due to the elevated concentration levels at the background station, which is located near a road (Harrison et al., 2004). The ratios at areas within London where the background station is located within parks are higher, as roadside emissions has a small effect on air quality within parks (Kuttler and Strassburger, 1999; Harrison et al., 2004).

City	Study Period	Ratio	Source
a) NO_2			
Hong Kong (Central)	2001-2005	1.79	HKEPD
Hong Kong (Mong Kok)	2001-2005	1.44	HKEPD
Hong Kong (Eastern)	2001-2005	1.67	HKEPD
Seoul	1999-2006	1.74	Pandey et al. (2008)
Central London	1998-2002	2.00	Carslaw and Beevers (2004)
Munich	1996-1998	1.59	Janssen et al. (2008)
b) PM_{10}			
Hong Kong (Central)	2001-2005	1.36	HKEPD
Hong Kong (Mong Kok)	2001-2005	1.25	HKEPD
Hong Kong (Eastern)	2001-2005	1.80	HKEPD
Stockholm (Hornsgatan)	2001-2005	2.50	Johansson et al. (2007)
Stockholm (Sveavägen)	2001-2005	2.10	Johansson et al. (2007)
Stockholm (Norrlandsgatan)	2001-2005	2.00	Johansson et al. (2007)
London (Camden)	2000-2002	1.33	Harrison et al. (2004)
London (Southwark)	2000-2002	1.73	Harrison et al. (2004)
London (Westminster)	2000-2002	1.75	Harrison et al. (2004)

Table 5.2 Ratio between concentrations at roadside and background monitoring stations in different cities

A large percentage of particulate emission from vehicles consists of elemental and organic carbon (Fujita et al., 2007; Ning et al., 2008). As a result, elemental and organic carbon contributes greatly to particulate matter levels observed at the roadside. At background stations, the contribution of elemental and organic carbon towards particulate emission is smaller (Qin et al., 1997). The difference between roadside and

background concentrations of particulate matter can mainly be attributed towards differences in elemental and organic carbon concentrations at roadside and background measurement sites (Hagler et al., 2006).

5.3.2 Statistical analysis of air quality in urban and sub-urban areas

PCA requires that observations be available at all monitoring stations. During the study period (2001–2005), a total of 14,640 and 16,932 NO_2 and PM_{10} concentration measurements were collected at all stations respectively. This set of measurements is considered for examination using PCA. Observations at each station are standardised so that observations at each station have zero mean and unit standard deviation (Pires et al., 2008). NO_2 and PM_{10} are chosen for statistical analysis as these two pollutants are monitored at all stations within the monitoring network and concentrations of these pollutants exceed standards outlined by local air quality objectives on a more frequent basis compared to others (HKEPD, 2006).

The plots for the variances accounted for by each un-rotated PC are shown in Fig. 5.5. It shows that the plots for NO_2 and PM_{10} become approximately linear beyond components 3 and 4, respectively. Thus, 3 and 4 PCs are retained for NO_2 and PM_{10}, respectively. The PCA results, after the factors are rotated, are shown in Table 5.3.

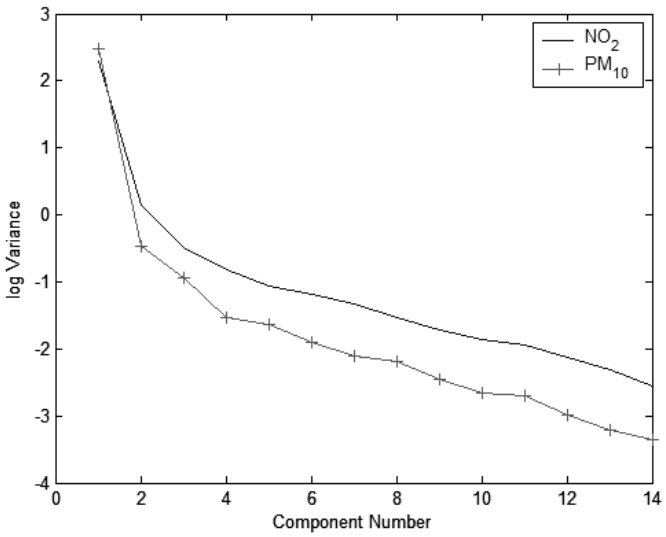

Fig. 5.5 Log of variance associated with individual PCs

For NO_2 (Table 5.3a), there are strong contributions towards factor 1 from the urban stations, in addition to TC. Factor 2 is mainly associated with stations within new towns, while contribution towards factor 3 is the strongest for the rural station TM. Table 5.3a shows that, for factor 1, the loadings associated with the roadside stations are the strongest amongst the monitoring stations. This suggests that this factor is associated with roadside sources, namely vehicle emissions. The loading of factor 2 is negative at all stations, suggesting that this factor is related with the level of ozone, whose concentration is negatively correlated with NO_2 concentration, at each station (Väkevä et al., 1999). The large loading of factor 3 found at TM suggests that the factor is associated with NO_2 in the regional background.

a)	Factor 1	Factor 2	Factor 3
C	**0.872**	-0.311	0.083
CB	**0.846**	-0.287	0.022
MK	**0.898**	-0.259	-0.044
CW	**0.726**	-0.440	0.197
E	**0.790**	-0.427	0.130
SSP	**0.833**	-0.435	0.034
KC	**0.739**	-0.527	0.023
KT	**0.783**	-0.446	0.087
TW	**0.784**	-0.466	0.033
ST	0.369	**-0.846**	0.125
TC	**0.558**	-0.555	0.229
TP	0.371	**-0.827**	0.154
YL	0.611	**-0.654**	0.071
TM	0.028	-0.162	**0.976**
Eigenvalue	6.86	3.667	1.125
% Variance	49.0	26.2	8.0
Cum. % Variance	49.0	75.2	83.2

b)	Factor 1	Factor 2	Factor 3	Factor 4
C	0.341	-0.374	**0.705**	0.413
CB	0.263	-0.259	0.274	**0.881**
MK	0.477	-0.361	0.480	**0.584**
CW	0.519	-0.446	**0.550**	0.402
E	**0.685**	-0.368	0.458	0.359
SSP	**0.566**	-0.440	0.510	0.420
KC	0.455	**-0.526**	0.516	0.396
KT	**0.641**	-0.370	0.465	0.433
TW	0.448	**-0.606**	0.458	0.373
ST	**0.607**	-0.512	0.423	0.335
TC	0.324	**-0.838**	0.266	0.228
TP	**0.634**	-0.558	0.342	0.275
YL	0.396	**-0.793**	0.266	0.272
TM	**0.819**	-0.415	0.213	0.239
Eigenvalue	3.993	3.722	2.751	2.609
% Variance	28.5	26.6	19.6	18.6
Cum. % Variance	28.5	55.1	74.8	93.4

Table 5.3 Results of Principal Component Analysis for a) NO_2; and b) PM_{10}. Bold figures indicate the Principal Component with the strongest loading at each station.

The dendrogram obtained through cluster analysis, using complete linkage between different clusters, is shown in Fig. 5.6a. It shows that the stations can be classified into five clusters:

1. C, CB, and MK,
2. CW, E, SSP, KT, KC, TW, and YL,
3. ST, and TP,
4. TC,
5. TM.

Examination of the factor loadings at each station (Table 5.3a) reveals that stations within the same cluster have similar factor loadings. In cluster 1, which consists of the roadside stations, stations are dominated by factor 1 and other factors have low values. In cluster 2, containing stations in the urban area and YL station, also have high values of factor 1. Meanwhile, clusters 3 and 5 consist of stations that are dominated by factors 2 and 3, respectively. The absolute loadings of factors 1 and 2 are nearly identical at TC, contained in cluster 4. Similar PC loadings are found at YL.

The above comparison indicates that variations in NO_2 concentration at most monitoring stations in the urban area of Hong Kong are highly similar to those found at roadside stations, suggesting that the variations in NO_2 concentration at monitoring stations in the urban area are mainly due to vehicle emissions. It appears that the effect is less pronounced at stations within the new towns.

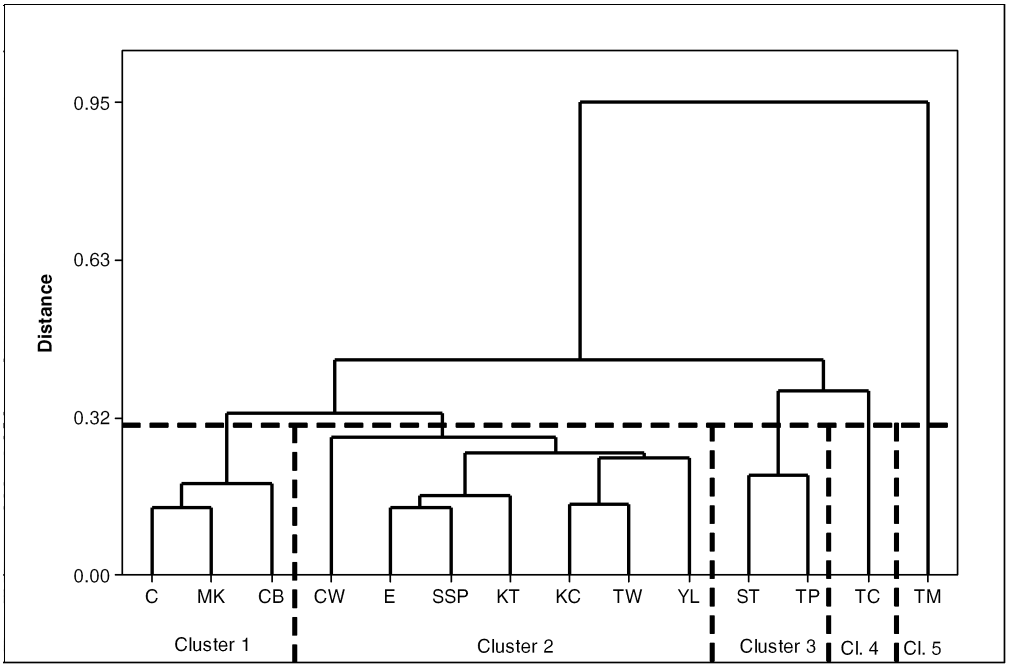

a)

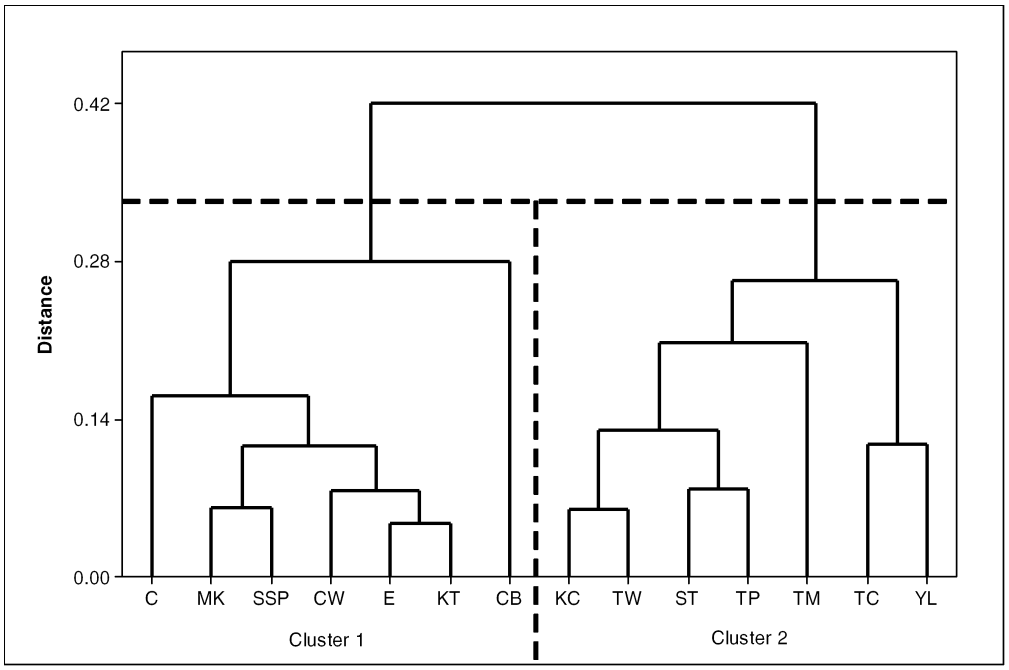

b)

Fig. 5.6 Cluster classification of monitoring stations based on a) NO_2; and b) PM_{10} monitoring data

The PCA results for PM_{10} are shown in Table 5.3b. It shows that, compared to NO_2, there is more ambiguity in the classification of stations—factor 1 is mainly associated

with the stations E, SSP, KT, ST, TP, and TM, which are located in the eastern part of the city (Fig. 5.1); the stations KC, TW, TC, and YL, located in the western part of Hong Kong, contribute mostly towards factor 2; and contributions from the stations C and CW towards factor 3 are the highest, while factor 4 is mainly associated with stations MK and CB. The table also shows that the variance accounted for by factors 1 and 2 is similar and likewise for factors 3 and 4.

The high loadings of factor 4 at the stations MK and CB suggest that this factor is associated with roadside emissions. The loading of this factor at C, however, is small. Similarly, the loading of factor 3 is the largest at C while the loading of this factor at CB is small. This suggests that while vehicle emissions have a strong impact on variations in PM_{10} level within a street canyon, roadside concentration of PM_{10} is also affected by street-level construction activity, roadwork, brake, road surface, and tyre wear (Wu et al., 2002; Johansson et al., 2007). This can result in PCA results showing that roadside variations in PM_{10} are associated with two distinct PCs—one with vehicle exhaust emissions and the other with non-exhaust emissions such as road dust and tyre wear (Almeida et al., 2005; Dongarrà et al., 2007).

Factor 1 loadings are the highest at background stations in the eastern part of Hong Kong (E, KT, SSP, ST, TP) while loadings of factor 2 are the highest at stations in the western part (KC, TW, TC, YL). The strong loadings of factor 2 in the western part of Hong Kong suggest that this factor is related to emissions from power plants (Yuan et al., 2006) while factor 1 appears to be related to regional sources, as indicated by the high loading found at the rural station TM.

The dendrogram produced from cluster analysis of PM_{10} monitoring data throughout Hong Kong is shown in Fig. 5.6b. It shows that, compared to NO_2, there is generally a

higher degree of similarity between variations in PM_{10} concentrations at different monitoring stations. This is mainly due to that the hourly PM_{10} concentrations at different stations within a monitoring network are often highly correlated (Monn, 2001).

Previous studies have shown that, throughout Hong Kong, PM_{10} concentrations are the highest when wind travels from the north-westerly direction, particularly when synoptic wind speed is low (Man and Shih, 2001; Physick and Goudey, 2001). This is likely due to the transport of emissions from industrial activities and power generation in the mainland towards the city. Concentrations are lower when wind originates from the north-east, where there is less development. PM_{10} concentrations are the lowest when wind travels from the south, where there are few emission sources (Man and Shih, 2001).

Fig. 5.6b shows that, based on PM_{10} measurements, the stations can be classified into two clusters—cluster 1 consists of the stations CB, C, MK, CW, E, SSP, and KT while cluster 2 consists of the stations KC, TW, ST, TP, TM, TC, and YL. Fig. 5.1 shows that the stations belonging in cluster 1 are located near the shores of the harbour area. Meanwhile, stations belonging to cluster 2 are located either in the port area or outside the urban area. The two station clusters are separated by hills of up to 500 metres in height. The wind patterns in the two regions differ greatly—winds in the western part of Hong Kong, containing most stations of cluster 2, mainly originates from the west, which increases the contribution of sources from the mainland towards PM_{10} levels there (Wang et al., 2001). Meanwhile, wind mainly travels from the east in the eastern part of the city, which includes most of the urban area (Fig. 5.4 and HKO, 2009). This results in a smaller contribution from regional sources towards PM_{10} concentrations in the urban area.

In Santiago and Oporto, similar station clusters are obtained from measurements of different pollutants. Likewise, PCA and CA results for a specific pollutant yielded similar station clusters. It was suggested that, in such instances, local sources have a minor influence on pollution levels (Gramsch et al., 2006; Pires et al., 2008). In contrast, vastly different station clusters are derived from NO_2 and PM_{10} measurements at monitoring stations in Hong Kong. This discrepancy may be due to the different level of contribution from various sources of pollutants in Hong Kong. For instance, by applying CA using PM_{10} measurements, the stations KC and TW belong to a different cluster from the other urban stations. These stations' proximity to the port area suggests that emissions from marine vessels have are larger influence on PM_{10} levels at KC and TW than the other urban stations (Yuan et al., 2006). This indicates that air quality at urban background stations in Hong Kong are strongly influenced by local sources.

5.3.3 Persistence of pollution in urban and rural areas

The ST method is applied to hourly CO concentration measurements at roadside (MK), urban background (TW), and rural (TM) air monitoring stations to examine the correlation between measurements observed from a station at different times. CO concentration is selected for study due to its inert nature. The variations in log of $\sigma(T)$ for T between 2 and 2000 are shown in Fig. 5.7. Since air quality in the urban area follows a weekly pattern (Fig. 5.3), CO concentration measurements are first subtracted by the mean of observations for that hour of the week to remove cyclic effects.

The figure shows that the slope of the fitted line of CO concentrations at the roadside and urban background stations are -0.34 and -0.41 respectively for larger values of T (T>50), indicating that correlation between high correlation between measurements observed a long time apart. Meanwhile, at TM, the log variance line has a slope of -0.53

for *T* greater than 50, indicating that there is little correlation between measurements that are observed far apart. This is expected as there is no source of CO in the neighbouring area of the station TM and the area surrounding the station is well ventilated. The origin of long-memory property in air quality monitoring data is not well understood (Varotsos et al., 2005). However, as persistence of air pollution appears to be greater at the roadside station than at the urban background station, effectiveness of dispersion may contribute to the persistence of air pollution within the urban area.

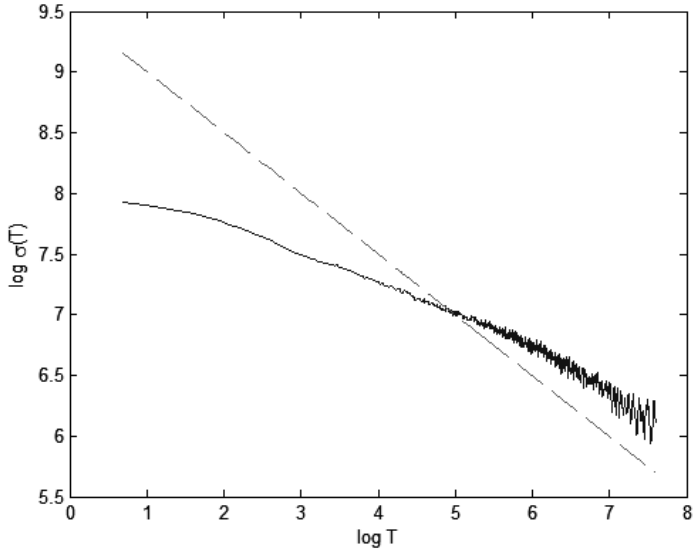

a)

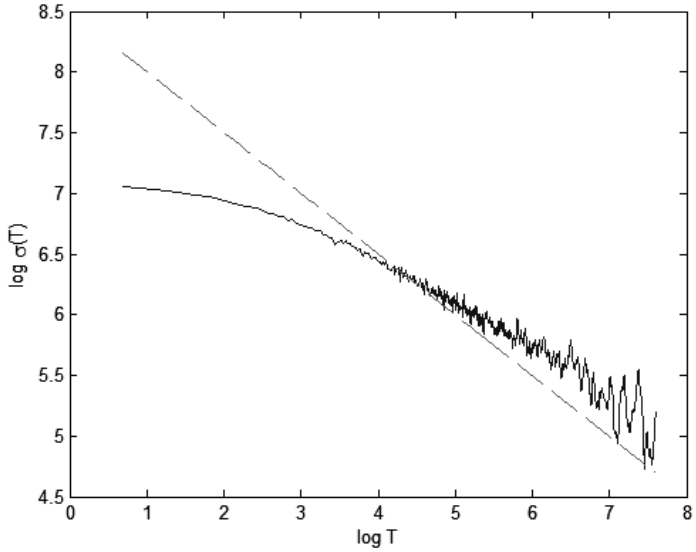

b)

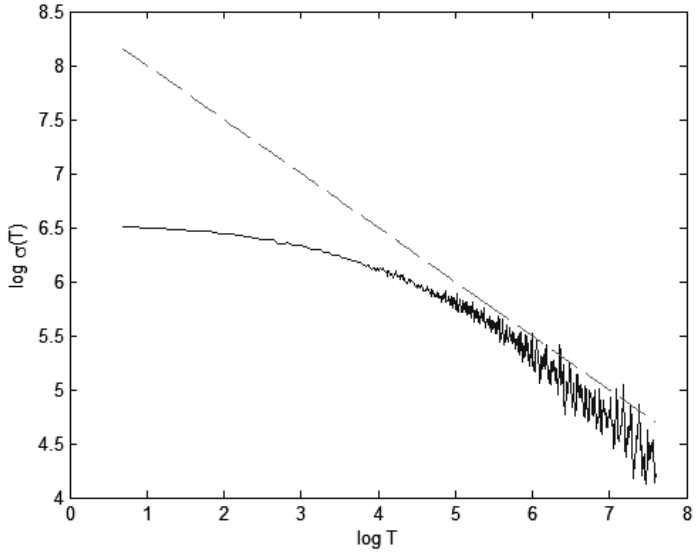

c)

Fig. 5.7 Plot of σ(*T*) vs. length of sub-series *T*, *T* = 2 to 2000, in loglog scale for CO measurements at a) roadside, b) urban background, and c) rural stations. A dotted line (with a slope of -0.5) is added for reference

5.4 Vehicle Emissions and its Dispersion in the Urban Area

In the previous section it is found that air quality measurements at roadside air quality monitoring stations are highly reflective of variations in traffic volume, due to the stations' proximity to roadways. Vehicle emissions appear to have a larger impact on background air quality within the urban area of Hong Kong than in new towns. A clear daily pattern, one that closely corresponds to traffic pattern, can also be found from air quality measurements at monitoring stations in the urban area. The discrepancies in the impact vehicle emission have on background air quality in the urban area and new towns may be due to the differences in dispersion effectiveness in the vicinity of the background monitoring stations in the two areas.

Ideally, background air quality monitoring stations should be located at a site where the pollution level is influenced by the integrated contribution from all sources upwind of

the station. The pollution level should not be dominated by a single source unless such a situation is typical for a larger urban area (EU, 2005). However, as shown in Table 5.4, a number of urban stations in Hong Kong are located close to roadways with heavy traffic and there may not be sufficient distance between the roadway and the station for effective dispersion to occur (USEPA, 1998). While most background stations in the urban area are located above the suggested height as indicated in USEPA (1998), variations in urban background air quality often follow variations in traffic closely. This indicates that dispersion of vehicle emissions may be impeded within the urban area.

NO_2						
Daily Average Traffic Volume (‘000)	<10	10-15	15-20	20-40	40-70	>70
Distance (m)	10	20	30	50	100	250
PM_{10}						
Daily Average Traffic Volume (‘000)	10	20	40	60	80	100
Distance (m)	10	20	40	60	80	100

Table 5.4 Recommended distance between background monitoring station and major roadways (USEPA, 1998).

Fig. 5.8 shows the daily variations in wind speed at weather stations located near the monitoring stations TW and TM. The stations are maintained by the Hong Kong Observatory and are located at similar heights as the air quality monitoring stations. The average wind speed for each hour is derived by computing the mean value of wind speed measurements during that hour of the week. The wind speed patterns shown are commonly observed in the urban and rural areas of Hong Kong. The plot shows that wind speed tends to be low (<3 m/s) for a majority of the time. While wind speed tends to be higher in the afternoon, variations in air quality in the urban area remain similar to variations in traffic volume. This indicates that wind speed may not be sufficiently high for effective dispersion to take place in the urban area.

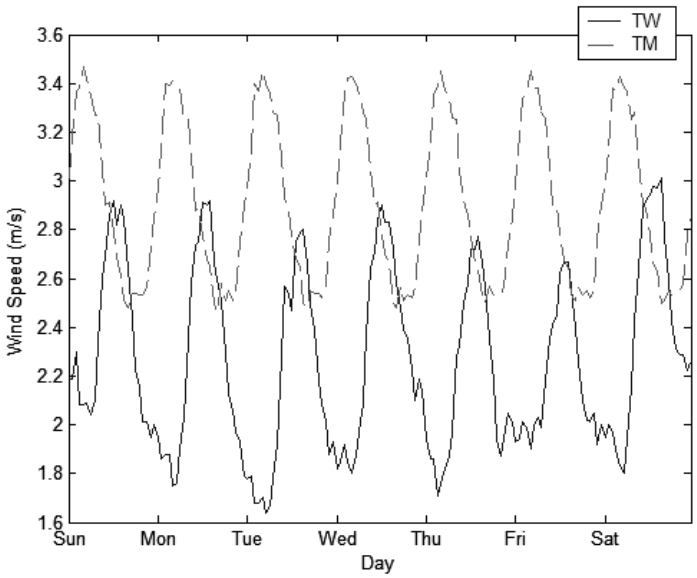

Fig. 5.8 Hourly variations in wind speed in the urban and rural areas of Hong Kong

The higher gaseous and particulate concentrations observed at urban background monitoring stations can be attributed urban traffic conditions. On-road measurements of vehicle emissions show that, under urban driving conditions, vehicles spend a majority of time idling or travelling at low speeds (Fig. 3.2), during which gaseous emission factors of vehicles are high. While gaseous emission rates of vehicles tend to be lower under idling and low speed driving conditions, long periods of idling increase trip length and raise total trip emissions (Unal et al., 2003; Silva et al., 2006b). During peaks in traffic volume, vehicles spend a large amount of time vehicles travelling at low speed and idling. In addition, changes in vehicle speed are more prevalent under urban driving conditions. This results in vehicles undergoing frequent acceleration, under which vehicles emit higher amounts of pollutants. This can result in higher emissions from vehicles and thus elevate concentrations of gaseous at roadside and urban background monitoring stations. Frequent stoppages due to traffic lights can also increase the amount of time vehicle undergo acceleration, which further increases levels of vehicle emissions. Since wind speed in the urban area of Hong Kong is low (Fig. 5.8), vehicle-induced turbulence can greatly affect dispersion of emissions (Kumar et al., 2008).

However, the low speed driving conditions observed in the urban area favours accumulation of vehicle emissions at street level, as low vehicle speed reduces the effectiveness of vehicle-induced turbulence in removing emissions near street level. This results in vehicle emissions remaining near street level for a longer period of time. Thus ineffective dispersion at street level contributes to the persistence of air pollution and leads to roadside air quality exhibiting the long-memory property. Long-memory property, while weaker than at the roadside, can also be observed from air quality measurements at the urban background station. This indicates that dispersion of emissions is impeded within the urban area.

Dispersion of emissions originating from the urban area of a city can be obstructed by surrounding objects such as hills (Gramsch et al., 2006). In addition to the hills surrounding the urban area of Hong Kong, the configuration of buildings within the urban area can also hinder dispersion of vehicle emissions in the area. For instance, high density of tall buildings can create an enclosed setting where the dispersion of vehicle emission within the enclosed space is separated from that outside (Harrison et al., 2004; Pires et al., 2008). Specifically, the high-rise buildings surrounding a monitoring station may create a setting where air flow is obstructed and vehicle emission is accumulated. This can lead to pollution behaviour at the background stations reflecting those found in street canyons, where persistence of air pollution can be observed, instead of pollution patterns of the greater urban area. Meanwhile, within new towns, density of buildings is lower and there is generally more open space, resulting in less obstruction in air flow and monitoring station measurements that are more reflective of background air quality in the area.

5.5 Chapter Summary

Variations in concentrations of CO, NO_2, and PM_{10} at monitoring stations located in different parts of Hong Kong are examined. Air quality in the urban area, both at the roadside and at the background, closely follows traffic volume while the correlation between air quality and traffic volume measurements is weaker in new towns. Statistical analysis of air quality measurements indicates that variations in air quality in the urban area are mainly due to vehicle emissions. Meanwhile, within new towns, vehicle emission has a smaller effect on air quality compared to regional sources. This is likely due to different wind patterns observed in the urban and new town areas. A test of long-memory shows persistence in urban air quality. Similarities in traffic volume and urban air quality may be due to the close distance between monitoring stations and major roadways in the urban area. The low wind speed observed within the urban area may also result in less effective dispersion of vehicle emissions there.

Statistical analysis indicates that dispersion of vehicle emissions may be impeded by high-rise buildings surrounding monitoring stations in the urban area. Traffic conditions, particularly the lack of vehicle movement, in the urban area can contribute to elevated levels of gaseous pollutants emitted by vehicles in the urban area, which results in persistence of air pollution in the urban area and observation of long-memory property from urban air quality measurements.

Chapter 6

Conclusions and Recommendations for Future Work

6.1 Conclusions

In this work on-road emissions of CO, NO, and HC from taxis, fuelled by LPG, and light goods vehicles (LGVs), fuelled by diesel, adhering to Euro 2, 3, and 4 emission standards were measured using a portable emission measurement system (PEMS). During road tests, vehicles followed vehicles of the same type to simulate urban driving conditions of the vehicle type. Road tests reveal that vehicles operate at idle mode for a large percentage of time. Acceleration and deceleration are frequent under urban driving conditions. The results show that newer model vehicles generally emit lower amounts of gaseous pollutants due to vehicle adhering to more stringent emission standards.

On-road measurements show that gaseous emission factors of vehicles decrease as vehicle speed increase. The low gaseous emissions observed from one LGV can be attributed to the installation of an oxidation catalytic converter. On-road measurements of LGVs indicate that emissions of NO may be related to vehicle weight while the relationship between vehicle weight and emissions of CO and HC appears to be weak. The lowest gaseous emission rates are observed when vehicles operate at idle mode. Meanwhile, gaseous emissions from test vehicles are generally the highest when undergoing acceleration, due to the vehicles' higher exhaust flow rate and heavier engine work under such driving conditions. CO and HC emissions of one taxi are extraordinarily high under idling and low-speed driving conditions. Examination of instantaneous emissions of the vehicles indicates that it is caused by malfunction in the control of fuel supply to the engine. These results help improve the understanding of on-

road gaseous emissions from light-duty vehicles. In particular, this work enhances the knowledge of gaseous emissions characteristics of LPG vehicles under urban driving conditions.

On-road gaseous emissions from a number of vehicle classes, measured using the remote sensing measurement system, are examined. This system enables measurement of vehicle emissions from a large number of vehicles without interruption in traffic. Regardless of fuel type, newer model vehicles produce lower amounts of gaseous pollutants. This can be attributed to the increasingly stringent emission standards that newer model vehicles adhere to. The decrease is more pronounced for vehicles running on LPG. However, emissions from such vehicles are generally higher than levels set by emission standards. Diesel vehicles emit smaller amounts of CO and HC and higher amounts of NO in comparison to petrol and LPG vehicles. LPG vehicles have higher gaseous emission factors compared to petrol vehicles. Older model LPG vehicles tend to produce higher amounts of gaseous emissions compared to light-duty vehicles running on petrol and diesel. This may be the result of intensive commercial use and poor maintenance of LPG vehicles, which can hasten deterioration of engine performance.

The relationship between vehicle speed and gaseous emission indices appears to be weak while gaseous emission factors are lower when vehicles travel at higher speeds. Gaseous emissions from light-duty vehicles are the lowest during deceleration and the highest when undergoing aggressive acceleration. The effect of road gradient of emissions from passenger cars and taxis are examined. The results show that NO emission increases as road gradient increases. Meanwhile, road gradient has minimal effect on emissions of CO and HC from passenger cars, due to variability of emissions

from individual vehicles.

Emission factors of taxis and LGVs derived from measurements collected by PEMS and remote sensing systems are compared in order to gain a better understanding of discrepancies in emission factors derived from different measurement methods. In general, gaseous emission factors from taxis are higher when measurements are collected using a PEMS. This is likely due to that the PEMS measures a vehicle's emissions directly in the exhaust while remote sensing instruments measure a vehicle's emission after it is expelled into the atmosphere, where it is diluted by ambient air. The difference between emission factors of LGVs derived from PEMS and remote sensing measurements may be due to the presence or absence of emission control within the test vehicles. NO emission factors of taxis and LGVs derived from PEMS measurements are generally higher. This can be attributed to the conversion of NO emitted by vehicles to NO_2 in the atmosphere, which lowers NO concentration measured by remote sensing instruments. How differences in sample size and computation methods limit such comparisons are discussed.

To explore the impact vehicle emission has on urban air quality, air quality variations in the urban and new town areas in Hong Kong are investigated through examination of CO, NO_2, and PM_{10} concentrations at roadside and background monitoring stations located at various districts of the city. It is found that variations in air quality follow variations in traffic volume closely. The amplitude of variations in concentrations of CO, NO_2, and PM_{10} are larger at background stations located in the urban area, indicating that the effect vehicle emissions have on background air quality is larger within the urban area than in new towns.

Results from statistical analysis of variations in air quality at monitoring stations show

that variations in background NO_2 concentrations in the urban area is largely dependent on vehicle emissions while vehicle emission has a smaller impact on background levels of NO_2 in new towns. Results from principal component analysis and cluster analysis show that variations in background PM_{10} concentrations outside the urban centre appear to be more dependent on regional sources and less dependent on vehicle emissions. This discrepancy likely results from differences in wind patterns within and outside the urban area. The variations in NO_2 and PM_{10} concentrations at a number of background stations in the urban area are similar to those found within street canyons, suggesting that the variations found at these stations may be due to insufficient distance between the monitoring station and nearby roadways for dispersion to take place.

The strong influence of roadside emission on air quality at background stations in the urban area may be due to the high density of tall buildings surrounding each station. The analysis has found for the first time that there is a long memory phenomenon of the air pollutants at the air monitoring stations. This suggests that high-rise buildings within the urban area of a densely-developed city such as Hong Kong may create an enclosed setting which favours the accumulation of roadside emissions. Thus air quality observed at urban background monitoring stations in such a city may reflect air quality of the enclosed space rather than that of a larger urban area. This leads to the observation of long-memory property from urban air quality measurements.

The results from this work indicates that discrepancies in vehicle emission factors can be bridged by comparing emission factors, derived from measurements collected from multiple methods within a city, of vehicles of the same type operating under similar conditions. This work also shows that vehicle emission's contribution towards deterioration of air quality in a densely-built city such as Hong Kong can be estimated

through statistical analysis of roadside and background air quality in the urban area of the city.

6.2 Recommendations for Future Work

On-road emission measurements show that vehicles in a densely-built city such as Hong Kong operate at idle mode for a large percentage of the time. Such driving conditions often result in higher amounts of emissions produced by a vehicle over a trip. In addition, vehicles travelling in the urban area undergo frequent acceleration and deceleration, conditions under which higher amounts of gaseous emissions are produced. This indicates that vehicle emission in the urban area can be reduced by improving traffic flow on urban roadways. This would decrease the amount of time vehicles operate in idle and acceleration modes and thus reduce the amount of pollutants emitted by vehicles. Traffic management schemes can be developed so that better traffic flow can be achieved. Such schemes may help reduce vehicle emission hotspots and total vehicle emissions in the urban area.

Results from this work show that gaseous emission factors derived from direct measurements from the exhaust are higher than those derived from remote sensing measurements, where concentrations of gaseous pollutants emitted by a vehicle is measured after being released into the atmosphere. However, the number of vehicles considered for on-road emission testing may not be sufficient to confirm this conclusion. As shown in this work, results can be skewed by a single high-emitting vehicle. Thus on-road measurement of emissions from a larger number of vehicles should be carried out so that more definitive on-road emission levels can be reached. Multiple vehicles adhering to each emission standard should be selected to the test fleet so that results are more representative of each class of vehicles.

In addition, the relationship between the two sets of measurements cannot be fully established due to that emissions from different sets of vehicles were measured. By setting up an emission measurement site at the roadside and driving a test vehicle, whose exhaust pipe is connected to on-road emission measurement instruments, to pass the site under a set of predefined driving conditions, better correlation between roadside and on-road measurements of vehicle emissions can be established. Such experiments may also help improve the understanding of dispersion of vehicle emissions in the vicinity of a roadway.

References

Almeida, S.M., Pio, C.A., Freitas, M.C., Reis, M.A., Trancos, M.A. (2005) Source apportionment of fine and coarse particulate matter in a sub-urban area at the Western European Coast. *Atmospheric Environment*, Vol. 39, pp. 3127–3138

Alvarez, R., Weilenmann, M., Favez J.-Y. (2008) Evidence of increased mass fraction of NO_2 within real-world NO_x emissions of modern light vehicles — derived from a reliable online measuring method. *Atmospheric Environment*, Vol. 42, pp. 4699–4707

André, M., Joumard, R., Vidon, R., Tassel, P., Perret, P. (2006) Real-world European driving cycles, for measuring pollutant emissions from high- and low-powered cars. *Atmospheric Environment*, Vol. 40, pp. 5944–5953

Australian Department of Climate Change (ADCC) (2009) *National Greenhouse and Energy Technical Guidelines*. National Inventory Systems Team, Canberra.

Ban-Weiss, G.A., Lunden, M.M., Kirchstetter T.W., and Harley, R.A. (2009) Measurement of Black Carbon and Particle Number Emission Factors from Individual Heavy-Duty Trucks. *Environmental Science & Technology*, Vol. 43, pp. 1419-1424

Baik, J.J., Kang, Y.S., Kim, J.J. (2007) Modeling reactive pollutant dispersion in an urban street canyon. *Atmospheric Environment*, Vol. 41, pp. 934–949

Benson, P.E. (1992) A Review of the Development and Application of the CALINE3 and 4 Models. *Atmospheric Environment*, Vol. 26B, pp. 379-390

Beran, J. (1994) *Statistics for Long-Memory Processes. Monographs on Statistics and Applied Probability, Vol. 61*. Chapman & Hall, New York.

Bergmann, M., Kirchner, U., Vogt, R., Benter, T. (2009) On-road and laboratory investigation of low-level PM emissions of a modern diesel particulate filter equipped diesel passenger car. *Atmospheric Environment*, Vol. 43, pp. 1908-1916

Berkowicz, R. (2000) OSPM – A parametrised street pollution model, *Environmental*

Monitoring and Assessment, Vol. 65, pp. 323–331

Bishop, G.A. Stedman, D.H. (1996) Motor vehicle emissions variability. *Journal of the Air & Waste Management Association*, Vol. 46, pp. 667-675

Bishop, G.A., Stedman, D.H. (2008) A Decade of On-road Emissions Measurements. *Environmental Science & Technology*, Vol. 42, pp 1651–1656

Booker, D.R., Giannelli, R.A., Hu, J. (2007) Road Test of an On-Board Particulate Matter Mass Measurement System. *SAE Paper* 2007-01-1116

Bukowiecki, N., Dommen, J., Prévôt, A. S. H., Richter, R., Weingartner, E., Baltensperger, U. (2002) A mobile pollutant measurement laboratory—measuring gas phase and aerosol ambient concentrations with high spatial and temporal resolution. *Atmospheric Environment*, Vol. 36, pp. 5569-5579

Bush, T., Tsagatakis, I., King, K., Passant, N. (2008) *NAEI UK Emission Mapping Methodology 2006*. Prepared on behalf of the UK Department for Environment, Food & Rural Affairs and the Devolved Administrations

Carslaw, D.C., Beevers, S.D. (2004). Investigating the potential importance of primary NO2 emissions in a street canyon. *Atmospheric Environment*, Vol. 38, pp. 3585–3594

Carslaw, D.C., Ropkins, K., Bell, M.C. (2006) Change-point detection of gaseous and particulate traffic-related pollutants at a roadside location. *Environmental Science & Technology*, Vol. 40, pp. 6912-6918

Castanho, A.D.A. and Artaxo, P. (2001) Wintertime and summertime São Paulo aerosol source apportionment study. *Atmospheric Environment*, Vol. 35, pp. 4889-4902

Ceviz, M.A., Yüksel, F. (2006) Cyclic variations on LPG and gasoline-fuelled lean burn SI engine. *Renewable Energy*, Vol. 31, pp. 1950-1960

Chan, T.L., Ning, Z. (2005) On-road remote sensing of diesel vehicle emissions measurement and emission factors estimation in Hong Kong. *Atmospheric Environment*, Vol. 39, pp. 6843-6856

Chatfield, C. (1996) *The Analysis of Time Series: An Introduction, 5th Ed*. Chapman & Hall, London.

Chen, C., Huang, C., Jing, Q., Wang, H., Pan, H., Li, L., Zhao, J., Dai, Y., Huang, H., Schipper, L., Streets, D.G. (2007) On-road emission characteristics of heavy-duty diesel vehicles in Shanghai. *Atmospheric Environment*, Vol. 41, pp. 5334-5344

Cheng, Y., Lee, S.C., Ho, K.F., Louie, P.K.K. (2006) On-road particulate matter (PM2.5) and gaseous emissions in the Shing Mun Tunnel, Hong Kong. *Atmospheric Environment*, Vol. 40, pp. 4235-4245

Colberg, C.A., Tona, B., Catone, G., Sangiorgio, C., Stahel, W.A., Sturm, P., Staehelin, J. (2005) Statistical analysis of the vehicle pollutant emissions derived from several European road tunnel studies. *Atmospheric Environment*, Vol. 39, pp. 2499-2511

Collett, R.S., Oduyemi, K. (1997) Air quality modelling: a technical review of mathematical approaches. *Meteorological Applications*, Vol. 4, pp. 235-246

Collins, J.F., Shepherd, P., Durbin, T.D., Lents, J., Norbeck, J., Barth, M. (2007) Measurements of in-use emissions from modern vehicles using an on-board measurement system. *Environmental Science &* Technology, Vol., 41, pp. 6554–6561

Corsmeier, U., Kohler, M., Vogel, B., Vogel, H., Fiedler, F. (2005) BAB II: a project to evaluate the accuracy of real-world traffic emissions for a motorway. *Atmospheric Environment*, Vol. 39, pp. 5627-5641

Curtis, L., Rea, W., Smith-Willis, P., Fenyves, E., Pan, Y. (2006) Adverse health effects of outdoor air pollutants. *Environment International*, Vol. 32, pp. 815–830

Dearth, M.A., Butler, J.W., Colvin, A., Gierczak, C., Kaberline, S., Korniski, T. (2005) SemtechD: The Chassis Roll Evaluation of a Commercial Portable Emission Measurement System (PEMS). *SAE Paper* 2005-01-0673

Di Sabatino, S., Buccolieri, R., Pulvirenti, B., Britter, R. E. (2008) Flow and pollutant dispersion in street canyons using FLUENT and ADMS-Urban. *Environmental*

Modeling & Assessment, Vol. 13, pp. 369-381

Dongarrà, G., Manno, E., Varrica, D., Vultaggio, M. (2007) Mass levels, crustal component and trace elements in PM10 in Palermo, Italy. *Atmospheric Environment*, Vol. 41, pp. 7977-7986

Dueñas, C., Fernández, M.C., Cañete, S., Carretero, J., Liger, E. (2005) Stochastic model to forecast ground-level ozone concentration at urban and rural areas. *Chemosphere*, Vol. 61, pp. 1379-1389

Durbin, T.D., Zhu, X., Norbeck, J.M. (2003) The effects of diesel particulate filters and a low-aromatic, low-sulfur diesel fuel on emissions for medium-duty diesel trucks. *Atmospheric Environment*, Vol. 37, pp. 2105-2116

El-Shawarby, I., Ahn, K., Rakha H. (2005) Comparative field evaluation of vehicle cruise speed and acceleration level impacts on hot stabilized emissions. *Transportation Research Part D: Transport and Environment*, Vol. 10, pp. 13-30

European Union (EU) (2005) *Directive on Ambient Air Quality and Cleaner Air for Europe (the "CAFE" Directive)*

Ferguson, C.R., Kirkpatrick, A.T. (2001) *Internal Combustion Engines, 2nd Ed*. John Wiley & Sons, New York

Fruin, S., Westerdahl, D., Sax, T., Sioutas, C., Fine, P.M. (2008) Measurements and predictors of on-road ultrafine particle concentrations and associated pollutants in Los Angeles. *Atmospheric Environment*, Vol. 42, pp. 207-219

Fujita, E.M., Campbell, D.E., Arnott, W.P., Chow, J.C., Zielinska, B. (2007) Evaluations of the chemical mass balance method for determining contributions of gasoline and diesel exhaust to ambient carbonaceous aerosols. *Journal of the Air and Waste Management Association*, Vol. 57, pp. 721–740

Gajendran, P., Clark, N.N. (2003) Effect of Truck Operating Weight on Heavy-Duty Diesel Emissions. *Environmental Science & Technology*, Vol. 37, pp. 4309-4317

Galindo, J., Luján, J.M., Serrano, J.R., Hernández, L. (2005) Combustion simulation of turbocharger HSDI Diesel engines during transient operation using neural networks. *Applied Thermal Engineering*, Vol. 25, pp. 877-898

Gao, Y., Checkel, M.D. (2007) Emission Factor Analysis for Multiple Vehicles Using an On-Board, In-use Emissions Measurement System. *SAE Paper* 2007-01-1327

Geller, M.D., Sardar, S.B., Phuleria, H., Fine, P.M., Sioutas, C. (2005) Measurements of Particle Number and Mass Concentrations and Size Distributions in a Tunnel Environment. *Environmental Science & Technology,* Vol. 39, pp. 8653–8663

Gidhagen, L., Johansson, C., Langner, J., Olivares, G. (2004) Simulation of NO_x and ultrafine particles in a street canyon in Stockholm, Sweden. *Atmospheric Environment*, Vol. 38, pp. 2029-2044

Giechaskiel, B., Dilara, P., Andersson, J. (2008) Particle measurement programme (PMP) light-duty inter-laboratory exercise: Repeatability and reproducibility of the particle number method. *Aerosol Science and Technology,* Vol. 42, pp. 528-543

Gokhale, S., Pandian, S. (2007) A semi-empirical box modeling approach for predicting the carbon monoxide concentrations at an urban traffic intersection. *Atmospheric Environment*, Vol. 41, pp. 7940-7950

Gramotnev, G., Brown, R., Ristovski, Z., Hitchins, J., Morawska, L. (2003) Determination of average emission factors for vehicles on a busy road. *Atmospheric Environment*, Vol. 37, pp. 465-474

Gramsch, E., Cereceda-Balic, F., Oyola, P., von Baer, D. (2006) Examination of pollution trends in Santiago de Chile with cluster analysis of PM10 and ozone data. *Atmospheric Environment*, Vol. 40, pp. 5464–5475

Greco, S.L., Wilson, A.M., Hanna, S.R., Levy, J.I. (2007) Factors Influencing Mobile Source Particulate Matter Emissions-to-Exposure Relationships in the Boston Urban Area. *Environmental Science & Technology,* Vol. 41, pp. 7675–7682

Gross, D.S., Barron, A.R., Sukovich, E.M., Warren, B.S., Jarvis, J.C., Suess, D.T., Prather, K.A. (2005) Stability of single particle tracers for differentiating between heavy- and light-duty vehicle emissions. *Atmospheric Environment*, Vol. 39, pp. 2889–2901

Hagler, G.S.W., Bergin, M.H., Salmon, L.G., Yu, J.Z., et al. (2006) Source areas and chemical composition of fine particulate matter in the Pearl River Delta region of China. *Atmospheric Environment*, Vol. 40, pp. 3802–3815

Hak, C.S., Hallquist, M., Ljungström, E., Svane, M., Pettersson, J.B.C. (2009) A new approach to in-situ determination of roadside particle emission factors of individual vehicles under conventional driving conditions. *Atmospheric Environment*, Vol. 43, pp. 2481-2488

Harrison, R.M., Jones, A.M., Barrowcliffe, R. (2004) Field study of the influence of meteorological factors and traffic volumes upon suspended particle mass at urban roadside sites of differing geometries. *Atmospheric Environment*, Vol. 38, pp. 6361–6369

He, L.Y., Hu, M., Zhang, Y.H., Huang, X.F., Yao, T.T. (2008) Fine Particle Emissions from On-Road Vehicles in the Zhujiang Tunnel, China. *Environmental Science & Technology*. Vol. 42, pp. 4461-4466

Heeb, N.V. Saxer, C.J., Forss, A., Brühlmann, S. (2006) Correlation of hydrogen, ammonia, and nitrogen monoxide (nitric oxide) emissions of gasoline-fueled Euro-3 passenger cars at transient driving. *Atmospheric Environment*, Vol. 40, pp. 3750-3763

Heywood, J.B. (1988) *Internal combustion engine fundamentals.* McGraw-Hill, New York

Holmén, B.A., Niemeier, D.A. (1998) Characterizing the effects of driver variability on real-world vehicle emissions. *Transportation Research Part D: Transport and Environment*, Vol. 3, pp. 117-128

Holmén, B.A., Ayala, A. (2002) Ultrafine PM Emissions from Natural Gas, Oxidation-

Catalyst Diesel, and Particle-Trap Diesel Heavy-Duty Transit Buses. *Environmental Science & Technology*, Vol. 36, pp. 5041–5050

Hong Kong Environmental Protection Department (HKEPD) (2006) *Air Quality in Hong Kong, 2005*. Air Science Group. Hong Kong

Hong Kong Environmental Protection Department (HKEPD) (2008) *Air Pollutants and Greenhouse Gas Emissions Inventory* (http://www.epd.gov.hk/epd/english/environmentinhk/air/data/emission_inve06.html)

Hong Kong Observatory (HKO) (2009) *Annual wind roses for Hong Kong Observatory, 1971-2000* (http://www.hko.gov.hk/cis/region_climat/HKO/HKO_windrose_year_e.htm)

Hong Kong Transportation Department (HKTD) (2009) *Annual Traffic Census 2008*. Traffic and Transport Services Division. Hong Kong

Huo, H., Zhang, Q., He, K.B., Wang, Q.D., Yao, Z.L., Streets, D.G. (2009) High-Resolution Vehicular Emission Inventory Using a Link-Based Method: A Case Study of Light-Duty Vehicles in Beijing. *Environmental Science & Technology*, Vol. 43, pp. 2394-2399

Imhof, D., Weingartner, E., Ordóñez, C., Gehrig, R., Hill, M., Buchmann, B., Baltensperger, U. (2005) Real-World Emission Factors of Fine and Ultrafine Aerosol Particles for Different Traffic Situations in Switzerland. *Environmental Science & Technology*, Vol. 39, pp. 8341-8350

Imhof, D., Weingartner, E., Prévôt, A.S.H., Ordóñez, C., Kurtenbach, R., Wiesen, P., Rodler, J., Sturm, P., McCrae, I., Ekström, M., Baltensperger, U. (2006) Aerosol and NOx emission factors and submicron particle number size distributions in two road tunnels with different traffic regimes. *Atmospheric Chemistry and Physics*, Vol. 6, pp. 2215-2230

Jamriska, M., Morawska, L. (2001) A model for determination of motor vehicle emission factors from on-road measurements with a focus on submicrometer particles. *Science of the Total Environment*, Vol. 264, pp. 241-255

Janssen, N.A.H., Meliefste, K., Fuchs, O., Weiland, S.K., Cassee, F., Brunekreef, B., Sandstrom, T. (2008) High and low volume sampling of particulate matter at sites with different traffic profiles in the Netherlands and Germany: Results from the HEPMEAP study. *Atmospheric Environment*, Vol. 42, pp. 1110-1120

Jayaratne, E.R., Morawska, L., Ristovski, Z.D., He, C. (2007) Rapid Identification of High Particle Number Emitting On-Road Vehicles and its Application to a Large Fleet of Diesel Buses. *Environmental Science & Technology*, Vol. 41, pp. 5022-5027

Jayaratne, E.R., He, C., Ristovski, Z.D., Morawska, L., Johnson G.R. (2008) A Comparative Investigation of Ultrafine Particle Number and Mass Emissions from a Fleet of On-Road Diesel and CNG Buses. *Environmental Science & Technology*, Vol. 42, pp. 6736-6742

Jiang, M., Marr, L.C., Dunlea, E.J., Herndon, S.C., Jayne, J.T., Kolb, C.E., Knighton, W.B., Rogers, T.M., Zavala, M., Molina L.T., Molina, M.J. (2005) Vehicle fleet emissions of black carbon, polycyclic aromatic hydrocarbons, and other pollutants measured by a mobile laboratory in Mexico City. *Atmospheric Chemistry & Physics*, Vol. 5, pp. 3377-3387

Johansson, C., Norman, M., Gidhagen, L. (2007) Spatial & temporal variations of PM_{10} and particle number concentrations in urban air. *Environmental Monitoring and Assessment*, Vol. 127, pp. 477–487

Johnson, J.P., Kittelson, D.B., Watts, W.F. (2005) Source apportionment of diesel and spark ignition exhaust aerosol using on-road data from the Minneapolis metropolitan area. *Atmospheric Environment*, Vol. 39, pp. 2111-2121

Johnson, K.C., Durbin, T.D., Cocker III, D.R., Miller, W.J., Bishnu, D.K., Maldonado, H., Moynahan, N., Ensfield, C., Laroo, C.A. (2009a) On-road comparison of a portable emission measurement system with a mobile reference laboratory for a heavy-duty diesel vehicle. *Atmospheric Environment*, Vol. 43, pp. 2877-2883

Johnson, J.P., Kittelson, D.B., Watts, W.F. (2009b) The Effect of Federal Fuel Sulfur Regulations on In-Use Fleets: On-Road Heavy-Duty Source Apportionment.

Environmental Science & Technology, Vol. 43, pp. 5358-5364

Jolliffe, I.T. (2002) *Principal Component Analysis, 2nd Edition*. Springer-Verlag, New York

Jones, A.M., Harrison, R.M. (2006) Estimation of the emission factors of particle number and mass fractions from traffic at a site where mean vehicle speeds vary over short distances. *Atmospheric Environment*, Vol. 40, pp. 7125-7137

Karanasiou, A.A., Siskos, P.A., Eleftheriadis, K. (2009) Assessment of source apportionment by Positive Matrix Factorization analysis on fine and coarse urban aerosol size fractions. *Atmospheric Environment*, Vol. 43, pp. 3385–3395

Karar, K., Gupta, A. K. (2007) Source apportionment of PM10 at residential and industrial sites of an urban region of Kolkata, India. *Atmospheric Research*, Vol. 84, pp. 30-41

Kean, A.J., Grosjean, E., Grosjean, D., Harley, R.A. (2001) On-Road Measurement of Carbonyls in California Light-Duty Vehicle Emissions. *Environmental Science & Technology*, Vol. 35, pp. 4198–4204

Kean, A.J., Harley, R.A., Kendall, G.R. (2003) Effects of Vehicle Speed and Engine Load on Motor Vehicle Emissions. *Environmental Science & Technology*, Vol. 37, pp. 3739–3746

Kent, J.H., Mudford, N.R., (1979) Motor vehicle emissions and fuel consumption modelling. *Transportation Research Part A: General*, Vol. 13, pp. 395-406

Kenty, K. L., Poor, N.D., Kronmiller, K.G., McClenny, W., King, C., Atkeson, T., Campbell, S.W. (2007) Application of CALINE4 to roadside NO/NO2 transformations. *Atmospheric Environment*, Vol. 41, pp. 4270–4280

Ketzel, M., Wahlin, P., Berkowicz, R., Palmgren, F. (2003) Particle and trace gas emission factors under urban driving conditions in Copenhagen based on street and roof-level observations. *Atmospheric Environment*, Vol. 37, pp. 2735–2749

Kim, H.N., Choi, B.C. (2008). Effect of ethanol-diesel blend fuels on emission and particle size distribution in a common-rail direct injection diesel engine with warm-up catalytic converter. *Renewable Energy*, Vol. 33, pp. 2222-2228

Kirchstetter, T.W., Harley, R.A., Kreisberg, N.M., Stolzenburg, M.R., Hering, S.V. (1999) On-road measurement of fine particle and nitrogen oxide emissions from light- and heavy-duty motor vehicles. *Atmospheric Environment*, Vol. 33, pp. 2955-2968

Kittelson, D.B., Watts, W.F., Johnson, J.P. (2004) Nanoparticle emissions on Minnesota highways. *Atmospheric Environment*, Vol. 38, pp. 9-19

Kittelson, D.B., Watts, W.F., Johnson, J.P., Thorne, C., Higham, C., Payne, M., Goodier, S., Warrens, C., Preston, H., Zink, U., Pickles, D., Goersmann, C., Twigg, M.V., Walkerand, A.P., Boddy, R. (2008) Effect of Fuel and Lube Oil Sulfur on the Performance of a Diesel Exhaust Gas Continuously Regenerating Trap. *Environmental Science & Technology*, Vol. 42, pp. 9276–9282

Ko, Y.W., Cho, C.H., (2006) Characterization of large fleets of vehicle exhaust emissions in middle Taiwan by remote sensing. *Science of the Total Environment*, Vol. 354, pp.75-82

Kohler, M., Corsmeier, U., Vogt, U., Vogel, B. (2005) Estimation of gaseous real-world emissions downstream a motorway. *Atmospheric Environment*, Vol. 39, pp. 5665-5684

Kristensson, A., Johansson, C., Westerholm, R., Swietlicki, E., Gidhagen, L., Wideqvist, U., Vesely, V. (2004) Real-world traffic emission factors of gases and particles measured in a road tunnel in Stockholm, Sweden. *Atmospheric Environment*, Vol. 38, pp. 657-673

Kudoh, Y., Kondo, Y., Matsuhashi, K., Kobayashi, S., Moriguchi, Y. (2004) Current status of actual fuel-consumptions of petrol-fuelled passenger vehicles in Japan. *Applied Energy*, Vol. 79, pp. 291-308

Kühlwein, J., Friedrich, R. (2005) Traffic measurements and high-performance modelling of motorway emission rates. *Atmospheric Environment*, Vol. 39, pp. 5722–5736

Kuhns, H.D., Mazzoleni, C., Moosmüller, H., Nikolic, D., Keislar, R.E., Barber, P.W., Li, Z., Etyemezian, V., Watson, J.G.. (2004) Remote sensing of PM, NO, CO and HC emission factors for on-road gasoline and diesel engine vehicles in Las Vegas, NV. *Science of the Total Environment*, Vol. 322, pp. 123-137

Kukkonen, J., Harkonen, J., Karppinen, A., Pohjola, M., Pietarila, H., Koskentalo, T. (2001) A semi-empirical model for urban PM_{10} concentrations, and its evaluation against data from an urban measurement network. *Atmospheric Environment*, Vol. 35, pp. 4433–4442

Kumar, P., Fennell, P., Britter, R. (2008) Effect of wind direction and speed on the dispersion of nucleation and accumulation mode particles in an urban street canyon. *Science of the Total Environment*, Vol. 402, pp. 82-94

Kurniawan, A., Schmidt-Ott, A. (2006) Monitoring the Soot Emissions of Passing Cars. *Environmental Science & Technology*, Vol. 40, pp. 1911–1915

Kuttler, W., Strassburger, A. (1999) Air quality measurements in urban green areas – a case study. *Atmospheric Environment*, Vol. 33, pp. 4101–4108

Laschober, C., Limbeck, A., Rendl, J., Puxbaum, H. (2004) Particulate emissions from on-road vehicles in the Kaisermühlen-tunnel (Vienna, Austria). *Atmospheric Environment*, Vol. 38, pp. 2187-2195

Lee, B.K., Jun, N.Y., Lee, H.K. (2005) Analysis of impacts on urban air quality by restricting the operation of passenger vehicles during Asian Game events in Busan, Korea. *Atmospheric Environment*, Vol. 39, pp. 2323-2338

Lenaers, G. (1996) On-board real life emission measurements on a 3 way catalyst gasoline car in motor way-, rural- and city traffic and on two Euro-1 diesel city buses. *Science of the Total Environment*, Vol. 189-190, pp. 139-147

Li., H., Andrews, G.E., Daham, B., Bell, M., Tate, J., Ropkins, K., (2007) Impact of Traffic Conditions and Road Geometry on Real World Urban Emissions using a SI Car. *SAE Paper* 2007-01-0308

Li., H., Andrews, G.E., Savvidis, D., Daham, B., Ropkins, K., Bell, M., Tate, J., (2008) Comparisons of the Exhaust Emissions for Different Generations of SI Cars under Real World Urban Driving Conditions. *SAE Paper* 2008-01-0754

Lonati, G., Giugliano, M., Cernuschi, S. (2006) The role of traffic emissions from weekends' and weekdays' fine PM data in Milan. *Atmospheric Environment*, Vol. 40, pp. 5998–6011

Lu, H.C., Chang, T.S. (2005) Meteorologically adjusted trends of daily maximum ozone concentrations in Taipei, Taiwan. *Atmospheric Environment*, Vol. 39, pp. 6491–6501

Lu, W.Z., Wang, X.K. (2008) Investigation of respirable suspended particulate trend and relevant environmental factors in Hong Kong downtown areas. *Chemosphere*, Vol. 71, pp. 561-567

Man, C.K., Shih, M.Y. (2001) Identification of sources of PM10 aerosols in Hong Kong by wind trajectory analysis. *Journal of Aerosol Science*, Vol. 32, pp. 1213-1223

Martins, L.D., Andrade, M.F., Freitas, E.D., Pretto, A., Gatti, L.V., Albuquerque, E.L., Tomaz, E. Guardani, M.L., Martins, M.H.R.B., Olimpio M. A. Jr. (2006) Emission Factors for Gas-Powered Vehicles Traveling Through Road Tunnels in São Paulo, Brazil. *Environmental Science & Technology*, Vol. 40, pp. 6722–6729

Mazzoleni, C., Moosmüller, H., Kuhns, H.D., Keislar, R.E., Barber, P.W., Nikolic, D., Nussbaum, N.J., Watson, J.G. (2004a) Correlation between automotive CO, HC, NO, and PM emission factors from on-road remote sensing: implications for inspection and maintenance programs. *Transportation Research Part D: Transport and Environment*, Vol. 9, pp. 477-496

Mazzoleni, C., Kuhns, H.D., Moosmüller, H., Keislar, R.E., Barber, P.W.; Robinson, N.F., Watson, J.G.., Nikolic, D. (2004b) On-road Vehicle Particulate Matter and Gaseous Emission Distributions in Las Vegas, NV, compared with other areas. *Journal of the Air and Waste Management Association*, Vol. 54, pp. 711-726

Mediavilla-Sahagún, A., ApSimon, H. M. (2003) Urban scale integrated assessment of

options to reduce PM_{10} in London towards attainment of air quality objectives. *Atmospheric Environment*, Vol. 37, pp. 4651-4665

Mellios, G., Van Aalst, R., Samaras, Z. (2006) Validation of road traffic urban emission inventories by means of concentration data measured at air quality monitoring stations in Europe. *Atmospheric Environment*, Vol. 40, pp. 7362-7377

Moeckli, M.A., Fierz, M., Sigrist, M.W. (1996) Emission Factors for Ethene and Ammonia from a Tunnel Study with a Photoacoustic Trace Gas Detection System. *Environmental Science & Technology*, Vol. 30, pp. 2864–2867

Monn, C., Carabias, V., Junker, M., Waeber, R., Karrer, M., Wanner, H.U. (1997) Small-scale spatial variability of particulate matter <10 μm (PM_{10}) and nitrogen dioxide. *Atmospheric Environment*, Vol. 31, pp. 2243-2247

Monn, C. (2001) Exposure assessment of air pollutants: a review on spatial heterogeneity and indoor/outdoor/personal exposure to suspended particulate matter, nitrogen dioxide and ozone. *Atmospheric Environment*, Vol. 35, pp. 1–32

Morawska, L., Jamriska, M., Thomas, S., Ferreira, L., Mengersen, K., Wraith, D., McGregor, F. (2005) Quantification of Particle Number Emission Factors for Motor Vehicles from On-Road Measurements. *Environmental Science & Technology*, Vol. 39, pp. 9130–9139

Morawska, L., Ristovski, Z.D., Johnson, G.R., Jayaratne, E.R., Mengersen, K. (2007) Novel Method for On-road Emission Factor Measurements using a Plume Capture Trailer. *Environmental Science & Technology*, Vol. 41, pp. 574–579

Nagendra, S.M.S., Khare, M. (2002) Line Source Emission Modelling. *Atmospheric Environment*, Vol. 36, pp. 2083-2098

Nagendra, S.M.S., Khare, M. (2004) Artificial neural network based line source models for vehicular exhaust emission predictions of an urban roadway. *Transportation Research Part D: Transport and Environment*, Vol. 9, pp. 199-208

Namdeo, A., Bell, M.C. (2005) Characteristics and health implications of fine and coarse particulates at roadside, urban background and rural sites in UK. *Environment International*, Vol. 31, pp. 565–573

Ning, Z., Chan, T.L. (2007) On-road remote sensing of liquefied petroleum gas (LPG) vehicle emissions measurement and emission factors estimation. *Atmospheric Environment*, Vol. 41, pp. 9099-9110

Ning, Z., Polidori, A., Schauer, J.J., Sioutas, C. (2008) Emission factors of PM species based on freeway measurements and comparison with tunnel and dynamometer studies. *Atmospheric Environment*, Vol. 42, pp. 3099-3114

Nurrohim, A., Sakugawa, H. (2005) Fuel-based inventory of NO_x and SO_2 emissions from motor vehicles in the Hiroshima Prefecture, Japan. *Applied Energy*, Vol. 80, pp. 291-305

Oestergaard, K., Akard, M., Porter, S., Carder, D. (2004) Further Investigation into the Performance of Two Different On-board Emissions Measurement System Compared to Laboratory Measurement. *SAE Paper* 2004-01-3480

O'Sullivan, S.T., Timoney, D.J. (2005) On-road Measurement of Diesel Particulate Matter from In-Service Vehicles. *SAE Paper* 2005-01-0678

Pandey, S.K., Kim, K.H., Chung, S.Y., Cho, S.-J., Kim, M.-Y., Shon, Z.H. (2008) Long term study of NOx behavior at urban roadside and background locations in Seoul, Korea. *Atmospheric Environment*, Vol. 42, pp. 607–622

Panis, L.I., Broekx, S., Liu, R. (2006) Modelling instantaneous traffic emission and the influence of traffic speed limits. *Science of the Total Environment*, Vol. 371, pp. 270-285

Park, S.S., Kim, Y.J. (2005) Source contributions to fine particulate matter in an urban atmosphere. *Chemosphere*, Vol. 59, pp. 217-226

Park, S., Rakha, H. (2006) Energy and Environmental Impacts of Roadway grades. *Transportation Research Record*, Vol. 1987, pp. 148-160

Paterson, K.G., Sagady, J.L., Hooper, D.L., (1999) Analysis of Air Quality Data Using Positive Matrix Factorization. *Environmental Science & Technology*, Vol. 33, pp. 635-641

Peace, H., Owen, B., Raper, D.W. (2004) Identifying the contribution of different urban highway air pollution sources. *Science of the Total Environment*, Vol. 334-335, pp. 347-357

Phuleria, H.C. Geller, M.D., Fine, P.M. Sioutas, C. (2006) Size-Resolved Emissions of Organic Tracers from Light- and Heavy-Duty Vehicles Measured in a California Roadway Tunnel. *Environmental Science & Technology*, Vol. 40, pp. 4109-4118

Physick, W.L., Goudey, R. (2001) Estimating an annual-average RSP concentration for Hong Kong using days characteristic of the dominant weather patterns. *Atmospheric Environment*, Vol. 35, pp. 2697-2705

Pierson, W.R., Gertler, A.W., Robinson, N.F., Sagebiel, J.C., Zielinska, B., Bishop, G.A., Stedman, D.H., Zweidinger, R.B., Ray, W.D. (1996) Real-world automotive emissions – summary of studies in the Fort McHenry and Tuscarora mountain tunnels. *Atmospheric Environment*, Vol. 30, pp. 2233-2256

Pires, J.C.M., Sousa, S.I.V., Pereira, M.C., Alvim-Ferraz, M.C.M., Martins, F.G. (2008) Management of air quality monitoring using principal component and cluster analysis—part II: CO, NO_2 and O_3. *Atmospheric Environment*, Vol. 42, pp. 1261–1274

Pirjola, L., Parviainen, H., Hussein, T., Valli, A., Hämeri, K., Aaalto, P., Virtanen, A., Keskinen, J., Pakkanen, T. A., Mäkelä, T., Hillamo, R.E. (2004) “Sniffer”—a novel tool for chasing vehicles and measuring traffic pollutants. *Atmospheric Environment*, Vol. 38, pp. 3625–3635

Post, K., Kent, J.H., Tomlin, J., Carruthers, N. (1984) Fuel consumption and emission modelling by power demand and a comparison with other models. *Transportation Research Part A: General*, Vol. 18, pp. 191-213

Prybutok, V.R., Yi, J., Mitchell, D. (2000) Comparison of neural network models with

ARIMA and regression models for prediction of Houston's daily maximum ozone concentrations. *European Journal of Operational Research*, Vol. 122, pp. 31-40

Qin, Y., Chan, C.K., Chan, L.Y. (1997) Characteristics of chemical compositions of atmospheric aerosols in Hong Kong: spatial and seasonal distributions. *Science of the Total Environment*, Vol. 206, 25–37

Ristovski, Z., Morawska, L., Ayoko, G.A., Johnson, G., Gilbert, D., Greenaway, C. (2004) Emissions from a vehicle fitted to operate on either petrol or compressed natural gas. *Science of the Total Environment*, Vol. 323, pp. 179-194

Robert, M.A., Kleeman, M.J., Jakober, C.A. (2007) Size and composition distributions of particulate matter emissions: Part 2—Heavy-duty diesel vehicles. *Journal of the Air and Waste Management Association*, Vol. 57, pp. 1429-1438

Saleh, W., Kumar, R., Kirby, H., Kumar, P. (2009) Real world driving cycle for motorcycles in Edinburgh. *Transportation Research Part D: Transport and Environment*, Vol. 14, pp. 326-333

Samuel, S., Morrey, D., Fowkes, M., Taylor, D.H.C., Garner, C.P., Austin, L. (2005) Real-world performance of catalytic converters. *Proceedings of the Institution of Mechanical Engineers Part D—Journal of Automobile Engineering*, Vol. 219, pp. 881-888

Scoggins, A., Kjellstrom, T., Fisher, G., Connor, J., Gimson, N. (2004) Spatial analysis of annual air pollution exposure and mortality. *Science of the Total Environment*, Vol. 321, pp. 71–85

Shah, S.D., Cocker, D.R., III, Miller, J. W., Norbeck, J. M. (2004) Emission Rates of Particulate Matter and Elemental and Organic Carbon from In-Use Diesel Engines. *Environmental Science & Technology*, Vol. 38, pp. 2544-2550

Shi, J.P., Harrison, R.M. (1997) Rapid NO_2 formation in diluted petrol-fuelled engine exhaust—a source of NO_2 in winter smog episodes. *Atmospheric Environment*, Vol. 31, pp. 3857–3866

Shorter, J.H., Herndon, S., Zahniser, M.S., Nelson, D.D., Wormhoudt, J., Demerjian, K.L., Kolb, C.E. (2005) Real-Time Measurements of Nitrogen Oxide Emissions from In-Use New York City Transit Buses Using a Chase Vehicle. *Environmental Science & Technology*, Vol. 39, pp. 7991-8000

Silva, C.M., Costa, M., Farias, T.L., Santos, H. (2006a) Evaluation of SI engine exhaust gas emissions upstream and downstream of the catalytic converter. *Energy Conversion and Management*, Vol. 47, pp. 2811-2828

Silva, C.M., Farias, T.L., Frey, H.C., Rouphail, N.M. (2006b) Evaluation of numerical models for simulation of real-world hot-stabilized fuel consumption and emissions of gasoline light-duty vehicles. *Transportation Research Part D: Transport and Environment*, Vol. 11, pp. 377-385

Slini, Th., Karatzas, K., Moussiopoulos, N. (2002) Statistical analysis of environmental data as the basis of forecasting: an air quality application. *Science of the Total Environment*, Vol. 288, pp. 227–237

Sodeman, D.A., Toner, S.M., Prather, K.A. (2005) Determination of Single Particle Mass Spectral Signatures from Light-Duty Vehicle Emissions. *Environmental Science & Technology*, Vol. 39, pp. 4569-4580

Song, Y., Shao, M., Liu, Y., Lu, S., Kuster, W., Goldan, P., Xie, S. (2007) Source Apportionment of Ambient Volatile Organic Compounds in Beijing. *Environmental Science & Technology*, Vol. 41, pp. 4348-4353

Song, G.H., Yu, L., Wang, Z.Q.L. (2009) Aggregate Fuel Consumption Model of Light-Duty Vehicles for Evaluating Effectiveness of Traffic Management Strategies on Fuels. *Journal of Transportation Engineering-ASCE*, Vol. 135, pp. 611-618

Sousa, S.I.V., Martins, F.G., Pereira, M.C., Alvim-Ferraz, M.C.M. (2006) Prediction of ozone concentrations in Oporto city with statistical approaches. *Chemosphere*, Vol. 64, pp. 1141-1149

Tang, U.W., Wang, Z. (2006) Determining gaseous emission factors and driver's particle

exposures during traffic congestion by vehicle-following measurement techniques. *Journal of the Air and Waste Management Association*, Vol. 56, pp. 1532-1539

Tsai, J.H., Hsu, Y.C. Weng, H.C., Lin, W.Y., Jeng, F.T. (2000) Air pollutant emission factors from new and in-use motorcycles. *Atmospheric Environment*, Vol. 34, pp. 4747-4754

Unal, A., Rouphail, N.M., Frey, H.C. (2003) Effect of Arterial Signalization and Level of Service on Measured Vehicle Emissions. *Transportation Research Record*, Vol. 1842, pp. 47-56

Unal, A., Frey, H.C., Rouphail, N.M. (2004) Quantification of highway vehicle emissions hot spots based upon on-board measurements. *Journal of the Air and Waste Management Association*, Vol. 54, pp. 130-140

US Environmental Protection Agency (USEPA) (1998) *Quality Assurance Handbook for Air Pollution Measurement Systems: Volume II, Part I: Ambient Air Quality Monitoring Program Quality System Development*. Office of Air Quality Planning and Standards, Research Triangle Park, NC.

Väkevä, M., Hämeri, K., Kulmala, M., Lahdes, R., Ruuskanen, J., Laitinen, T. (1999) Street level versus rooftop concentrations of submicron aerosol particles and gaseous pollutants in an urban street canyon. *Atmospheric Environment*, Vol. 33, pp. 1385–1397

Vardoulakis, S., Fisher, B.E.A., Pericleous, K., Gonzalez-Flesca, N. (2003) Modelling air quality in street canyons: a review. *Atmospheric Environment*, Vol. 37, pp. 155–182

Vardoulakis, S., Gonzalez-Flesca, N., Fisher, B.E.A., Pericleous, K. (2005) Spatial variability of air pollution in the vicinity of a permanent monitoring station in central Paris. *Atmospheric Environment*, Vol. 39, pp. 2725–2736

Varotsos, C., Ondov, J., Efstathiou, M. (2005) Scaling properties of air pollution in Athens, Greece and Baltimore, Maryland. *Atmospheric Environment*, Vol. 39, pp. 4041–4047

Viana, M., Querol, X., Alastuey, A. (2006) Chemical characterisation of PM episodes in NE Spain. *Chemosphere*, Vol. 62, pp. 947-956

Vogt, R., Scheer, V., Casati, R., Benter, T. (2003) On-Road Measurement of Particle Emission in the Exhaust Plume of a Diesel Passenger Car. *Environmental Science & Technology*, Vol. 37, pp. 4070-4076

Wåhlin, P., Palmgren F., Van Dingenen, R. (2001) Experimental studies of ultrafine particlesin streets and the relationship to traffic. *Atmospheric Environment*, Vol. 35, Supplement 1, pp. 63-69

Wang, T., Wu, Y.Y., Cheung, T.F., Lam, K.S. (2001) A study of surface ozone and the relation to complex wind flow in Hong Kong. *Atmospheric Environment*, Vol. 35, pp. 3203-3215

Wang, W.G., Lyons, D.W., Clark, N.N., Gautam, M., Norton, P.M. (2000) Emissions from Nine Heavy Trucks Fueled by Diesel and Biodiesel Blend without Engine Modification. *Environmental Science & Technology*, Vol. 34, pp. 933-939

Wang, X.K., Lu, W.Z. (2006) Seasonal variation of air pollution index: Hong Kong case study. *Chemosphere*, Vol. 63, pp. 1261-1272

Weijers, E.P., Khlystov, A.Y., Kos, G.P.A., Erisman, J.W. (2004) Variability of particulate matter concentrations along roads and motorways determined by a moving measurement unit. *Atmospheric Environment*, Vol. 38, pp. 2993-3002

Weng, Y.C., Chang, N.B., Lee, T.Y. (2008) Nonlinear time series analysis of ground-level ozone dynamics in Southern Taiwan. *Journal of Environmental Management*, Vol. 87, pp. 405-414

Westerdahl, D., Fruin, S., Sax, T., Fine, P.M., Sioutas, C. (2005) Mobile platform measurements of ultrafine particles and associated pollutant concentrations on freeways and residential streets in Los Angeles. *Atmospheric Environment*, Vol. 39, pp. 3597-3610

Westerdahl, D., Wang, X., Pan, X.C., Zhang, K.M. (2009) Characterization of on-road vehicle emission factors and microenvironmental air quality in Beijing, China. *Atmospheric Environment*, Vol. 43, pp. 697-705

Windsor, H.L., Toumi, R. (2001) Scaling and persistence of UK pollution. *Atmospheric Environment*, Vol. 35, pp. 4545-4556

Won, J.H., Park, J.Y., Lee, T.G. (2007) Mercury emissions from automobiles using gasoline, diesel, and LPG. *Atmospheric Environment*, Vol. 41, pp. 7547-7552

Wu, Y., Hao, J., Fu, L., Wang, Z., Tang, U. (2002) Vertical and horizontal profiles of airborne particulate matter near major roads in Macao. China. *Atmospheric Environment*, Vol. 36, pp. 4907–4918

Xie, S., Zhang, Y., Qi, L., Tang, X. (2003) Spatial distribution of traffic-related pollutant concentrations in street canyons. *Atmospheric Environment*, Vol. 37, pp. 3213–3224

Yang, H.H., Hsieh, L.T., Liu, H.C., Mi, H.H. (2005) Polycyclic aromatic hydrocarbon emissions from motorcycles. *Atmospheric Environment*, Vol. 39, pp. 17-25

Yang, H.H., Chien, S.M., Cheng, M.T., Peng, C.Y. (2007) Comparative Study of Regulated and Unregulated Air Pollutant Emissions before and after Conversion of Automobiles from Gasoline Power to Liquefied Petroleum Gas/Gasoline Dual-Fuel Retrofits. *Environmental Science & Technology*, Vol. 41, pp. 8471–8476

Yao, Y.C. Tsai, J.H., Chiang, H.L. (2009) Effects of ethanol-blended gasoline on air pollutant emissions from motorcycle. *Science of the Total Environment*, Vol. 407, pp. 5257-5262

Yuan, Z., Lau, A.K.H., Zhang, H., Yu, J. Z., Louie, P.K.K., Fung, J.C.H. (2006) Identification and spatiotemporal variations of dominant PM_{10} sources over Hong Kong. *Atmospheric Environment*, Vol. 40, pp. 1803-1815

Yura, E.A., Kear, T., Niemeier D. (2007) Using CALINE dispersion to assess vehicular PM2.5 emissions. *Atmospheric Environment*, Vol. 41, pp. 8747–8757

Zamboni, G., Capobianco, M., Daminelli, E. (2009) Estimation of road vehicle exhaust emissions from 1992 to 2010 and comparison with air quality measurements in Genoa, Italy. *Atmospheric Environment*, Vol. 43, pp. 1086-1092

Zavala, M., Herndon, S.C., Wood, E.C., Onasch, T.B., Knighton, W.B., Marr, L.C., Kolb, C.E., Molina, L.T. (2009) Evaluation of mobile emissions contributions to Mexico City's emissions inventory using on-road and cross-road emission measurements and ambient data. *Atmospheric Chemistry and Physics*, Vol. 9, pp. 6305-6317

Zhai, H., Frey, H.C., Rouphail, N.M. (2008) A Vehicle-Specific Power Approach to Speed- and Facility-Specific Emissions Estimates for Diesel Transit Buses. *Environmental Science & Technology*, Vol. 42, pp. 7985–7991

Zhang, Y., Stedman, D.H., Bishop, G.A., Guenther, P.L., Beaton, S.P., Peterson, J.E. (1993) On-road hydrocarbon remote sensing in the Denver area. *Environmental Science & Technology*, Vol. 27, pp. 1885–1891